Development of a CO_2 Cooling Test Facility from the Vertex Locator Thermal Control System

Stuart Lunt

A dissertation presented for the degree of
Master of Science in Engineering

Department of Electrical Engineering
University of Cape Town
South Africa

May 29, 2024

EP-DT
Detector Technologies

Abstract

The Vertex Locator Thermal Control System (VTCS) was a mechanically pumped, evaporative CO_2 cooling system developed for silicon strip detectors in the Large Hadron Collider beauty (LHCb) experiment at the European Organisation for Nuclear Physics (CERN). This type of cooling has become increasingly common in high-energy physics experiments, making their design and testing increasingly more important. The Detector Technologies (DT) group chose to reuse the hardware from the VTCS after it was retired and convert it into a test facility for future detectors. This dissertation describes the analysis and redesign of the electrical, fluid and control systems which was undertaken to optimise the design for its new role and to bring it into line with current standards in the field. Alongside the hardware design, a model of the system was developed in Simulink, enabling the performance to be simulated with different hardware configurations and to assess its suitability for different applications. Delays in travel and procurement caused by the COVID-19 pandemic did not allow final construction and commissioning to be fully completed by the end of the project.

Declaration

I know the meaning of plagiarism and declare that all the work in the document, save for that which is properly acknowledged, is my own. This dissertation has been submitted to the Turnitin module and I confirm that my supervisor has seen my report and that any concerns revealed by such have been resolved with my supervisor.

Signed by candidate | 25/05/2024

Stuart Lunt | Date

Acknowledgements

These last few years have been turbulent times for the world with many unexpected and unprecedented events changing life as we know it. It has required plans to become flexible and adaptation to become the norm. Many people have helped me navigate these new conditions successfully and it reflects in the work produced.

Firstly, to Professor Edward Boje and Dr Sahal Yacoob from UCT and Bart Verlaat and Lukasz Zwalinski from CERN for their continuous support, technically, financially and administratively, in the ever-changing circumstances. You accompanied me the whole way with your expert knowledge and years of experience.

Furthermore, to Loïc Davoine, Cédric Landraud and Wojciech Hulek for sharing their knowledge on the design and construction of the group's systems.

Viren Bhanot for his expertise in modelling.

Eric Thabuis and Loïc Curtat for their assistance in the construction of the electrical and mechanical systems.

Isabelle, David, Derek, Noémie, Camila, Dani, Bartek and Dominik, my fellow students, for always being there for a coffee or a discussion about the problems with the project.

To my friends and fellow students for the entertainment and distraction from work.

Finally to my family, for their support, grounding and advice.

My heartfelt thanks to you all, you have all influenced my journey in different ways. It would not be the same without your support.

Contents

List of Figures

List of Tables

Acronyms

2PACL Two-phase Accumulator Controlled Loop. vii, 3, 13–15, 50, 65, 69, 71, 75, 78

AHOT Any Heater Over Temperature. 41

ATLAS A Toroidal LHC Apparatus. 1, 11

CERN European Organisation for Nuclear Research. 1, 22, 23, 27, 34–36, 46, 84–86

CFC Chloroflurocarbon. 5

CMS Compact Muon Solenoid. 1

COP Coefficient of Performance. vii, 7, 8

DT Detector Technologies. 1, 46, 78, 90

DTCS Detector Technologies Cooling System. viii, 37, 38, 40, 63

EP Experimental Physics. 1, 46, 78

FS Fluid Systems. 1, 3, 86

GPN General Purpose Network. 34, 35

GWP Global Warming Potential. 6, 7

HCA Heat Controlled Accumulator. 13, 14

HCFC Hydrochlorofluorocarbon. 5

HFC Hydroflurocarbon. 5–7

HFO Hydrofluoroolefin. 7

I2PACL Integrated Two-phase Accumulator Controlled Loop. vii, 14–17, 19, 49, 50, 61, 62, 65, 69, 71, 75, 78

IPCC Intergovernmental Panel on Climate Change. 6

LHC Large Hadron Collider. 1, 10, 86

LHCb Large Hadron Collider beauty. 1

LUCASZ Light Use Cooling Apparatus for Surface Zones. 19, 22, 49

NIKHEF Dutch National Institute for Subatomic Physics. 27, 50

P&ID Process and Instrumentation Diagram. 4, 16, 25, 50

PCA Pressure Controlled Accumulator. 13, 14

PCO Process Control Object. viii, 37, 38, 40, 42–46

PID Proportional Integral Derivative. 26, 43, 64

PLC Programmable Logic Controller. ix, 20, 26–29, 31, 34–37, 44–46, 48, 62, 63, 71

PTC Positive Temperature Coefficient. 29

RCD Residual Current Device. 29, 32

RF Radiative Forcing. 6

SCADA Supervisory Control and Data Acquisition. viii, 4, 26, 34, 36, 46–48, 78

TN Technical Network. 34, 35

UAB UNICOS Application Builder. 37, 48

UNICOS Unified Industrial Control System. vii, 4, 26, 27, 36–38, 43, 46, 48, 64–66, 78, 92

VELO Vertex Locator. vii, ix, 1, 9, 11

VTCS VELO Thermal Control System. vii, viii, 1–3, 10, 17, 49, 50, 56, 59, 61, 62, 78, 79

Chapter 1

Introduction

1.1 Background

The European Organisation for Nuclear Research (CERN) is an institute in Geneva, Switzerland which studies the physics of subatomic particles. This is done by accelerating particles in the Large Hadron Collider (LHC) and colliding them with other materials or particles and observing the results with particle detectors.

The Fluid Systems (FS) section in the Detector Technologies (DT) group of the Experimental Physics (EP) department at CERN has pioneered the use of two-phase CO_2 cooling for silicon tracking detectors. These detectors are placed close to the collision point to measure the direction and momentum of particles created after a collision. They degrade rapidly after they are exposed to radiation which can be prevented only by keeping them cold.

The use of two-phase CO_2 is desirable because it has a high latent heat of vaporisation, can be distributed with small lines, and provides accurate temperature control over long distances through pressure regulation allowing radiation sensitive components to be kept a safe distance from the experimental zone.

The first system was installed in the Vertex Locator (VELO) sub-detector which was part of the Large Hadron Collider beauty (LHCb) experiment in 2007. VELO had specific cooling requirements that were suited to this two-phase cooling system. The original VTCS was replaced in 2019 with an upgraded system which is larger and more capable than the VTCS.

CO_2 cooling systems developed by the DT group are installed in the A Toroidal LHC Apparatus (ATLAS), Compact Muon Solenoid (CMS) and LHCb experiments at CERN. Similar cooling systems have also been deployed on the International Space Station for the Alpha Magnetic Spectrometer 2 (AMS-02) experiment that measures cosmic radiation.

The DT group decided to refurbish the VTCS so it can be used for internal research and development purposes. The VTCS can provide a cooling environment

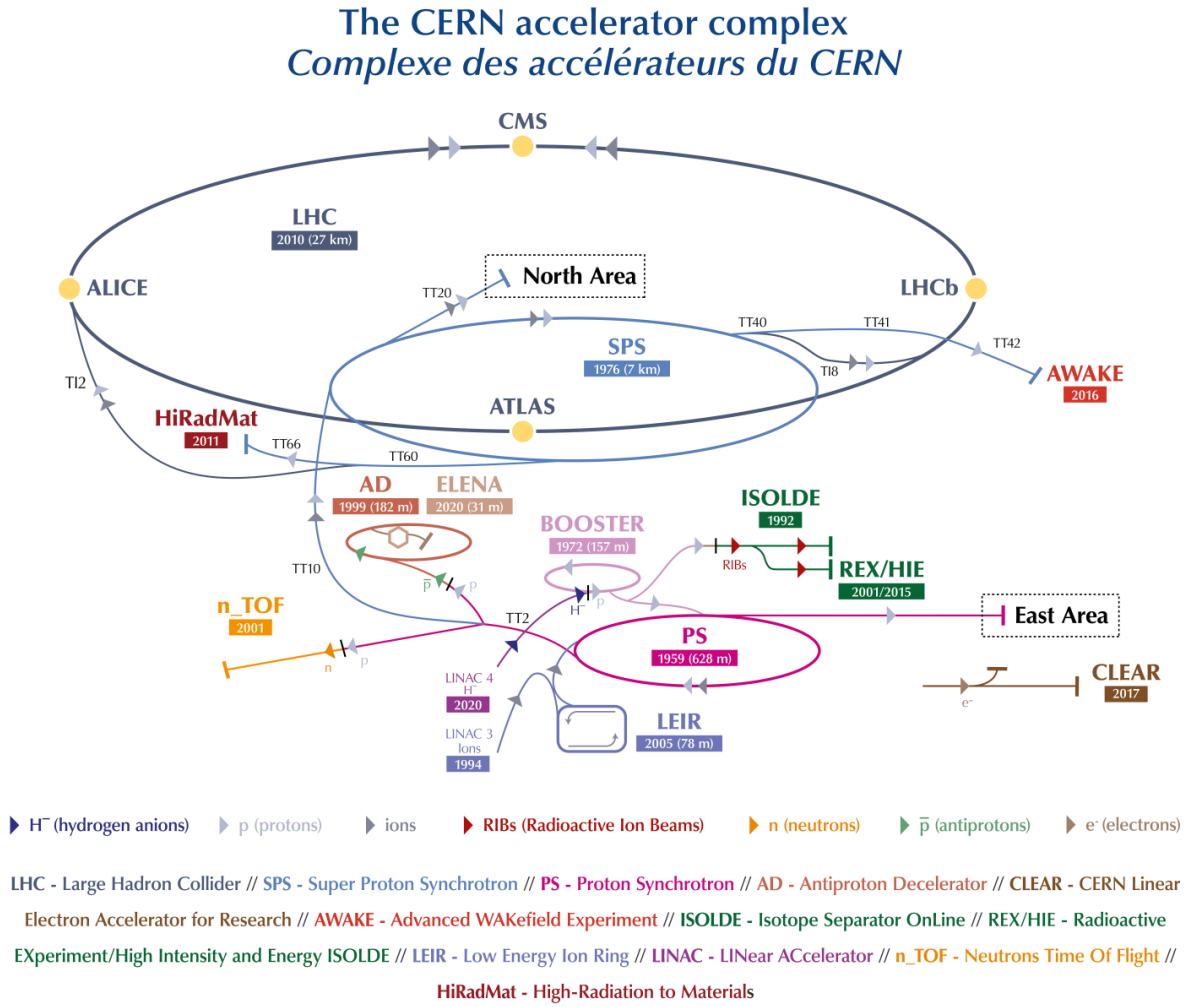

Figure 1.1: The CERN accelerator complex [1]

that is almost identical to what a detector may receive when it is installed and could provide valuable test data for future detector development.

The VTCS had been partially decommissioned in 2019 after which it had been in storage. It consisted of two mechanical equipment frames and one electrical cabinet. Some components had already been removed with others no longer in usable condition.

1.2 Objectives

This project aimed to develop a two-phase CO_2 cooling system that performs similarly to the systems installed in the experimental cavern for use at a fixed surface location for research and development of future detectors. A retired CO_2 cooling system was used as the basis to minimise cost and material waste.

The system should operate as autonomously as possible because it will be used by detector engineers who may not have experience with cooling. It must be able to operate in a surface building without services other than electricity. The new system should meet the current design and safety standards used in the section.

1.2.1 Problems to be investigated

The FS section needed a detector cooling system that they could use for the development and testing of prototypes without designing and building a completely new one. The system was based on the retired VTCS which has been modified and upgraded to perform best in the new role while retaining as many components as possible.

1.2.2 Outcomes

The project should:

- Adapt the P&ID of the VTCS to allow it to function as a test facility
- Write a new functional analysis to describe the functionality of the system
- Be capable of operating in both normal and integrated 2PACL modes
- Have two independently operated CO_2 systems
- Be cooled by a single air-cooled chiller
- Have a capacity of 3 kW at $-25\,^{\circ}\mathrm{C}$, equally divided between the two CO_2 systems
- Have a minimum operating range between $-25\,^{\circ}\mathrm{C}$ and $15\,^{\circ}\mathrm{C}$
- Maintain the standard temperature change rate of $1\,^{\circ}\mathrm{C\,s^{-1}}$
- Maintain a steady state temperature within $\pm 0.1\,^{\circ}\mathrm{C}$ of the set point

1.3 Scope and limitations

The physical construction of the project was limited to the components that were installed in the two skids where the original system was constructed. Any components that will be remote or on the user side were considered in diagrams but will not be procured or connected as part of the project.

1.4 Plan of development

First, the final system requirements were discussed with the project stakeholders. This ensured that the performance limitations were made clear to all involved and

The condition of the existing hardware was assessed. To do this the system was disassembled and the suitability of the components for the new system was considered. Unsuitable components were recycled. Useful components were set aside to be used at a later stage or for spare stock.

A new Process and Instrumentation Diagram (P&ID) was developed based on the existing pipe and sensor configuration. This showed what changes need to be made to the mechanical and electrical systems to achieve the desired result. The Functional Analysis was written based on the P&ID and the intended use of the system. It describes, in detail, how the control program will function.

The system piping will be modified to match the new P&ID. A combination of in-house assembly and contracted manufacturing is to be used as appropriate.

New electrical schematics were designed based on the sensors required in the P&ID. These were used to construct the new electrical system.

A representative model was created using MATLAB and Simulink. It used the fluid and material thermal properties to get a representative model of the system. The model was used to gain insight into the new system's behaviour and prepare the control design accordingly.

The UNICOS project was developed from the Functional Analysis. To do this the Specification file had to be filled with the information from the Functional Analysis and any customised functions were written in template files.

SCADA panels were then created to visually represent the system and allow the operator to interact with it. These panels were made using UNICOS visual objects in the section's server and deployed on it.

Chapter 2

Literature review

2.1 Refrigeration

The vapour-compression refrigeration cycle has been continuously developed since 1834 with several significant changes occurring in the twentieth century due to increased environmental impact regulations. Early systems used naturally occurring refrigerants including carbon dioxide, ammonia, methyl chloride, butane, and propane. Many natural refrigerants are flammable, toxic or both, with others like carbon dioxide being originally technically difficult to use.

In the early twentieth century, as household refrigeration became more common, companies invested resources in finding a refrigerant suitable for domestic use which had to be stable, non-toxic and non-flammable. This research led to the development of halocarbons, commonly referred to as Chloroflurocarbons (CFCs) and Hydrochlorofluorocarbons (HCFCs). Their use continued until the 1980s when it was discovered that they were depleting the ozone layer.

2.1.1 The Montreal protocol

In 1987, the Montreal Protocol began phasing out CFCs, committing to a 50% reduction in 10 years, followed by the complete phase-out of ozone-depleting substances in favour of fluorine-based Hydroflurocarbons (HFCs). While the Montreal Protocol is one of the most successful international environmental treaties implemented, it did not consider the impact of new HFC refrigerants on climate change.

Early climate research by Ramanathan [2] in 1975, concluded that the effect of refrigerants on the earth's thermal energy balance must be given serious consideration. Their model found that at the rate that their atmospheric concentrations were rising, refrigerant emissions could cause a 0.5 K increase in surface temperatures by the year 2000.

2.1.2 Quantifying the impact of emissions

Different gases contribute diversely to the greenhouse effect per kilogram emitted. To express this, the Intergovernmental Panel on Climate Change (IPCC) developed the Global Warming Potential (GWP). This is defined as the time-integrated global mean Radiative Forcing (RF) of a pulse emission of 1 kg of a compound relative to that of 1 kg of the reference gas CO_2, which was adopted for use in the Kyoto Protocol with a time horizon of 100 years [3]. Equation 2.1 shows the mathematical representation where r is the reference gas, a is the radiative efficiency caused by a unit increase in atmospheric abundance ($\mathrm{W\,m^{-2}\,kg^{-1}}$) and $x(t)$ is the time dependant decay of the substance. This allows the emission of any gas to be compared to the equivalent emission of CO_2 and to judge its impact on climate.

$$GWP(x) = \frac{a_x}{a_r} \frac{\int_0^{TH} x(t)dt}{\int_0^{TH} r(t)dt} \tag{2.1}$$

The adequacy of GWP has been debated since its introduction because it fails to account for the decay of emissions in the atmosphere. The 100-year time horizon used for the Kyoto Protocol contains many shorter-lived greenhouse gases such as methane (CH_4). The IPCC has recognised the shortcomings of GWP; however, they still recommend it for long-lived greenhouse gases and it performs well in predicting the impact of sustained emissions of shorter-lived gases [3].

2.1.3 Climate impact of refrigerants

The United States Environmental Protection Agency produced a breakdown of global emissions by their CO_2 equivalent using data from the IPCC's Fifth Assessment report, shown in Figure 2.1. Atmospheric concentrations of fluorinated gases have been rising since the 1980s as refrigeration and air conditioning have become more common [4]. HFCs have a lifespan of up to 270 years with GWPs of up to 14 800 and as a result, they have a significant impact, even at low concentrations [5].

Additionally, there is a significant lag between the production and emissions of halocarbons because of the way they are used. Unless a large portion of them are properly destroyed, [6] current amounts of banked halocarbons will have a significant effect on radiative forcing.

Fluorinated gases (F-gases) do not occur naturally. Thus, all emissions must have come from leaks or incorrect disposal methods during decommissioning. Phasing out these refrigerants will limit the emissions of some of the most potent and long-lived greenhouse gases.

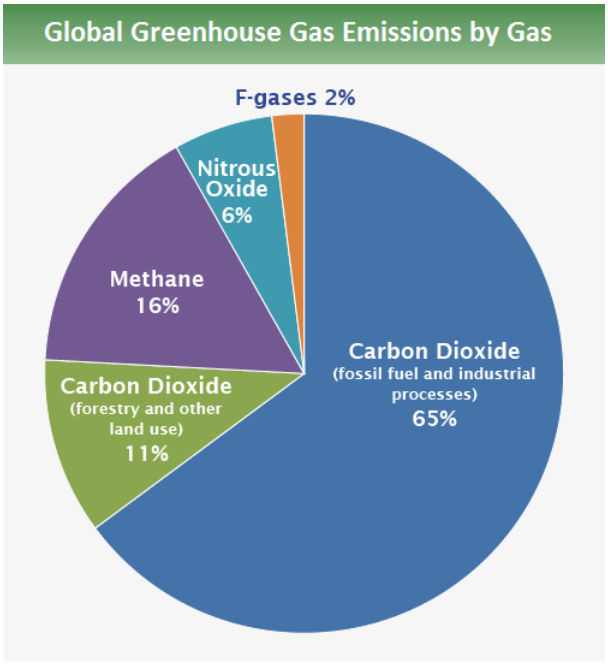

Figure 2.1: Global emissions broken down by gas, represented by their CO_2 equivalent [7]

2.1.4 The Kigali amendment

In 2016, the Kigali Amendment to the Montreal Protocol was signed, becoming effective in most developed countries on 1 January 2019. This amendment aims to replicate the success of the Montreal Protocol in protecting the ozone layer against climate change. This agreement adds HFCs to the list of controlled substances and creates a phase-down programme. The amendment requires parties to reduce their HFC consumption by 80% to 85% by the late 2040s [8].

In anticipation of the phase-out of HFCs, two different paths are being investigated. The first is the transition to Hydrofluoroolefins (HFOs), low-GWP HFCs, or blends of the two. These can be used as drop-in replacements for banned HFCs; however, the performance of the system will not be identical. Heredia-Aricapa, Belman-Flores, Mota-Babiloni, *et al.* [9] discussed proposed replacements for R404. They found that a new refrigerant would cause variation in the capacity, COP, and energy consumption, with a margin of $\pm 10\%$ depending on the operating envelope, indicated in Figure 2.2. It is expected that these low-GWP alternatives will also need to be phased out to meet the requirements of the treaty in the future.

The second path forward is to transition directly to natural refrigerants. These gases cannot be used in existing equipment, which significantly increases the up-front cost of new equipment, but they are expected to have lower running costs as the drop-in replacements will eventually be phased out under the rules shown in Figure 2.3.

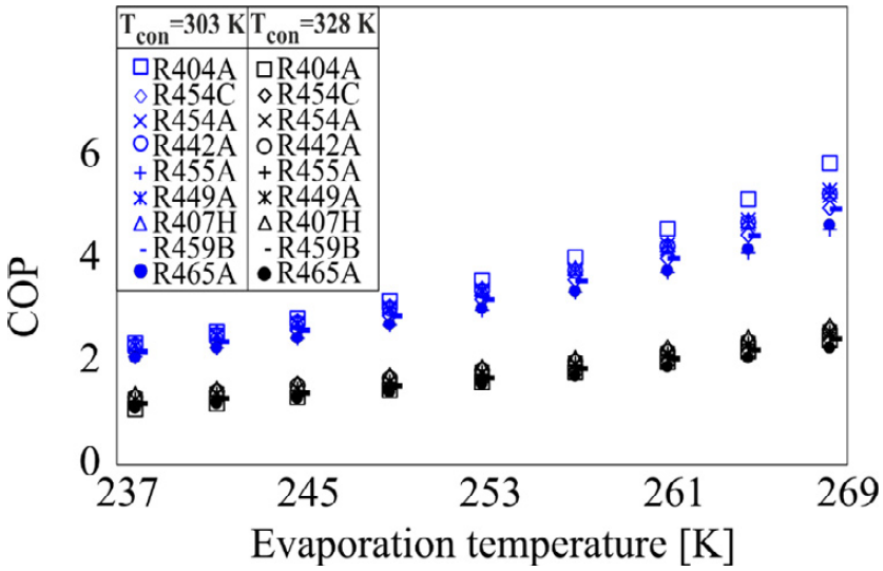

Figure 2.2: COP vs evaporation temperature for R404A alternatives [9].

2.1.5 F-gas regulation

The European Union updated the regulations governing the use of fluorinated gases in 2015 with Regulation (EU) No 517/2014 [10]. This directive phases out the amount of CO_2 equivalent that a refrigeration system may contain, shown in Figure 2.3. R404a was commonly used at CERN in previous systems; however, the F-gas regulation prohibited its use in new systems from the beginning of 2020.

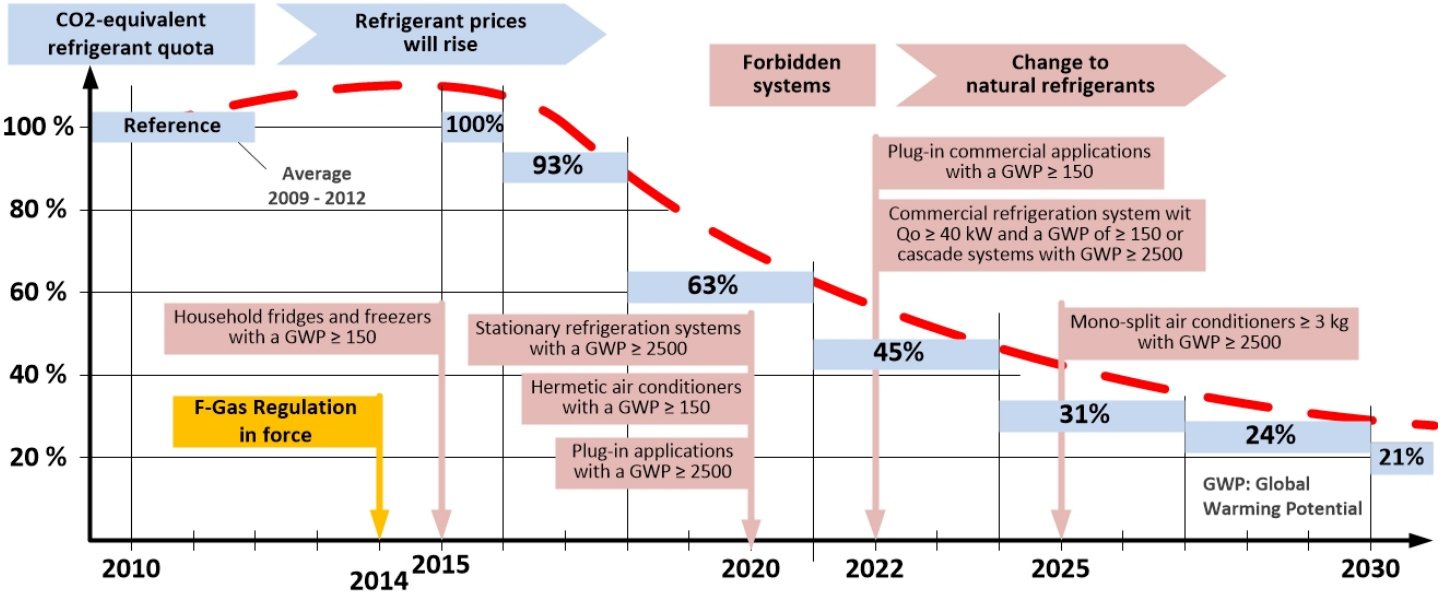

Figure 2.3: F-gas regulation phase-out [11]

2.2 Silicon tracking detectors

Silicon tracking detectors are solid-state ionisation chambers, that use semiconductors to read out the path of a particle. Both gas and solid-state ionisation chambers are used in particle detectors, with each type having a different role.

Solid-state detectors are used closer to the interaction point because they have good energy resolution and greater density than gaseous detectors. This allows higher spatial resolution close to the collision point to determine the position of the primary interaction vertex and secondary decays [12].

Proximity to the beam and collision point requires the detector to operate in a hostile environment with high levels of ionising radiation and a strong vacuum. Figure 2.4 shows an element of the VELO detector. The cutout in the middle allows the beam to pass between the detector elements. These detectors and their driving electronics are cooled at the periphery, where the green circuit board can be seen.

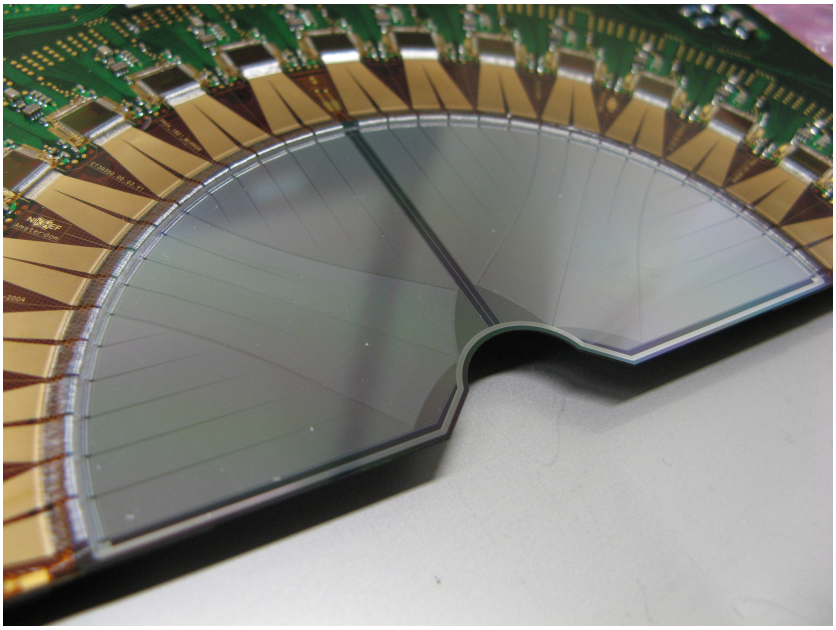

Figure 2.4: VELO Detector element [13]

2.2.1 Radiation length

Radiation length is a material property describing its transparency to radiation. It is defined as the mean length (in cm) needed to reduce the energy of an electron by a factor of e^{-1} [14]. This loss of energy is caused when the electron emits a photon after interacting with the electric field of an atom. This interaction is impacted by the number of electrons (atomic number Z) and the size (atomic weight A). It can be approximated with Equation 2.2. However, it should only be used when experimental data is not available.

$$Xo = \frac{716.4}{Z(Z+1)ln\frac{287}{\sqrt{Z}}} \tag{2.2}$$

The radiation length of the cooling system should be small compared to that of the detector itself. Therefore, minimising the mass of the cooling system is an important consideration during the design process.

2.2.2 Ionising radiation

A primary concern for the longevity of the detector is the effect of ionising radiation on the silicon. After irradiation, the leakage current and bias voltage increase due to defects introduced when the silicon crystal structure is disturbed by the radiation [12]. This causes more heat to be generated inside the sensor and could lead to thermal runaway if uncontrolled. To minimise the damage done by the radiation and reduce the leakage current, the silicon must be chilled to sub-zero temperatures after exposure and kept at or below $-20\,^{\circ}\mathrm{C}$ during operation [15].

When the proton beam is circulating in the LHC, the entire beam pipe and unshielded caverns are exposed to radiation. This requires the working fluid to be radiation-hard. It should not polymerise to maintain the heat transfer properties of the heat exchangers and any byproducts from the breakdown of the working fluid should be noncorrosive [16].

2.2.3 Stress

The silicon wafers, microchannels and fluid connectors are susceptible to thermal stresses if the temperature is changed too quickly. Whenever the temperature needs to be raised for maintenance or when the detector is shut down, it must be done in a controlled manner that will not damage the sensor [15]. The standard temperature change rate is generally set at a maximum of $1\,\mathrm{K\,min^{-1}}$ for silicon-based detectors; however, different detectors may have different requirements.

2.2.4 Thermal stability

The detectors measure particle tracks at micron level accuracy which requires the cooling system to provide a stable set point to the level of $\pm 0.1\,^{\circ}\mathrm{C}$. Variations beyond this could cause mechanical movement or deformation significant enough to spoil the measurements [15].

2.2.5 Cooling requirements of VELO

The original VTCS was designed to meet the requirements shown in Table 2.1. The designers of the detectors set these requirements to increase the life span and reliability of the detector.

Table 2.1: Temperature requirements of VELO [17]

Scenario	Temperature [range] (°C)
Operation	-7 [-12; -5]
Short term	[0; 24] for 100 hours
Long term	[-30; 0]
Unirradiated	[-30; 100]

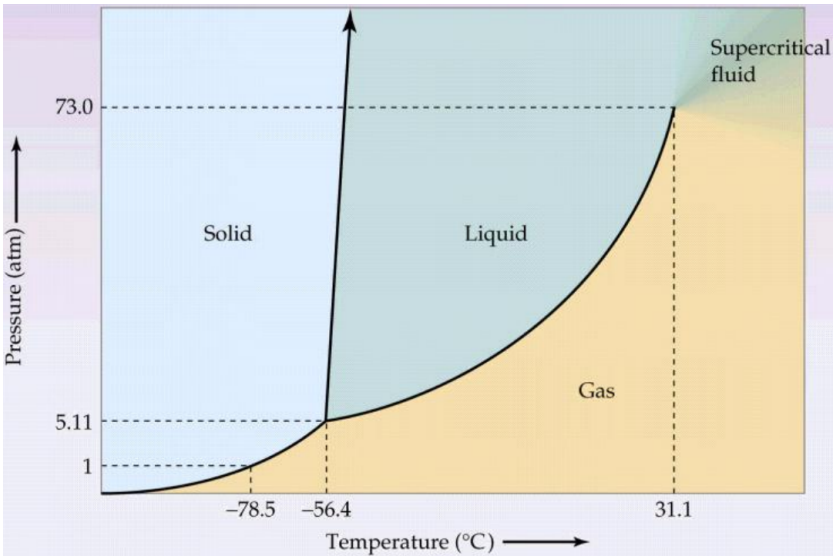

Figure 2.5: CO_2 phase diagram [19]

2.3 Carbon dioxide cooling

Carbon dioxide is a good candidate for detector cooling because it meets all the requirements outlined above. It does not degrade or produce toxic substances over time and it is radiation hard, recombining to CO_2 if disassociated by ionising radiation [18].

CO_2 systems operate at high pressures to ensure that the fluid does not freeze. The operational range of CO_2 is shown in Figure 2.5. This is beneficial because it allows the system to have a high pressure drop across the detector.

The high pressure drop across the detector allows the use of smaller pipes, reducing both the material budget and the radiation length of the cooling system [19]. This reduced pipe size allows more usable space for the detector components and provides significant gains in the radiation length of the cooling system, as shown in Figure 2.6.

CO_2 has a large latent heat allowing a lower flow rate, which leads to a lower pressure drop per metre of tubing. It also has a low viscosity, contributing to an even lower pressure drop [19]. Figure 2.7 shows a comparison to octafluoropropane, (C_3F_8) previously used in the ATLAS Inner Detector (ID) [20].

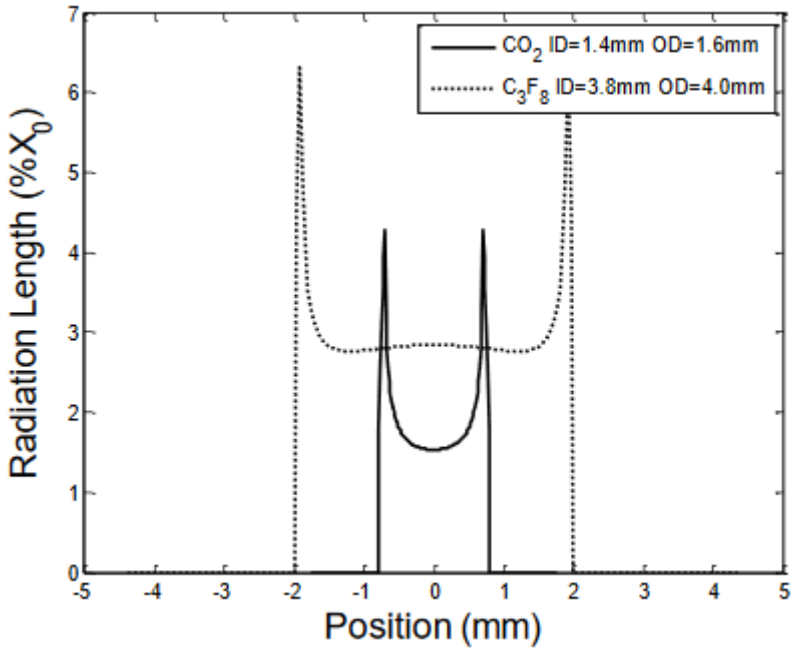

Figure 2.6: Radiation length of CO_2 compared to C_3F_8[19]

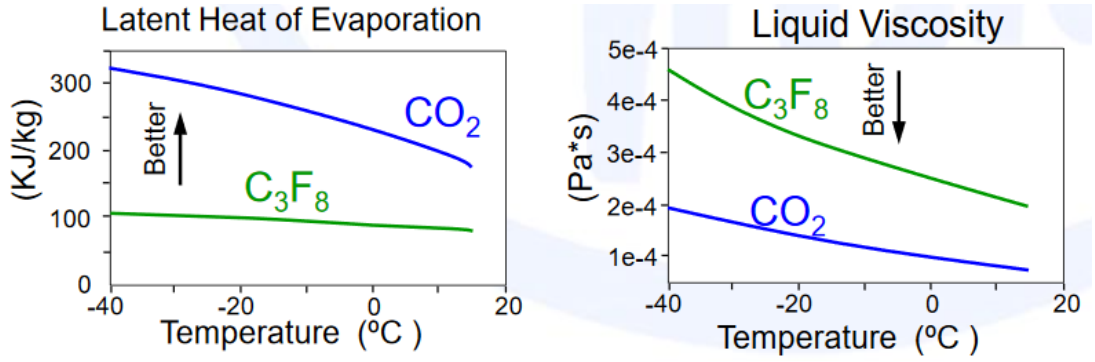

Figure 2.7: Properties of CO_2 compared with C_3F_8[19].

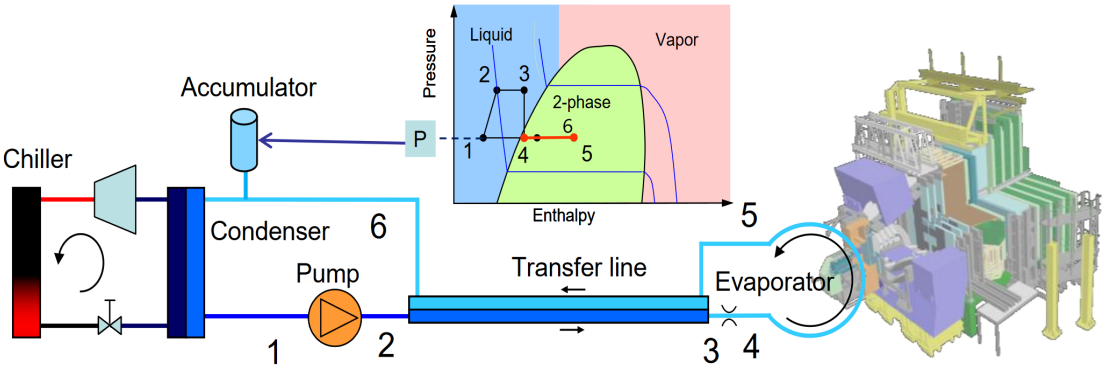

Figure 2.8: 2PACL system diagram [20]

2.4 Two-phase accumulator controlled loop

The 2PACL cycle (Fig 2.8) is an evaporative, bi-phase, mechanically pumped cooling system that allows accurate control of the evaporator temperature at long distance [19]. This cycle relies on the latent heat of evaporation to absorb the energy in the evaporator. This ensures that, as long as there is two-phase flow in the return line, the evaporator temperature will be the same as the boiling point of the liquid.

To ensure that the fluid boils in the evaporator, there must be a low pressure drop in the return line and the fluid must be saturated when it enters the evaporator. The pressure drop is minimised by using larger return lines with as few restrictions as possible. Saturation is achieved by adding a restriction just before the evaporator and allowing heat transfer between the liquid and two-phase flows in the transfer line.

The liquid's boiling point can be controlled by changing the pressure in the return line. This allows the evaporator's temperature to be accurately controlled over long distances by adding an accumulator, shown in Figure 2.8, to the return line. The accumulator pressure is controlled by evaporating or condensing the fluid inside it.

The cycle can operate at wide pressure ranges and is independent of heat load or condenser temperature. The only parameter that must be accurately controlled to maintain an accurate evaporator temperature is the accumulator pressure [21].

2.4.1 Accumulator control methods

The key function of the accumulator is to control the saturation temperature of the fluid through the pressure of the system. Jan van Gerner and Braaksma [22] describes the two types of pressure control accumulators that are possible; Pressure Controlled Accumulator (PCA) and Heat Controlled Accumulator (HCA).

Pressure controlled accumulator

In a PCA the accumulator volume is changed mechanically by an external force. Often this type of accumulator is comprised of a single pressure vessel separated by a flexible membrane. One chamber contains the working fluid of the system and the other an inert gas such as Nitrogen or Argon. Regulating the pressure of this second chamber controls the system pressure.

The main advantage is the fast response time. The disadvantages are that it adds additional complexity and may require the management of a consumable pressure source. Additionally, the membrane must be carefully managed to not exceed its maximum deformation during pressure changes.

Heat controlled accumulator

A HCA is a constant volume chamber which uses the density difference between the liquid and gas phases of the fluid to change the pressure, by heating or cooling the fluid as required. This is advantageous because it is simple and in a cooling application the needed hardware will already exist; however, it is limited by the cooling or heating power available which can slow the response.

2.4.2 Temperature variation

In two-phase cooling systems, the most significant heat inputs to the accumulator are required during load power changes. During these changes, the void fraction of the return line will change, which will change the density of the cooling loop. To restore equilibrium mass will move between the accumulator and the cooling loop, which the pressure control system will have to accommodate.

The disturbance can be accommodated by increasing the accumulator-to-plant volume ratio, as this will reduce the deviation [22]. If physical space or refrigerant mass is of little concern this is an effective way of physically aiding disturbance rejection. Alternatively, increasing the power available to the controller improves performance at the cost of energy.

2.4.3 Integrated two-phase accumulator controlled loop

The I2PACL is an evolution on the 2PACL cycle, simplifying the original concept. A traditional 2PACL system requires both heating and cooling of the accumulator to raise and lower the pressure. The accumulator needs a connection to the chiller and backup chiller for it to function properly, not shown in Fig 2.8.

In an I2PACL system the sub-cooled liquid is pumped through a heat exchanger inside the accumulator before it flows to the transfer lines, as shown in Figure 2.9 [23]. This removes energy from the accumulator, similar to the heat exchanged in the transfer line between points 2, 3 and 5, 6 in Figure 2.8.

The constant cooling can be negated by continuously running the accumulator heaters to reach net zero heat input to the vessel. This enables the system

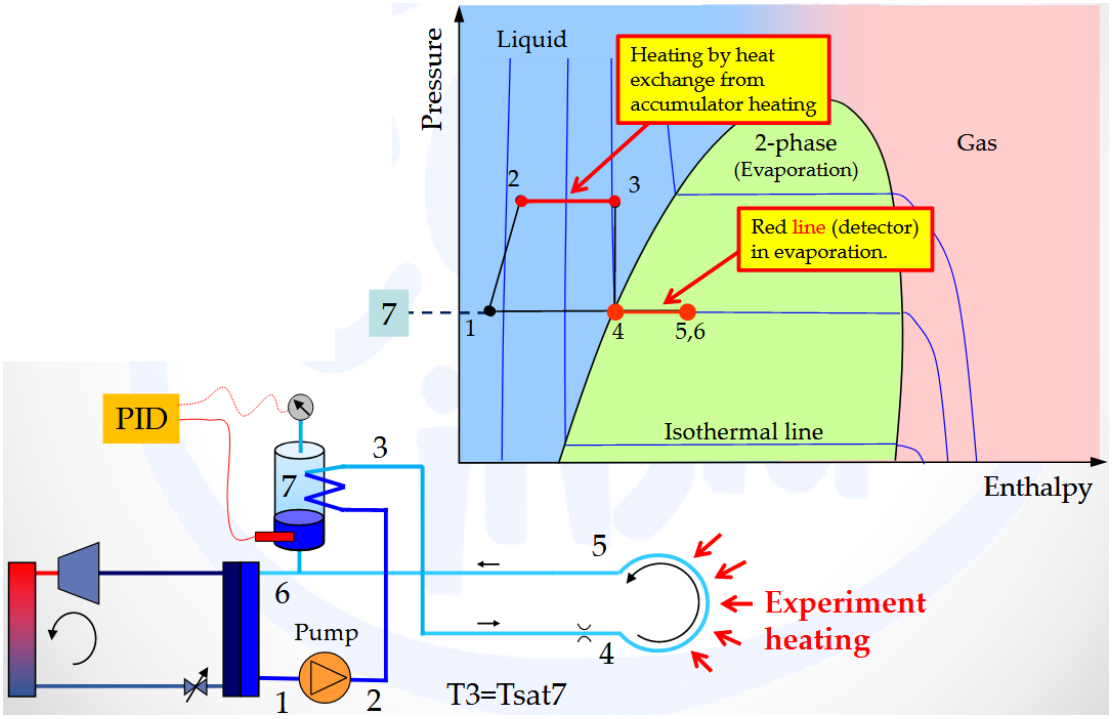

Figure 2.9: I2PACL cycle [24]

pressure to be regulated with one controller and one actuator. The system is simplified: the chiller has fewer evaporators to supply; the accumulator only requires a single heat exchanger; the control system has a reduced number of objects and complexity of controllers. This is inefficient as the fluid is both heated and cooled before reaching the evaporator; however, in this context, it is tolerable to achieve consistent cooling. The group is investigating designs which could eliminate the need for this for future development.

Additionally, the heat exchanger in the accumulator removes the sub-cooling from the liquid CO_2. For evaporative cooling to perform well, the liquid needs to be saturated when it reaches the evaporator. In a traditional 2PACL system this occurs in the concentric transfer line; however, in systems with short transfer the line may not fully saturate the liquid. In this case, the I2PACL system does this before the liquid enters the transfer line.

Knowing the maximum power output of the detector the flow rate is set to achieve a maximum vapour quality of 30%. This ensures that the evaporator will not dry out. Typically, a flow of $10\,\mathrm{g\,s^{-1}\,kW^{-1}}$ is required to ensure the return line remains in two-phase flow.

Chapter 3

Fluid system

This chapter details the changes to the fluid systems that were necessary to optimise the fluid process for the test facility application. The backup pump, primary and secondary chillers and their associated hardware were removed. The accumulators were moved to a new position to reduce the height so they would fit in the new building constructed outside the Building 154 clean room.

To meet the performance requirements the CO_2 systems must be able to deliver a mass flow rate of up to $15\,\mathrm{g\,s^{-1}}$ to the detector. There also must be enough heat transfer between the supply and return flows to ensure that the supply is saturated when it arrives at the heat load.

A new air-cooled chiller was designed, ordered and installed. The I2PACL operating mode was added to improve its versatility. The local boxes were designed to allow the simple connection and disconnection of experiments from the system.

After discussing these changes with the stakeholders involved in the project a new P&ID was produced using the current naming conventions of the group. The full design can be found in Appendix A.

3.1 VELO cooling system hardware

Figure 3.1 shows the block diagram of the original cooling system. Only the cooling plant was brought back to the lab with all components beyond the connections to the transfer line not being included in the redesign. Within the cooling plant, the chillers were recycled because water cooling is inconvenient for surface operation. These will be replaced with a single air-cooled chiller. The backup pump and its associated pipes were removed. This created a simplified architecture with two independent CO_2 systems interconnected only by manual valves for mechanical support and servicing.

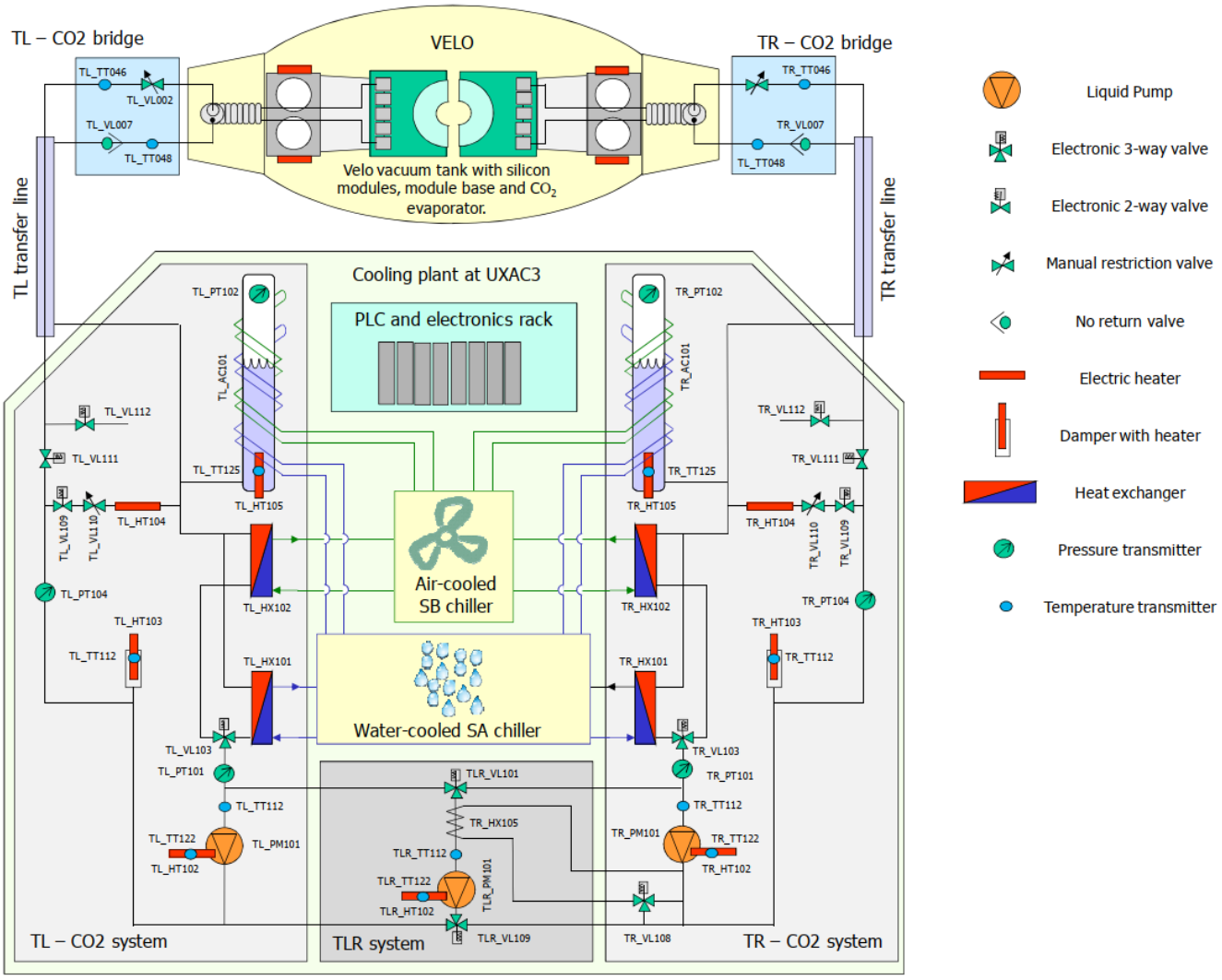

Figure 3.1: VTCS tertiary system block diagram [17]

3.2 CO_2 subsystem

The most significant change to the CO_2 system was the addition of the I2PACL operating mode. This was made possible by re-purposing the heat exchanger in the accumulator previously used by the backup chiller, HX1a10 in Fig. 3.2. The operator can enable this mode when required. The naming convention is described in Appendix C.

This mode can allow improved performance at higher operating temperatures due to the increased supply line heat exchange area. It does have limitations as the design was not initially intended to operate in this mode. The limitations can be explored using the energy balance of the accumulator.

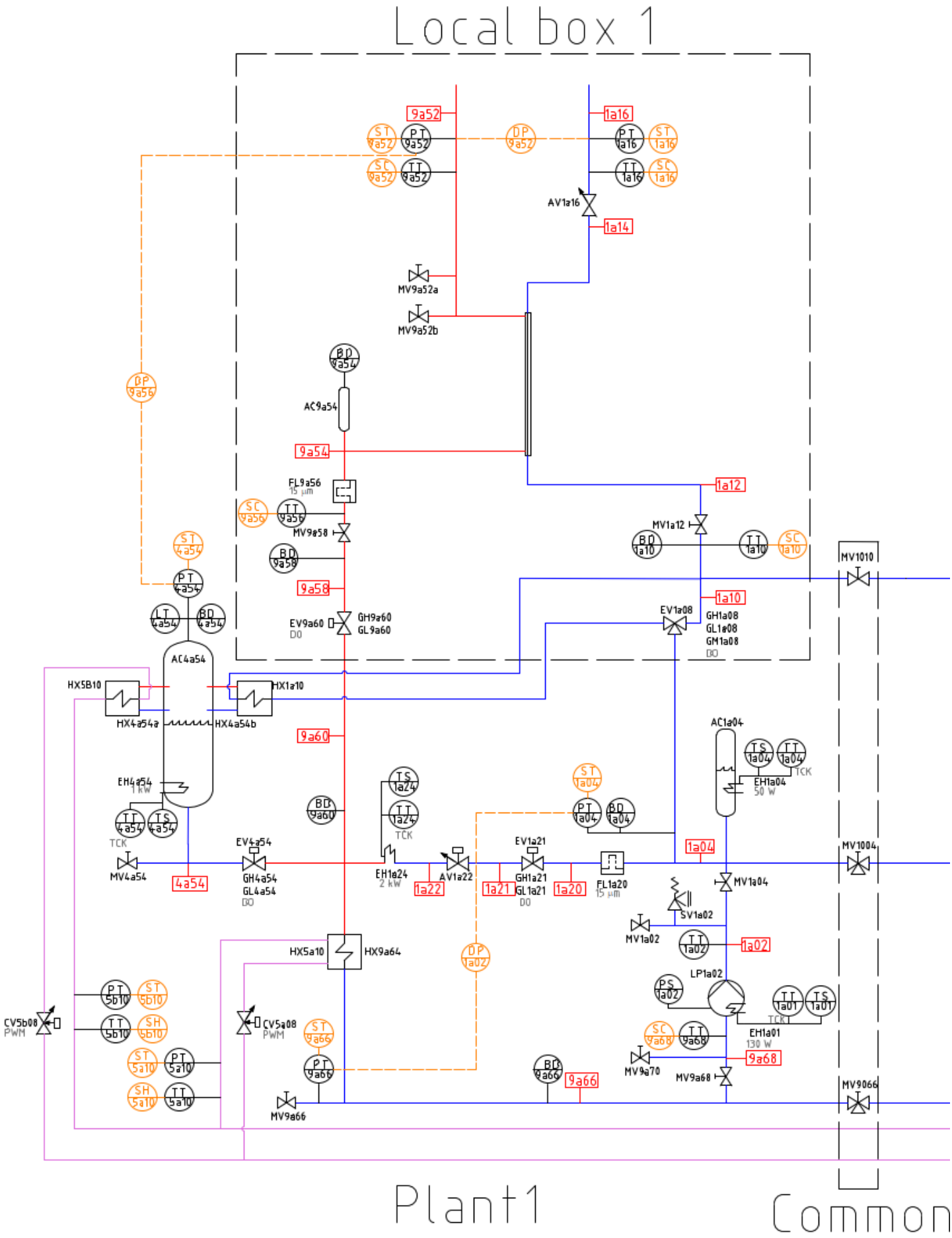

Figure 3.2: 2PACL P&ID diagram

3.2.1 I2PACL performance

To simplify the calculation, heat leak will be considered negligible. This is a reasonable assumption as the vessel is well insulated with Armaflex foam insulation and, in this case, heat leak will enhance performance in I2PACL mode providing a worst-case result. This is because energy is exchanged between the sub-cooled liquid exiting the pumps and the saturated two-phase accumulator. To hold the set point the energy removed from this system must be added by the heater, described in Equation 3.1.

$$P_H = \frac{\delta Q}{\delta t} = c\dot{m}\Delta h \tag{3.1}$$

The accumulators have 1 kW heaters which is the limiting factor for high-temperature operation. The Light Use Cooling Apparatus for Surface Zones (LUCASZ) systems built by the section have 3 kW heaters and have a maximum flow rate of $14\,\mathrm{g\,s^{-1}}$. They reach their heater limitation at 18 °C [24]. The default pump stroke is 7 mm which produces a nominal flow of $10\,\mathrm{g\,s^{-1}}$ at low temperatures. The flow can be up to $22\,\mathrm{g\,s^{-1}}$ depending on the temperature and stroke, as shown in Figure 3.3.

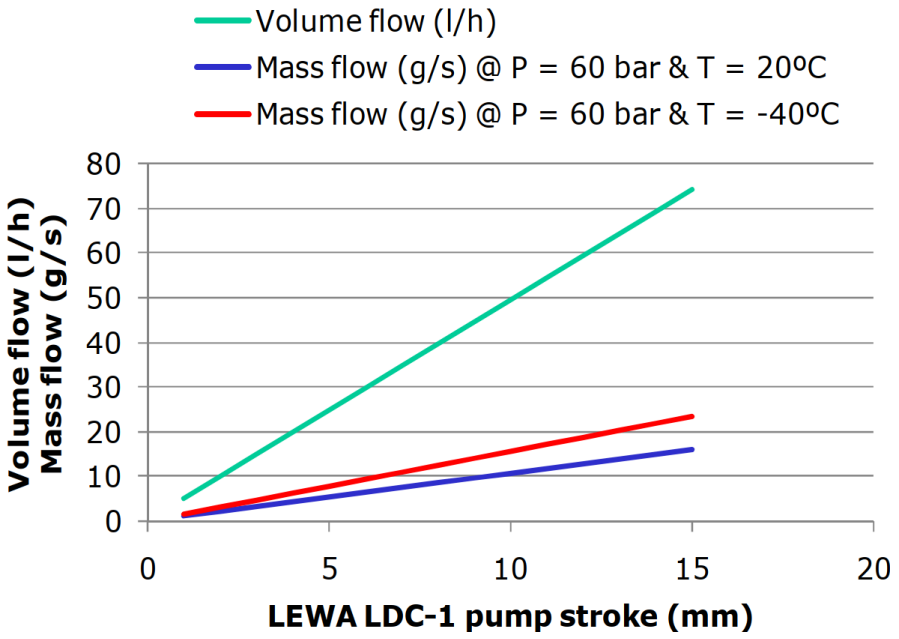

Figure 3.3: VELO pump performance [17]

Figure 3.4 shows the heater power required to maintain a stable set point at different mass flow rates. At the nominal operating flow rate of $10\,\mathrm{g\,s^{-1}}$ the heater saturates at a set point of 10 degrees. This excludes warm running from the I2PACL mode. At colder temperatures, it may improve the controller's performance as it can operate in heating mode only.

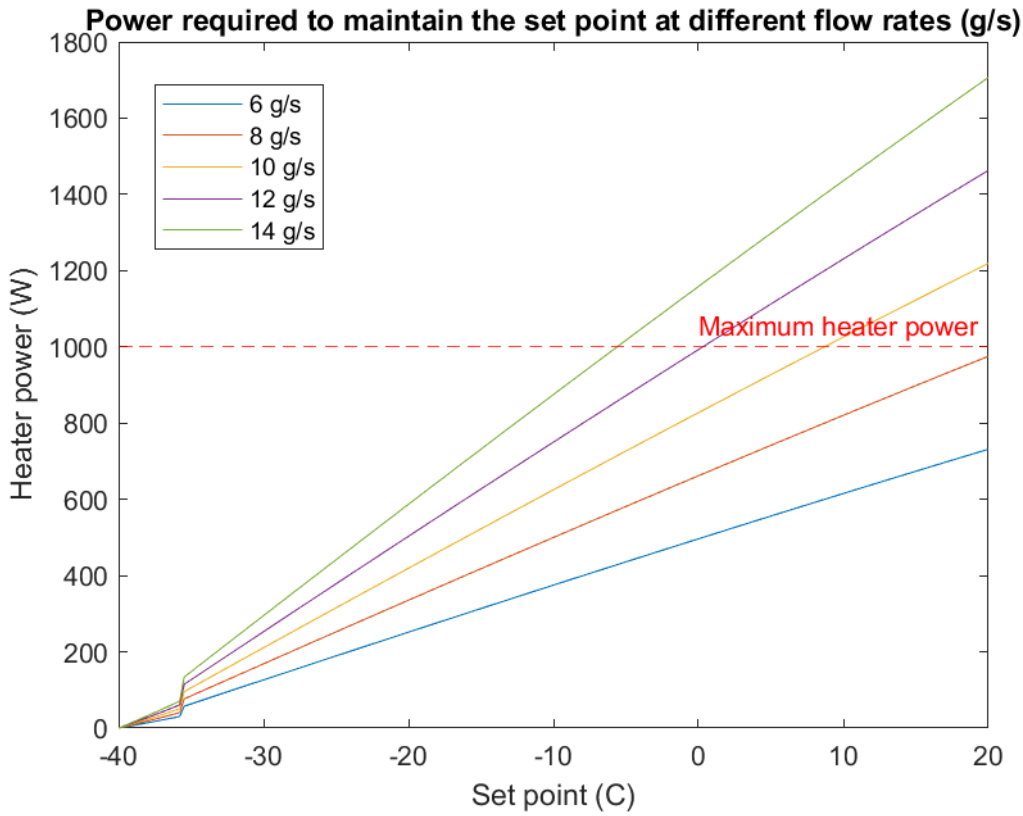

Figure 3.4: I2PACL limits due to heater power

3.2.2 Local boxes

The local boxes are the termination point to which the device that requires cooling can be connected. It is designed to be manually operated by the user with the required steps being monitored by the PLC to ensure the procedure is safely followed before the system can allow CO_2 supply to begin. The transfer line will bring the CO_2 supply through the wall into the building. The only components accessible to the user are those beyond the transfer line, the others are located in the plant but are part of the local box process.

3.2.3 Accumulators

The accumulators have been moved to make the system more compact. They were previously mounted at the top of the CO_2 skid and were significantly taller than the rest of the system. In the new design, they will be moved to the Chiller skid, shown in Figure 3.5. They will be mounted to the frame using pipe clamps rather than metal brackets. This will make the insulation of the system simpler because the pipes at the bottom of the accumulator are more exposed. It should also improve the thermal isolation of the system because the brackets are insulated with a rubber insert so no metal components will be in direct contact with the accumulator body.

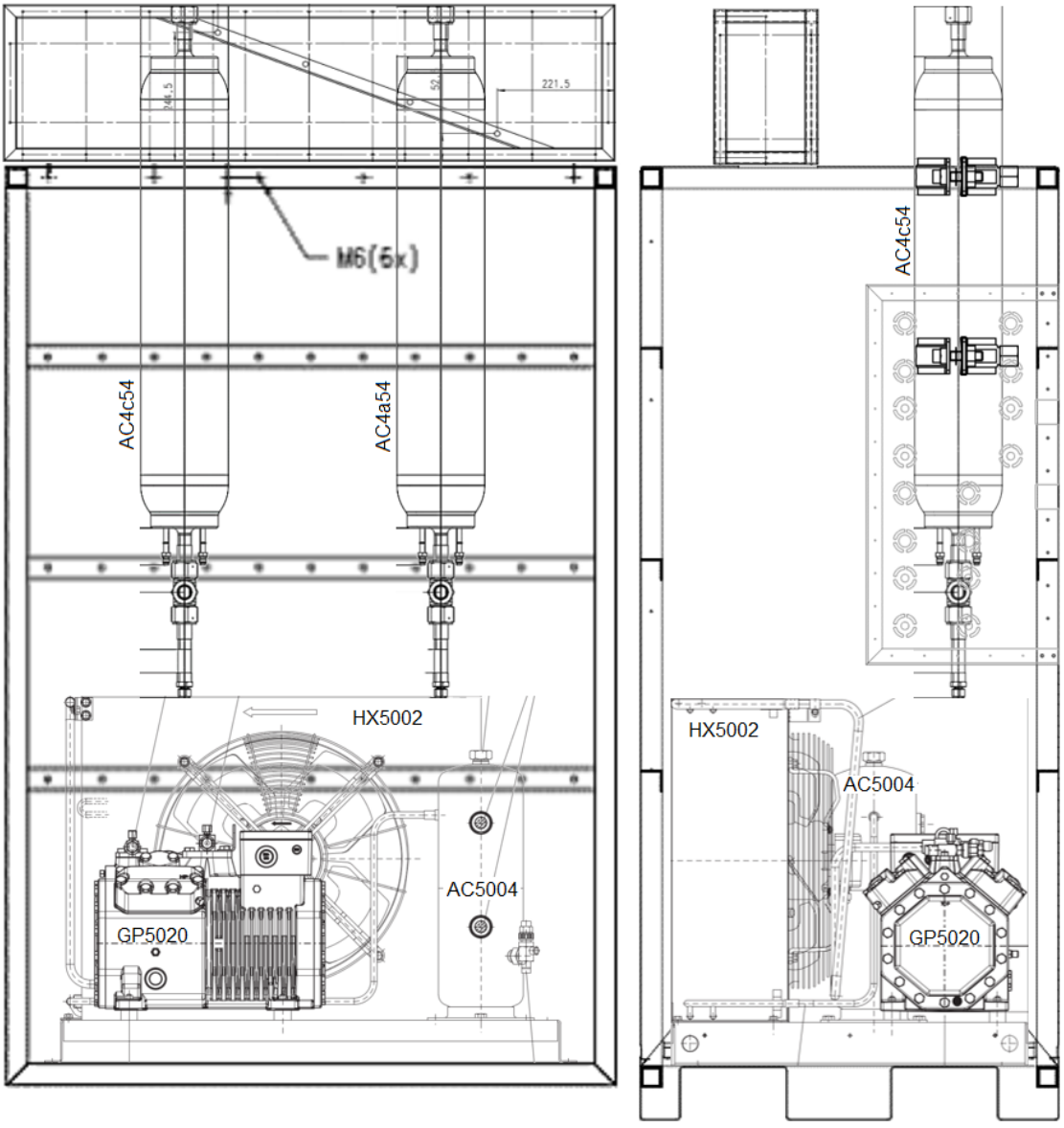

Figure 3.5: New chiller rack design showing the back (L) and right (R) views

3.3 Chiller

The new chiller is based on the LUCASZ chiller [24]. The Bitzer LH84E/4CES-6(Y) air-cooled compressor unit was selected for the new chiller because it is the model that provides the highest performance while still being small enough to fit into the frame of the system. This unit contains the compressor, condenser, condenser fan and refrigerant accumulator, as shown in Figure 3.6. It has a rated cooling power of 3.15 kW with R449A.

The chiller will include a hot gas bypass and cold liquid injection for safety and performance. This is atypical for refrigeration systems which are generally designed for fixed loads. This solution allows the chiller to run normally at a wide range of heat loads. These valves control the compressor inlet temperature and superheating independently of the load on the system. This is important to this system because each 2PACL system can operate independently and at varying heat loads which the chiller must be able to adapt to.

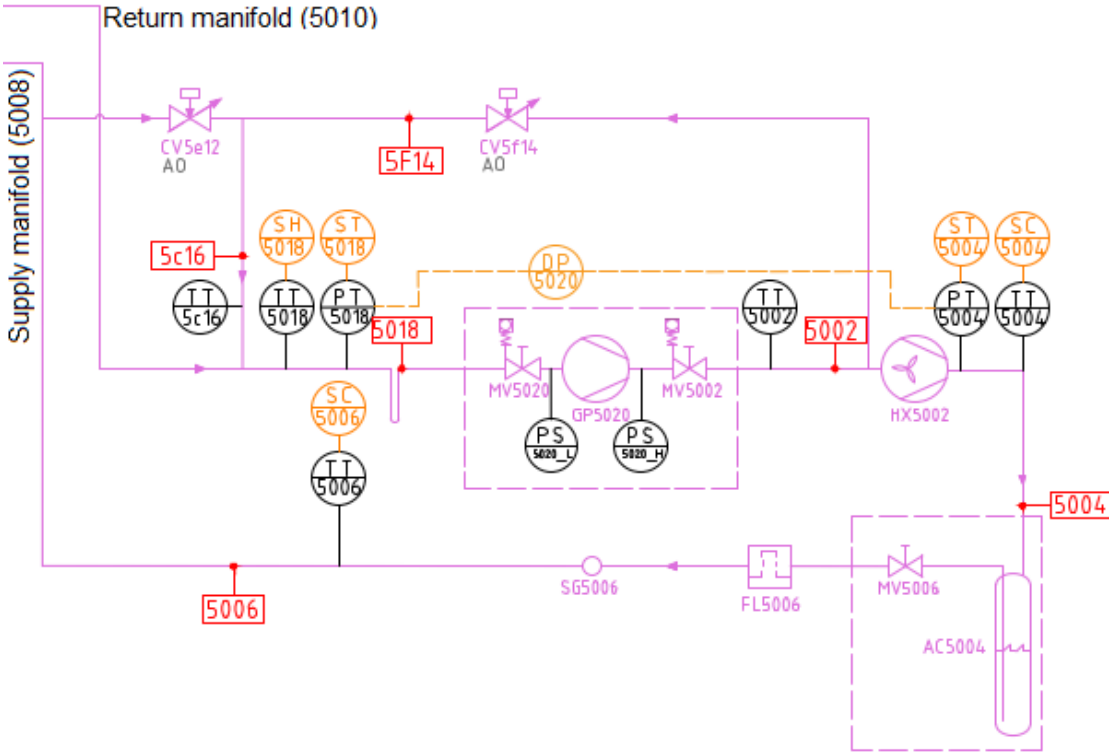

Figure 3.6: Chiller P&ID diagram

3.4 Commissioning

The system has a maximum operating pressure of 70 bar to avoid reaching the critical point and a maximum design pressure of 100 bar. The system must pass a proof test conducted by CERN's Department of Health and Safety before it can be put into operation.

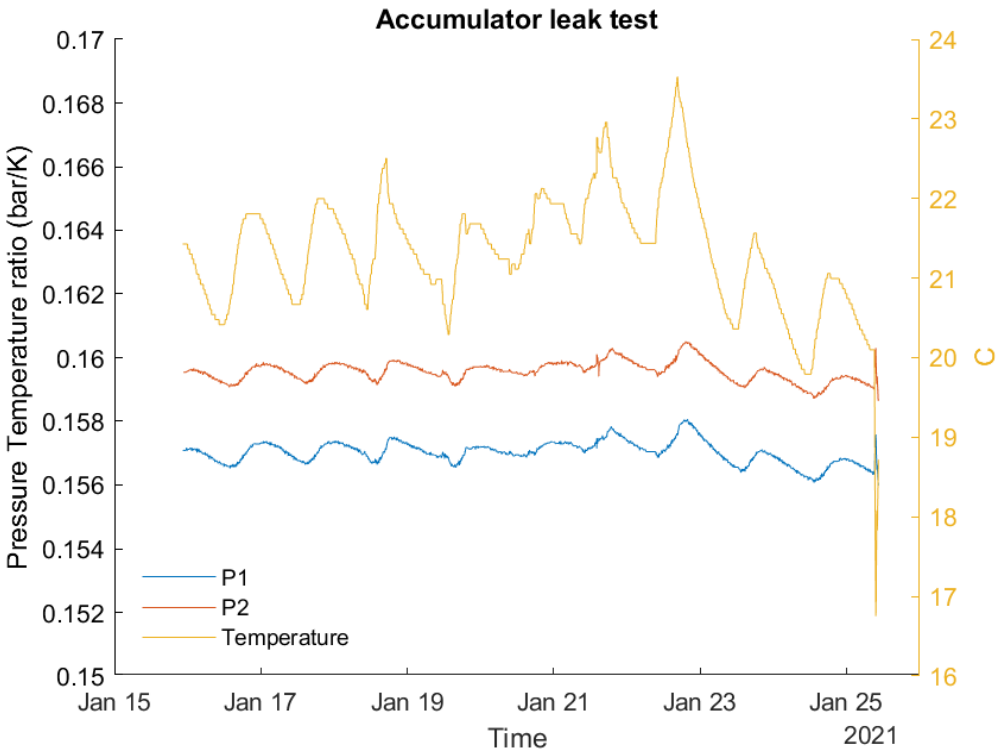

Figure 3.7: Leak test data for the accumulators

3.4.1 Leak tests

Leak detection is done using the ideal gas law in the form shown in Equation 3.2. In this case, the volume (V) is constant; therefore, any change in the pressure-temperature ratio indicates a change in the mass of gas contained within the volume under test. Leaks were sourced using a CO_2 sniffer and soap solution. They were commonly caused by faulty components or connections which were not fully tightened. Leak tests are always done after any new fitting is added.

$$n = \frac{PV}{RT} \tag{3.2}$$

3.4.2 Proof test

Pressure equipment with new welds needs to be proof tested by CERN safety officials before being operated. This test is supervised and uses argon to create pressures over 140 bar to ensure that all the welds can withstand the designed pressures. All safety valves and burst disks are capped during this test.

3.5 Conclusion

The updated fluid design provides a simpler platform which is more suited to surface operation and provides more flexibility to the user when choosing how

to configure the system for the operating conditions. The new chiller meets the power requirement and can run continuously with varying heat loads placed upon it for constant availability.

Each CO_2 subsystem can operate fully independently of each other giving the test team more flexibility. The Lewa pumps can reach the maximum flow requirement even at warm temperatures. This was accomplished while also minimising the changes which needed to be made, reducing the complexity and cost of the project. The Local Boxes allow the experiments to be isolated and changed with low charge loss and without needing significant training.

Chapter 4

Electrical system

This chapter discusses the design of the electrical cabinet and safety systems. To remain within the project budget the reuse of recovered hardware and existing spare stock was prioritised over purchasing new hardware. I developed a part list based on the specification of devices that needed to be powered on the P&ID. The recovered components and spare stock were assessed and as many suitable components that could be found were reserved for this build. Any components which remained outstanding were ordered from suppliers.

The new schematics were drawn in AutoCAD Electrical according to the department's conventions described in Appendix C and D. The schematics can be found in Appendix A. The electrical system was assembled and tested according to the applicable French and Swiss national standards.

4.1 Existing hardware

First, I removed and inspected all the existing hardware. No formal electrical schematics existed; however, there were some system block diagrams and electrical drawings of specific components which could be used for reference purposes, see Appendix B.

The inspection revealed that significant changes would be required to bring the existing system up to the department's conventions. We decided that a new panel would be built according to new schematics to remove any uncertainty in the old wiring.

4.1.1 Electrical boxes

The system used the older system of mounting the components in a drawer mounted in the rack, shown in Figure 4.1. Cables plugged into connectors mounted on the back of the drawer.

This system makes inspection, intervention and maintenance difficult as the

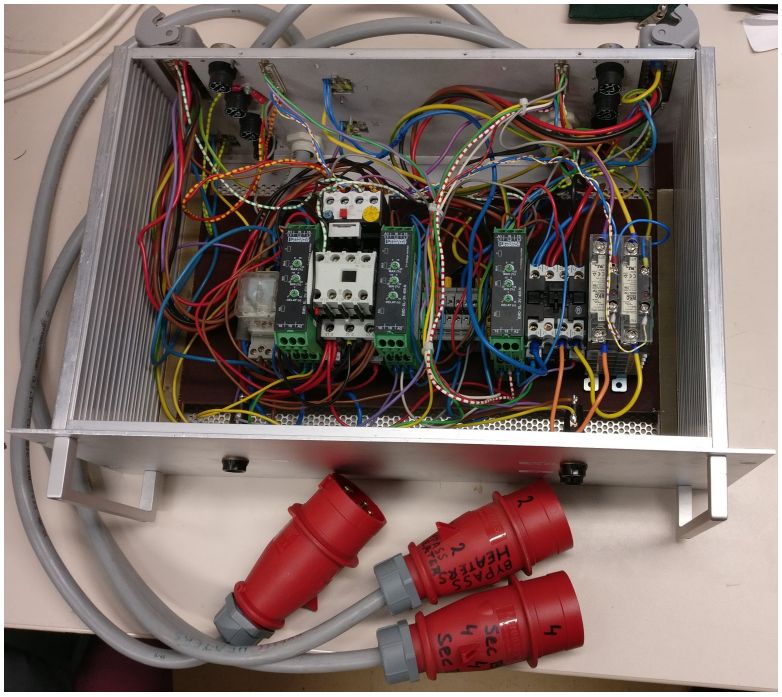

Figure 4.1: A rack-mounted power distribution drawer

components cannot be accessed without disconnecting and removing a box from the rack. These boxes will be reused elsewhere in the group and a new electrical panel was built with DIN rails on sheet metal which was mounted vertically in the mid-plane of the electrical cabinet.

4.1.2 Programmable logic controller

The PLC is a Siemens S7-400 model with additional cards providing Proportional Integral Derivative (PID) control, RS-232 and industrial ethernet features. The new design requires some analogue output channels on the FM 455 PID controller card; however, it is not compatible with UNICOS. The FM 455 was replaced with an Analogue Output module provided by another department.

The S7-400 product family is nearing the end of its life and CERN's Industrial Control Systems (BE-ICS) group has announced the end of support for the family. Upgrading to the replacement product, the S7-1500, was considered; however, it was too costly for a negligible performance improvement.

4.1.3 Human machine interface

The PLC was connected to a human-machine interface (HMI) touchscreen which will not be used as it is not compatible with the WinCC OA SCADA system. Instead, the system is controlled remotely by connecting to the DT group's SCADA server.

4.1.4 HAPTAS

HAPTAS is a purpose-built data acquisition system designed by the Dutch National Institute for Subatomic Physics (NIKHEF), which enables many resistive temperature sensors to be read over an RS-232 connection reducing the required number of PLC input channels. It was used previously but is incompatible with UNICOS, and the simplified system has fewer sensors which can be read directly by the PLC. It is thus not being used in the new system.

4.2 Component specification

To appropriately select the electrical hardware the nominal operating currents of each component was identified. From this, the specific capabilities of each component were extracted.

4.2.1 Power distribution

A single 440 V four-wire three-phase with neutral connection is used to power the system. The three-phase supply is used to power the motors. All other devices are single-phase, powered from individual phases split internally. The best practice when working with three-phase power is to balance the current between the phases as far as practical.

The system power requirements were analysed to balance phase distribution and size of wires and components. The nominal current consumption of all the devices is shown in Table 4.1 and the rating of the circuit breaker protecting them is shown in Table 4.2.

The circuit breaker ratings are chosen based on the rated current that the device draws and the inrush current that may occur when the device is switched on. The inrush current should not exceed the Type C performance curve shown in Figure 4.2.

The combined circuit breaker rating is used to determine the maximum current that the system must safely handle. This is used to size the main incoming wires and main disconnect switch at 63 A.

4.2.2 Safety systems

The design must comply with CERN's standards and industry norms to ensure there is no risk to the hardware or the operators.

Circuit breakers

Thermal-magnetic circuit breakers must be used for overcurrent protection. This device can be tripped by both a bimetallic switch and a solenoid. The solenoid trips the circuit breaker when there is a large, rapid increase in current through

Table 4.1: Nominal current consumption of each component

Device	L1 (A)	L2 (A)	L3 (A)
24V DC	1.04	-	-
PLC power supply	-	-	0.50
Cabinet Fan	-	0.33	-
24V AC	-	0.30	-
Level Transmitter	-	0.20	-
Pump 1	2.62	2.62	2.62
Pump 2	2.62	2.62	2.62
EH1a01	-	0.57	-
EH1a04	-	0.22	-
EH1a24	8.70	-	-
EH4a54	-	-	4.35 -
EH1c01	-	0.22	-
EH1c04	-	0.22	-
EH1c24	-	-	8.70
EH4c54	4.35	-	-
Compressor	17.7	17.7	17.7
Condenser Fan	-	1.50	
Voltage monitor	0.05	0.05	0.05
Total	37.07	26.88	36.53

Table 4.2: Protection rating for each component

Device	L1 (A)	L2 (A)	L3 (A)
24V DC	10.00		
PLC			6.00
Cabinet Fan		2.00	
24V AC		1.00	
Level Transmitter		2.00	
Pump 1	3.20	3.20	3.20
Pump 2	3.20	3.20	3.20
Heaters 1	10.00	10.00	10.00
Heaters 2	10.00	10.00	10.00
Compressor	18.00	18.00	18.00
Condenser Fan		4.00	
Voltage monitor	1.00	1.00	1.00
Total	55.40	54.40	51.40

the device. The bimetallic switch trips the circuit breaker when there is a smaller, but longer, overload of the protected circuit.

Circuit breakers are rated by their tripping curve. Class B, C and D are for overcurrent protection of cables. Class K protects motors and transformers with simultaneous cable protection. Class Z is for control circuits with high impedance, voltage converter circuits and cable protection. The circuit breakers used in the system are compliant with IEC/EN 60947-2; the standard for low-voltage switchgear for industrial applications. The response curves for these classes are shown in Figure 4.2.

Type C circuit breakers are commonly used for power supplies and resistive or low-inductance devices with standard tripping current ratings. The motor circuit breakers are Type K and are adjustable to allow the tripping point to be set close to the motor's nominal current rating.

Residual current devices

Residual Current Devices (RCDs) are safety devices that monitor the net current flow through a set of conductors. If there is a difference of more than 30 mA, the circuit breaker is tripped to protect anyone who may come into contact with the system. Because the heaters have metal bodies which are connected to the pipes and frame, they are mandatory. In the event of a short, the entire chassis could become live if the protective earth fails.

Motor thermal protection

The pumps and compressor are equipped with Positive Temperature Coefficient (PTC) resistors on the motor windings. These safety devices can shut down the affected motor if the winding overheats. This circuit disconnects the control signal to the motor contactor, ensuring power is removed until the temperature decreases, and sends a signal to the PLC to trigger an alarm on the affected motor.

Heater protection

There are three layers of heater protection in the system to ensure that the system is safe. Two of these layers are logical and the third is a thermal switch attached to the heater body. They trigger at 120 °C, opening the circuit. This removes power from a normally open relay which opens the heater power contactor circuit. Opening the power contactor mechanically removes power from all the heaters safely.

Emergency stop

The safety relay is included in the circuits that control all the power contactors and sends a signal to the PLC. If the emergency stop button is pressed, the relay opens and cuts power to the CO_2 pumps, compressor, condenser fan and heaters.

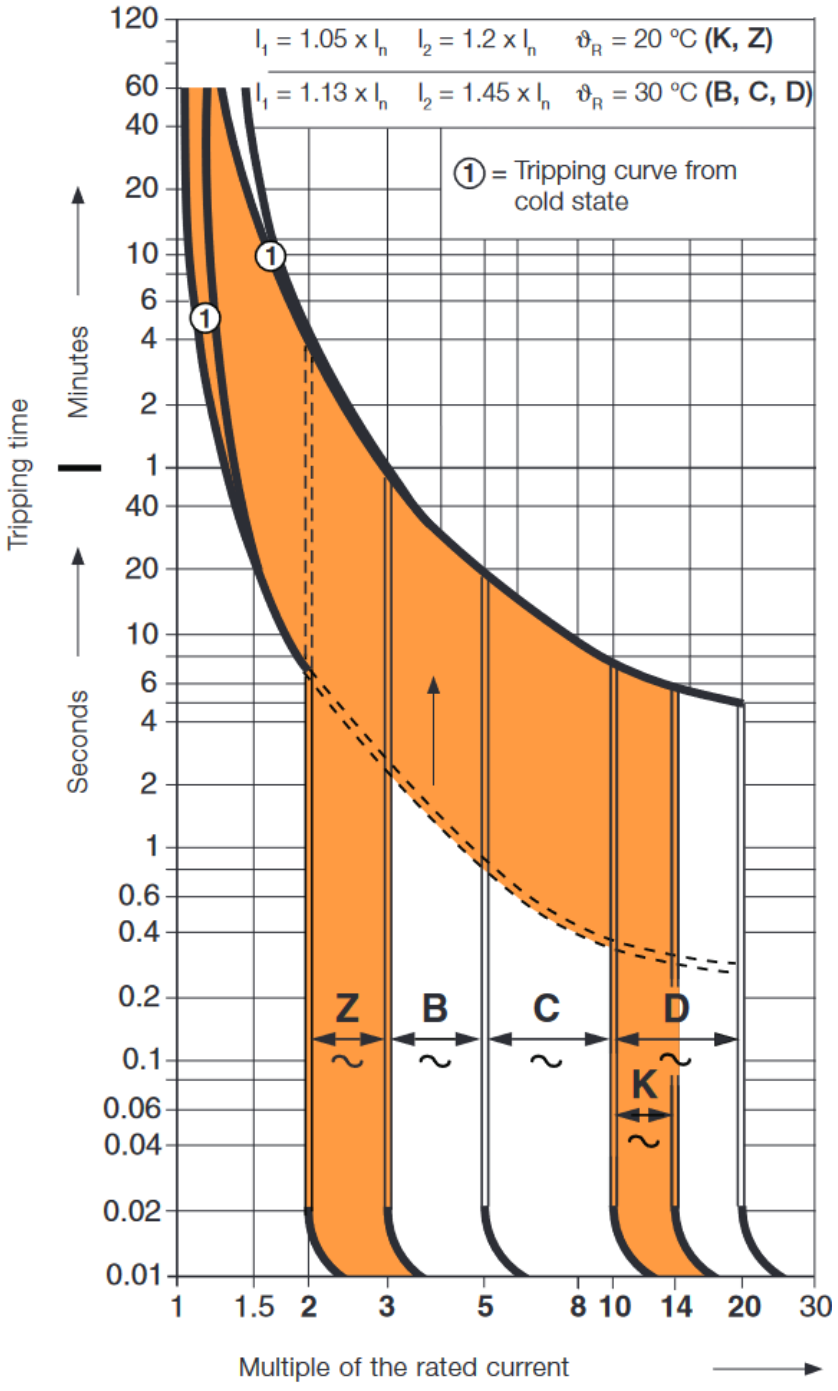

Figure 4.2: Circuit breaker response curves defined by IEC/EN 60898-1 and IEC/EN 60947-2 [25]

The PLC commands all actuators to go to their safe positions and to wait for an operator to assess the problem and reset the safety relay.

4.3 Electrical schematics

After the component selection and design proposal were agreed upon, a detailed electrical design was done in AutoCAD Electrical. This design includes all the information required to assemble the panel including wire colour, wire gauge, terminal numbers, and connection types.

4.3.1 Wire colours

CERN has chosen to use a standard set of colours to indicate a wire's purpose. This allows a visual inspection of an electrical cabinet to reveal potential dangers and aid in debugging and problem-solving. This project uses the standard wire colours with the addition of Violet for 24V AC. The standard colours are shown in Appendix D.

4.3.2 Wire gauge

Wire gauge, given in square millimetres, is selected based on the maximum current a wire will carry before the overcurrent protection is triggered. This ensures that the wire will not fail in the event of a short circuit. The maximum current is dependent on the installation type, ambient temperature, ventilation and wire type. The wire gauge also helps distinguish between signal and power wires, with signal wires typically being less than $1\,\mathrm{mm}^2$ and power wires typically being $1.5\,\mathrm{mm}^2$ or greater. This would be applicable when deciding if a grey wire is a digital output or a phase carrying 230V AC power.

4.4 Construction

Following the decommissioning and analysis of the electrical cabinet, the only reused components were the liquid-level sensor electronics and the PLC. The PLC is installed at the top of the cabinet and was left in place. The liquid level controller has been moved to be directly below the PLC. This keeps the devices that still use the drawer-style system together and visible just above eye level.

This leaves the remaining area of the front side of the rack for the new distribution panel. To make full use of the available area, an aluminium sheet was cut to $500\,\mathrm{mm} \times 1500\,\mathrm{mm}$ to fit in the midplane of the cabinet, just behind the PLC and level controller. This left some space for cables to run over or under the panel to reach the IO blocks and devices on the back of the rack.

The components or their placeholders were placed on the panel with the cable trays and DIN rails to ensure they would fit, as shown in Figure 4.3. The panel

was built, wired and installed in the cabinet, shown in Figure 4.4, by a qualified electrician who works in the department.

4.5 Commissioning

Before the cabinet was connected, it was checked for errors that may have been made during assembly. The first step was a visual inspection to confirm that there were no disconnected or exposed wires and to check that the correct wire colours had been used.

Following this, a multimeter was used to check for short circuits between all three phases, neutral, and ground. All circuit breakers were on for these tests and the other side of normally open contactors were tested separately.

After switching all the circuit breakers off, the system was plugged in and the main switch was turned on. Each circuit breaker was then turned on individually and the device it powers is cross-checked with the electrical schematics. The RCD breakers were tested using the test button on each device to confirm they were working correctly.

4.6 Conclusion

The new electrical design meets the most recent norms and standards applied in the department, including labelling and colours. The components are presented in an open, easily visible format so that the status of the system can be seen at a glance and so servicing can be done safely and reliably. Where possible, both hardware and software interlocks are implemented to provide a redundant layer of operator and machine protection.

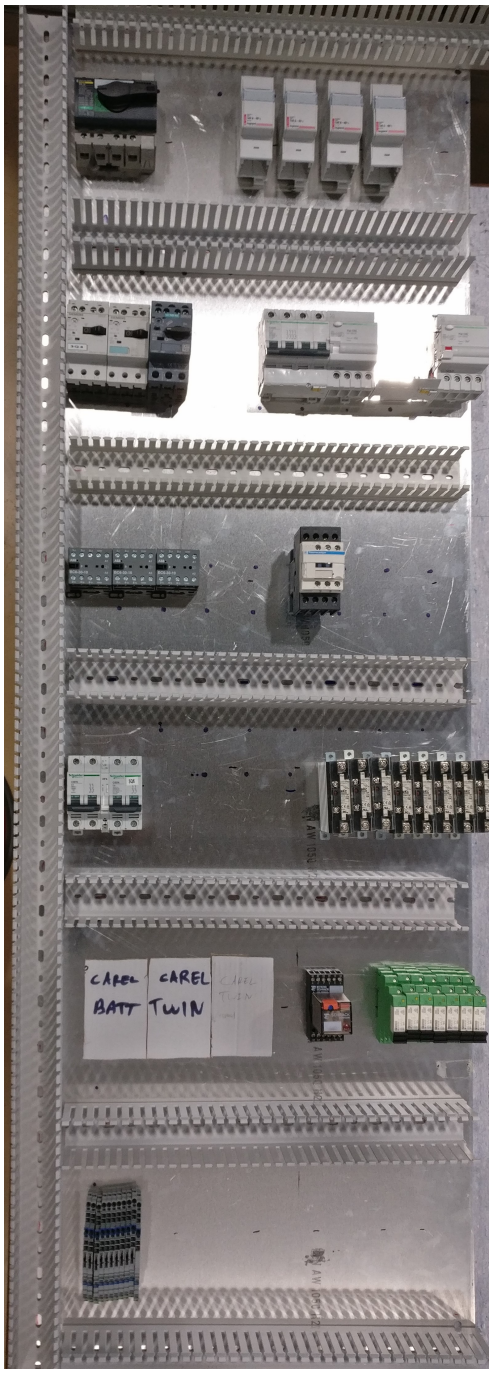

Figure 4.3: Panel mock-up during design

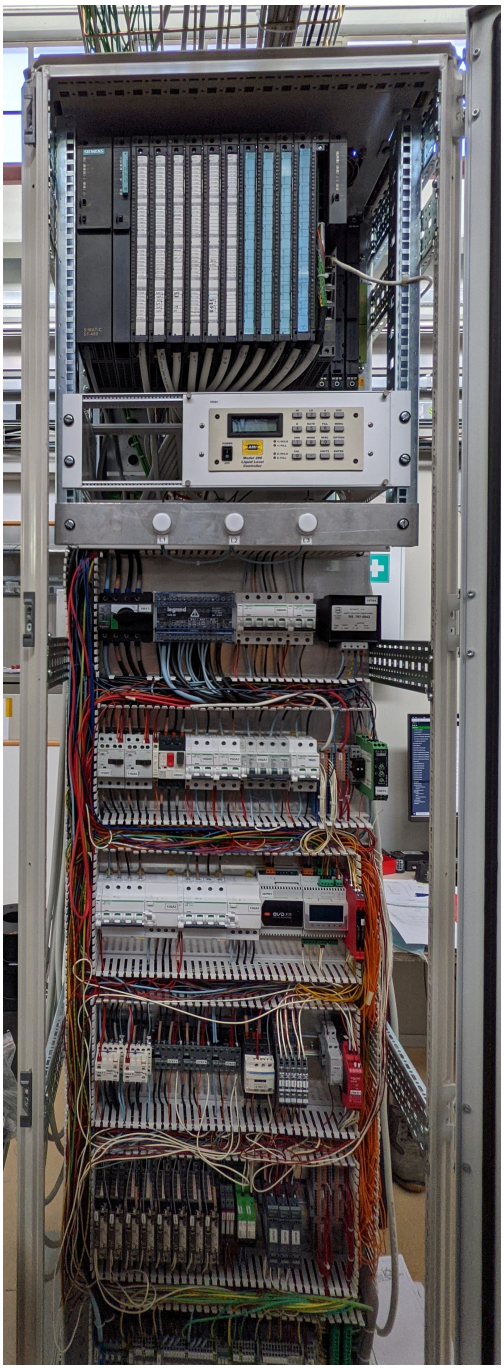

Figure 4.4: Final panel installed in the system

Chapter 5

Control architecture

This chapter shows the development of the control system architecture including networking, security, archiving, data acquisition, system logic and safety. All these aspects must function together to ensure the operator has a clear view of the functionality of each component and protect the operator and hardware from equipment failure.

In the case of networking and security, there are defined processes set out by the IT department that must be followed. In the other cases the configuration for each system and described below.

5.1 Control system architecture

The system is controlled by a Siemens S7-400 PLC which communicates with Siemens WinCC OA for SCADA over the Technical Network (TN). The structure of the system is shown in Figure 5.1.

5.2 Security

Network security is an increasingly important requirement in industrial applications as the internet expands and more devices are capable of connecting to networks. PLCs are particularly attractive and vulnerable targets because they typically control important processes and valuable equipment. Several worms have been discovered that specifically target PLCs, the most infamous being Stuxnet which targeted the Iranian nuclear program [26].

The Computer Security team of the CERN IT department is responsible for centrally monitoring and managing CERN's internal networks. They have several layers of protection for devices that are more vulnerable to attacks. The first layer of security is the main firewall which protects the internal General Purpose Network (GPN) from the public internet. All general-purpose networked devices, such as office computers and printers, are connected to this network.

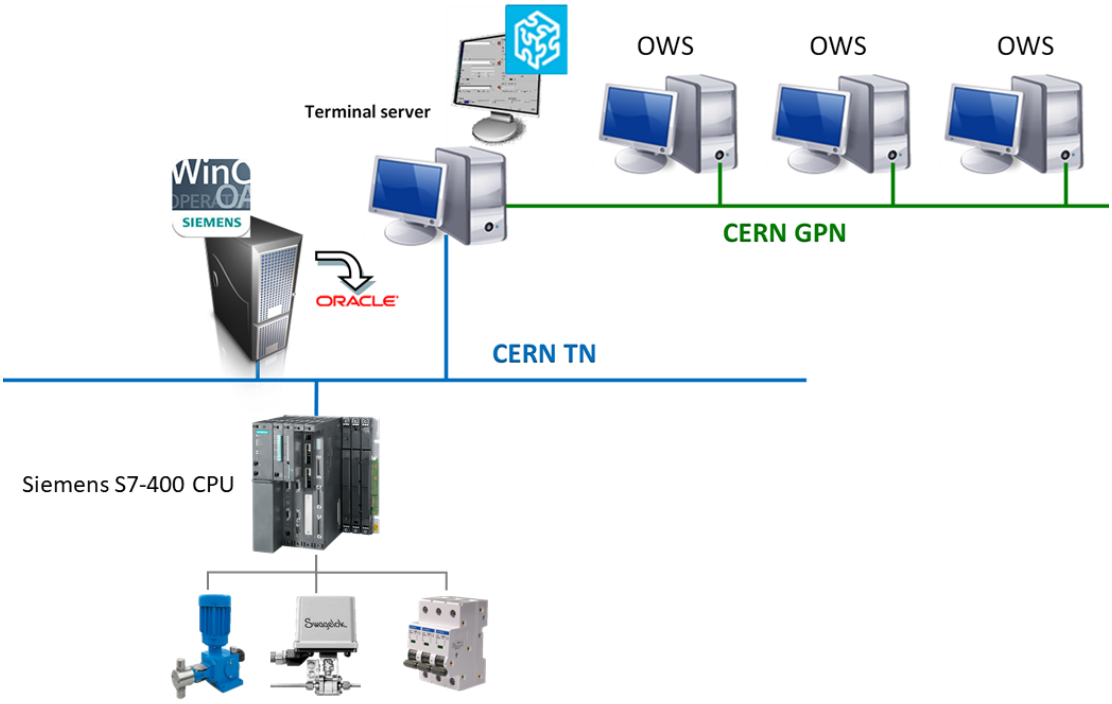

Figure 5.1: Control System Architecture

The TN is connected to the GPN through another firewall run by the terminal server, shown in Figure 5.1. Devices connected to the TN are not permitted to access the GPN or the internet.

Interacting with devices on the TN can only be done from the TN. This is done by connecting remotely to a trusted Virtual Machine in the CERN data centre that is connected to the TN. This way the hardware is secure and under the control of the IT department.

5.3 PLC

The PLC has a central rack back-plane with 15 slots available for cards to be added. The configuration of the system is shown in Table 5.1.

The utilisation of the PLC input channels is shown in Table 5.2. The required number of channels has been reduced with the simplification of the system. The unused channels were kept as spares to guard against card or channel failure. In each IO class apart from the analog output, an entire card can fail and the PLC can be restarted by switching to the spare card while a replacement is found. The S7-400 platform is reaching the end of its life and sourcing replacement parts may become more difficult with time.

Table 5.1: PLC configuration

Card	Number	Description
Power supply	1	Provides power for internal electronics
CPU	1	Stores and runs program data
Digital input	3	32 input channels
Digital output	3	32 output channels
Analog input	4	16×16-bit channels
Analog output	1	8×13-bit channels
Communication	1	Industrial ethernet and Profibus

Table 5.2: PLC IO channels

Type	Used	Total
Digital input	63	96
Digital output	41	96
Analog input	47	64
Analog output	2	8

5.4 UNICOS application

The control application was developed using CERN's Unified Industrial Control System Continuous Process Control version 6 framework (UNICOS CPC6) [27]. It standardises the types and behaviour of standard control objects that are used throughout CERN. UNICOS is used to generate the PLC program and SCADA configuration file so each can be uploaded to the devices. It provides tools that enable automated code generation and is compatible with both Siemens and Schneider PLCs and defines how the PLC and SCADA systems should communicate. After generating the PLC and SCADA code and configuration files it is not used.

This makes developing and maintaining the application much easier and reduces the risk of configuration mistakes. Siemens WinCC OA is deployed on servers to provide the SCADA element of the control system. To apply this framework, the process is broken down into standardised objects.

5.4.1 UNICOS objects

UNICOS programs are made up of four different object classes: IO, field, interface, and control. Each class fulfils a specific role in the program. The full UNICOS documentation is available online at the link in Appendix F.

Input/Output IO objects allow the UNICOS environment to interface with the signals the PLC is receiving and to send signals to the plant. They consist of Analog Input, Analog Input Real, Analog Output, Analog Output Real, Encoder,

Digital Input and Digital Output. They provide data for the other objects to act on.

Interface Interface objects represent items in the PLC's memory. They allow information to be transferred between the PLC and SCADA. Status objects represent data that is sent from the PLC memory to SCADA and can be of analog or word data type. Parameter objects represent data that is sent from SCADA to the PLC and can have digital, analog or word data types.

Field Field objects represent real objects and use field objects to send commands and read the status of the item. They include OnOff, Analog, AnaDig, AnaDO, Local, Mass Flow Controller, and Stepper Motor. These objects are chosen to represent physical devices such as valves, motors and heaters which may combine several interface objects to control.

Control Control objects manage actions in the field according to process logic by driving field objects. They include PCO, Controller, Analog Alarm and Digital Alarm.

5.4.2 Specification file

The spec file is the keystone of a UNICOS project. All the objects are populated in an XML document using a spreadsheet. Each row contains a single object with parameters that are configured in the columns. This file is the input for the UNICOS Application Builder (UAB) bootstrap client which generates the PLC logic, WinCC OA files, and commissioning documents. This ensures that any change made to the spec file is propagated to all other documents at the same time.

5.4.3 Logic templates

The spec file allows project-specific logic to be created through the use of logic templates. They are written in Python and are developed from the standard templates that UAB runs in the code generation section. They automate the generation of logic for commonly used functions and allow specific custom logic to be inserted when needed. For example, repetitive calculations such as sub-cooling and saturation temperature can be written once and then generated automatically at each object where they are needed, as shown in Figure 5.2.

The templates must be written specifically for the brand of PLC that is being used. A Schneider template will not work to generate code for a Siemens PLC. No Siemens templates were available in the group so these were all developed specifically for DTCS. Further details of the template files can be found in Appendix F. The template adds the required prefixes and suffixes for the variable name to be read by the PLC and checks that the inputs are valid. This occurs locally on the machine running the UAB, once the process is complete the PLC program

				LogicDeviceDefinitions CustomLogicParameters	
Parameter1	Parameter2	Parameter3	Parameter4	Parameter5	Parameter6
Subtraction	_P1_PT1a04, CS0d_P1_PT9a66				
SaturationCO2	CS0d_P1_PT1a04				
SaturationCO2	CS0d_P1_PT4a54				
SaturationCO2	CS0d_P1_PT9a66				
Subtraction	_P1_ST9a66, CS0d_P1_TT9a68				
MotorWorkingTimeCalc	CS0d_P1_LP1a02	CS0d_P1_LP1a02_WTr	CS0d_P1_LP1a02_WT		
LimitationDecr	04_OHL_tL, CS0d_P1_TC:	CS0d_P1_TT1a04			
LimitationDecr	4_OHL_tH, CS0d_P1_ST(	CS0d_P1_TT4a54			
LimitationDecr	4_OLL1_tH, CS0d_P1_ST(	CS0d_P1_SC9a68			
LimitationDecr	4_OLL2_tH, CS0d_P1_ST(	CS0d_C0_SH5b10			
MAX	4a54_OLL1, CS0d_P1_ST	4a54_OLL2			

Figure 5.2: Adding customised logic to UNICOS

is created and can be uploaded to the device. The process followed is shown in Figure 5.3

5.4.4 PCO structure

A PCO is a UNICOS process control object which represents a stand-alone unit in the system and can be made up of field objects or other control objects. The PCO structure of the DTCS is shown in Figure 5.4. Each CO_2 system can run independently of the other and will request the Chiller to start or stop as needed. The Local Box PCOs requires that the parent PCO be running before they can operate.

5.5 Safety

5.5.1 Alarms

There are three levels of alarms: 'full stop', 'temporary stop' and 'alarm'. These can be applied to any UNICOS object and will be propagated to other devices based on the hierarchy. Any stop on a parent object will also stop a child object until the alarm is cleared.

To make the alarm pages easier for the operator to understand, alarm groups are created. Figure 5.5 shows the alarm overview panel during the commissioning stage when each alarm was being checked. An alarm group is an alarm object that is activated by a set of other alarms that have a common source, such as temperature or pressure. The groups allow the source of a problem can be quickly identified while simplifying the overview.

From the overview page, the details of each group can be opened to identify the specific cause of the alarm. An example of the alarm page is shown in Figure

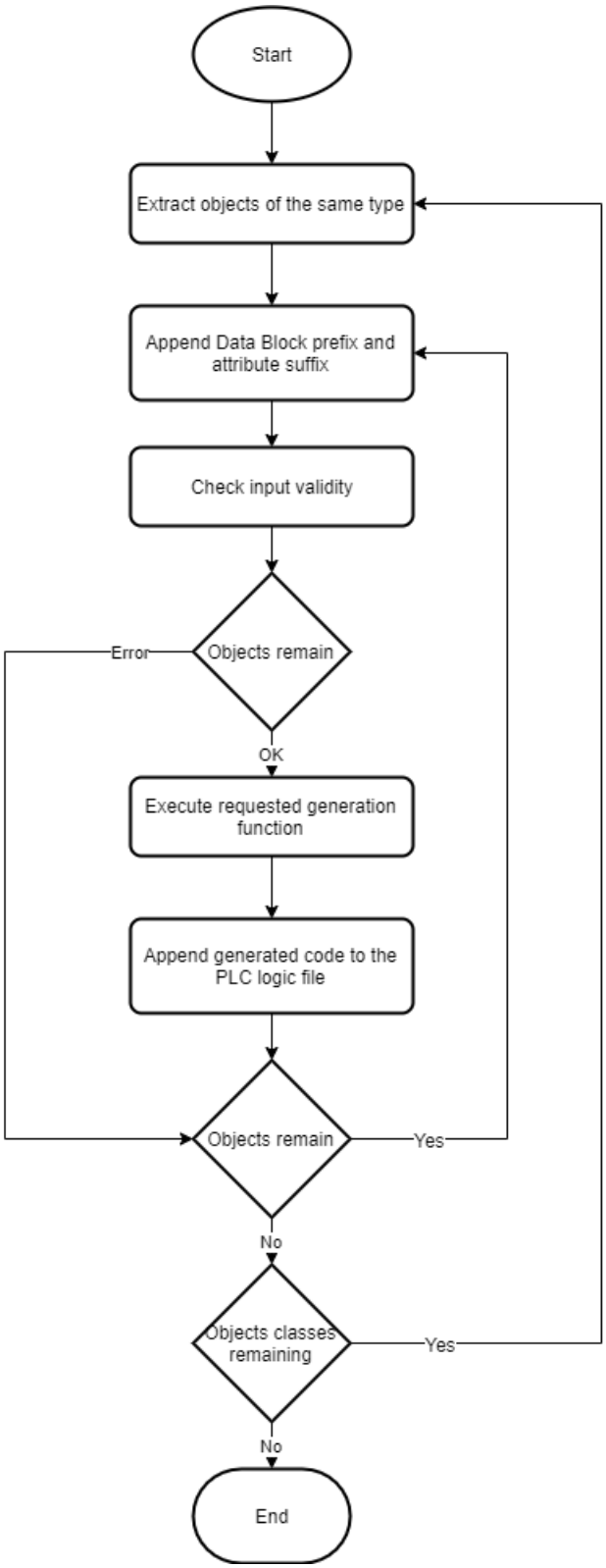

Figure 5.3: Actions performed in the logic template

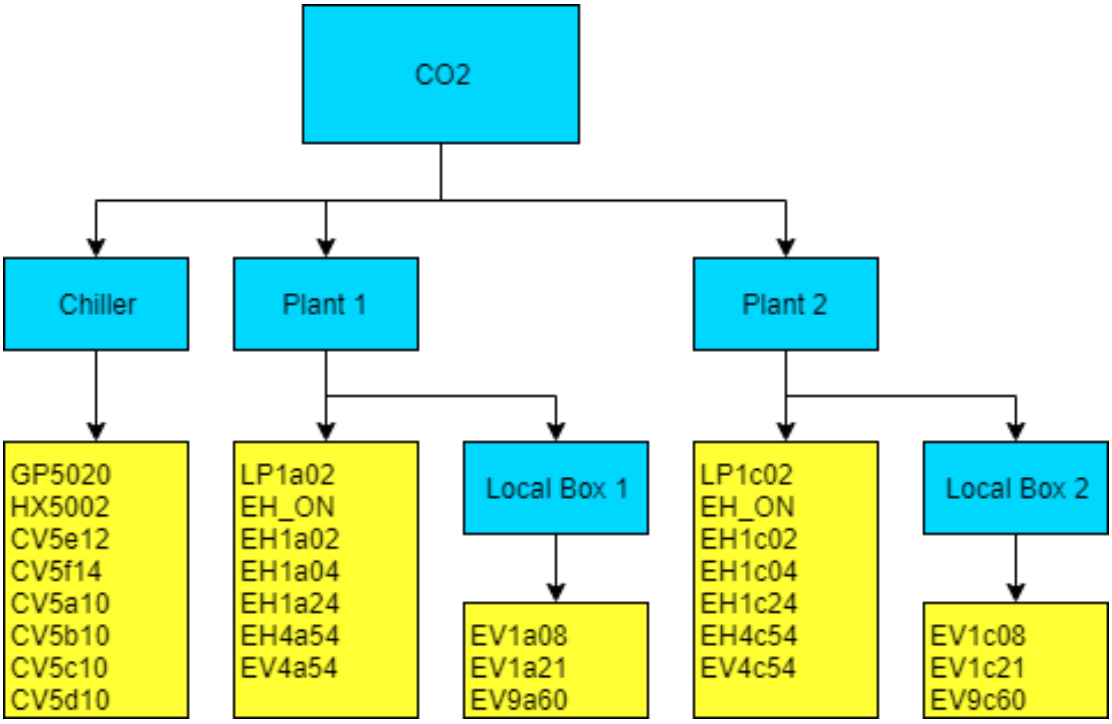

Figure 5.4: DTCS PCO structure

Figure 5.5: Alarm groups for all PCOs

Figure 5.6: Plant 1 Pump alarms

5.6. Significant alarms trigger the full stop group alarm which stops the PCO for safety. Other alarms trigger the warning level alarm to indicate there is an issue but it is not critical.

The full alarm breakdown is written in the Functional Analysis which can be found in Appendix A. In each case, the impact of the failure on the system was analysed and the appropriate action related to the alarm was implemented based on input from the process experts and experience from earlier systems.

5.5.2 Heaters

The heaters of the system could set off a fire or cause the pressure to rise above safe levels which poses a significant hazard. To protect the operators and system from failure or error, the heaters have three levels of safety protection, two logical and one at the hardware level.

1. Each heater has an internal thermocouple which monitors the temperature of the element. This triggers a warning and temporary stop interlock for that heater if the alarm threshold is exceeded.
2. The Any Heater Over Temperature (AHOT) full stop interlock is triggered when any heater is over temperature which will switch off all the heater power contactors in case a wiring fault is causing the wrong heater to be switched off by the first interlock. This alarm has a delayed action so it will

activate if the first alarm does not reduce the temperature.

3. Each heater is fitted with a thermal switch that opens at 120 °C. If this trips it electrically disconnects the input to the heater power contactor without any action from the PLC. This ensures that power is disconnected even if there is faulty logic on the PLC. The PLC also receives the signal that the thermal switch has tripped and triggers a full stop alarm on the PCO.

5.5.3 Output limits

An additional safeguard that is applied for heaters is a dynamic output limit for controllers, as shown in Figure 5.7. The output high or low limit parameter of a controller caps the maximum or minimum output of the controller within that which the actuator is capable of. In this case, as the internal temperature of the heater increases, the maximum output power is decreased to protect the heater.

This principle is also applied to expansion valves to protect the compressor from receiving liquid in the return line. If the super-heating of the return flow drops the maximum opening of the expansion valve is decreased to avoid triggering a full stop alarm.

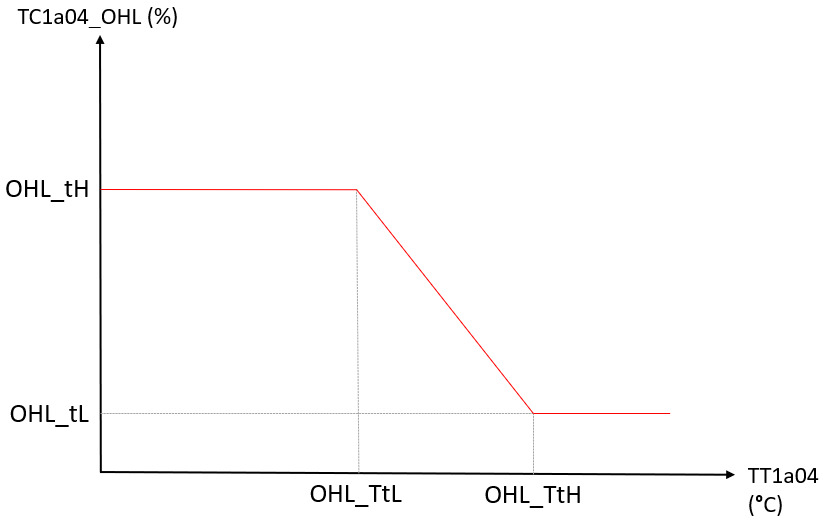

Figure 5.7: TC1a04 Output High Limit function

5.5.4 Trapped liquid

If cold liquid CO_2 is trapped in a line and warms up it will boil, causing an extremely high pressure to build up which may cause the pipe to burst. To protect against this happening, the safe or stopped mode of the system must make sure liquid is not trapped by keeping valves open where possible. Additionally, the sub-cooling at different points in the system is monitored.

5.6 Controllers

The PID controllers implemented in UNICOS have different operating modes which improve their usability when implemented in physical systems. The controller has three operating modes: 'Regulation', 'Tracking', and 'Output Positioning'.

In Regulation mode the controller is active and the output signal is driven by the PID algorithm. In Tracking mode, the output signal is not active due to a manual request on the actuator. The set point tracks the measured value. Output Positioning opens the control loop and sets the actuator to an external position request.

Two primary concerns when designing a controller are its response to a step input change and the response of the set point itself. The response of the controller is discussed in detail in Chapter 7 which will determine the performance of the controller. The response of the set point is governed by the set point speed parameter of each controller. In some cases, this limit is externally defined, such as the detector limit of $1\,^{\circ}\mathrm{C\,min^{-1}}$ for the accumulator saturation temperature controller. Faster than that risks damaging the detectors connected to the system.

In other cases, it may be useful in the process to slow the set point change down to allow devices such as the chiller to ramp the power delivery up and down more smoothly. When a controller is in Tracking mode the set point is equal to the measured value. When Regulation mode is requested the set point moves at the defined speed to the currently active set point. The set point speed for each controller is defined in the Functional Analysis with the Accumulator saturation temperature controller being the slowest.

5.7 Carbon dioxide plant

The CO_2 Plant PCOs runs in bypass mode by default unless the Local box is in Operation mode. It must be running before the Local box can operate.

5.8 Run conditions

The CO_2 system PCOs does not have a stepper that controls the startup or running of the system. The system begins running when the run status of the PCO is selected, however, the pump is interlocked and will not start until there is sufficient sub-cooling at the inlet. If the liquid CO_2 is not sub-cooled it will cavitate in the pump which significantly degrades performance.

5.9 Local box

The local box is the only PCO which has a sequential function chart stepper that allows the state of the program to move between states, as shown in Figure 5.8.

This PCO requires specific conditions to be fulfilled before it can safely proceed to the next step.

The local box shut-off valves are physically located in the CO_2 skid but are logically considered to be part of the local box, as indicated in Figure 3.2. The safe position of these valves is closed which protects the main CO_2 system from damage due to operator error. This allows for potentially large pressure differences between the two systems depending on the state in which it was shut down and what has happened since then.

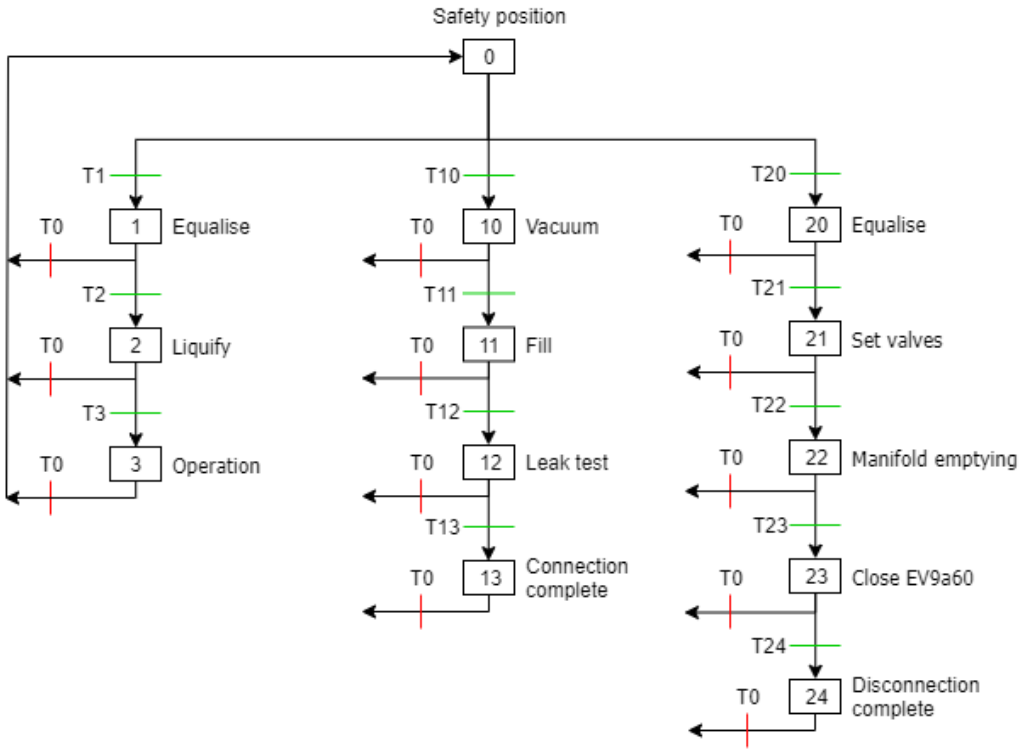

Figure 5.8: Stepper for local box operation

Operation These are the steps that must be taken when the system is restarted following a temporary shutdown or detector replacement. The set point is set to the saturation temperature of the local box. When the pressures are equal and the system reaches operation mode the set point is returned to the user set point.

Connection The PLC follows the steps that are required to properly connect an experiment. These steps are done manually by the user with the PLC only allowing the next step to continue when the conditions have been met.

Disconnection First, the system pressures are equalised and the valves are opened to allow the PLC to remove the CO_2 from the local box. The set point is set to the minimum allowable temperature to condense as much CO_2 in the accumulator as possible. When super-heating is detected in the local box the

Table 5.3: Transition condition descriptions for the stepper shown in Fig. 5.8

Transition	Condition
T0	Stop request
T1	Device connected and run request
T2	Pressure difference $<$ 1.2 bar or all pressures $>$ 52 bar
T3	Sub-cooling at the inlet and outlet of the experiment
T10	Device disconnected and connect request
T11	Vacuum applied
T12	Device filled with CO2
T13	Leak test OK
T20	Device connected and disconnect request
T21	Pressure difference $<$ 1.2 bar or all pressures $>$ 52 bar
T22	CO2 return valve open
T23	Super-heating in the local box
T24	Plant valves closed

valves can be closed and the experiment can be disconnected only losing a minimal amount of CO_2.

Set point management The set point needs to be controlled by both the user and logic at different points in the stepper. This is done by having two variables, the User set point (Usp) and the Automatic set point (Asp). At the appropriate steps (equalising, liquefying and emptying) the control of the set point is given to the PLC and handed back when the step is finished.

5.10 Chiller

The chiller PCO starts when either of the CO_2 Plants begins to run. The relevant expansion valves are enabled by the run condition of the associated CO_2 PCO.

5.10.1 Load management

The chiller is kept running at an optimum point using hot gas bypass and cold liquid injection. The cold liquid refrigerant is added to the suction line of the compressor to control the temperature of the gas entering the compressor. Hot gaseous refrigerant from the outlet is fed into the suction line which regulates the saturation temperature and super-heating on the suction side. This creates a false load on the compressor which allows it to continue running even if the load demanded by the CO_2 plants is small.

This results in a loss in efficiency which is tolerable due to the small size of the unit and the necessity to keep running. The compressor can only be restarted a fixed number of times before a wait time must be observed. If the chiller stops

and a load is added to the system it may not start fast enough to maintain pump sub-cooling or accumulator saturation temperature. Some loss in efficiency is an acceptable compromise for constant cooling availability.

Compressor surge is not a concern in this case as we use a reciprocating compressor. This is why we require a constant mass flow through it while it is running to avoid damage.

5.11 SCADA panels

CERN uses Siemens WinCC OA to monitor and control the PLC. I made the panels using a specific editor on the EP-DT projects server using UNICOS specific widgets. The main panel, shown in Figure 5.9, gives a high-level overview of the whole system. Each CO_2 system and chiller has a dedicated panel containing all the information required to monitor and operate it.

SCADA gives complete control over the objects in the PLC, including their status and values. In commissioning this is used to safely test that all the logic is operating correctly and can be used during operation to address issues as they arise.

Objects can be set in three different modes: Auto, Manual and Forced. Auto mode allows the object to act according to the logic applied to it. Manual mode sets it to the operator's requested position; this is reset when the PCO is switched on. Forced mode sets it to the operator's request and holds it there regardless of the status of the PCO. It also highlights it in yellow to distinguish the status.

Additionally, there are alarm panels segmented by PCO with an overview of the alarm groups with further detail provided in other panels, as discussed in Section 5.5.1.

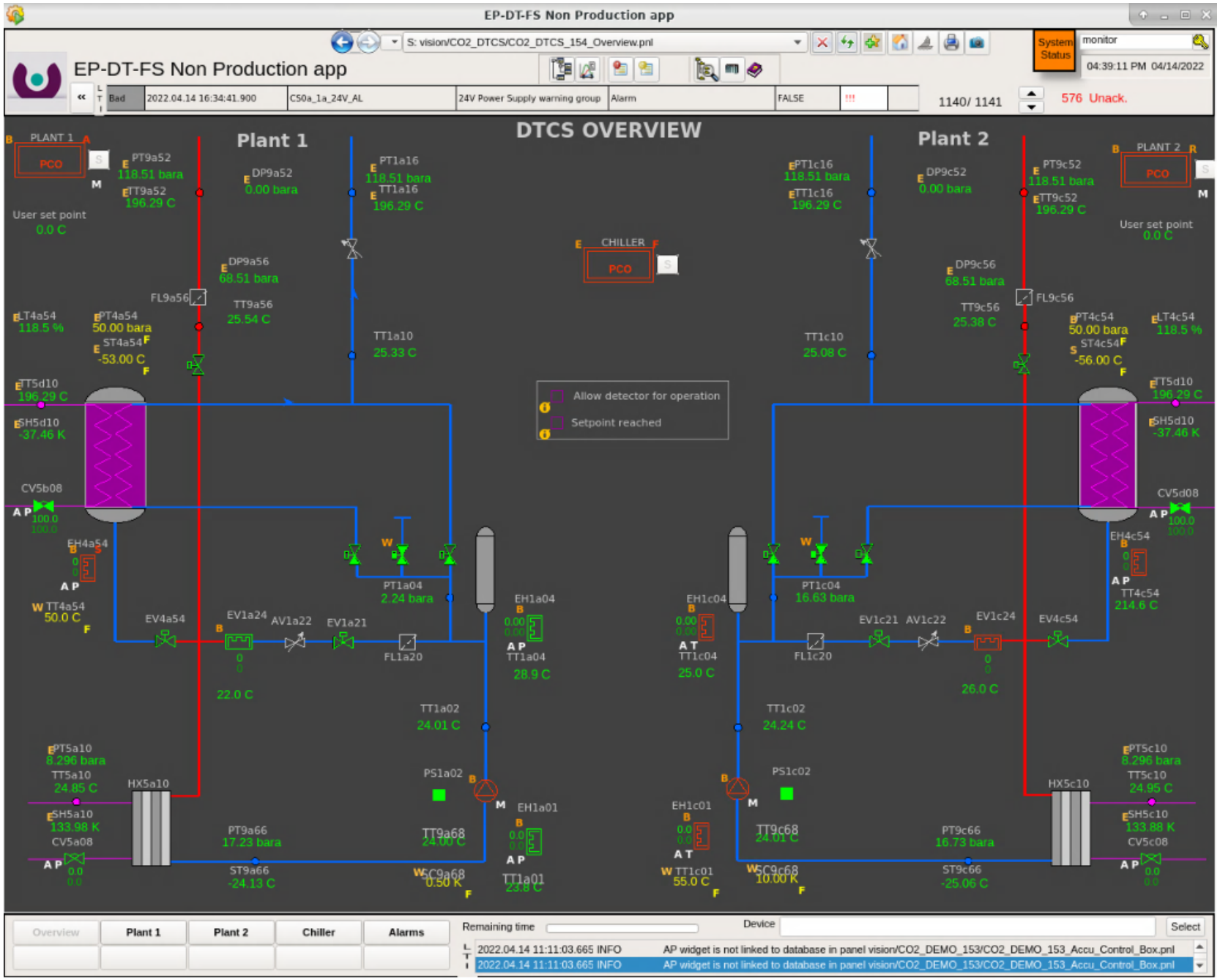

Figure 5.9: Overview SCADA panel

5.12 Commissioning

The commissioning of the control system is a rigorous and well-defined process to ensure the safety of the hardware and those operating it. To ensure that no objects are omitted, each test is noted in the Commissioning File, which is a spreadsheet generated by the UAB from the spec file which lists the IO objects, alarms and controllers.

First, all the IO channels are checked to confirm that the correct sensor is connected to the correct channel. This is done by activating the sensor manually or disconnecting it and monitoring the response in SCADA to see that the expected input responds. The conversion of the sensor value is also checked by comparing it to a known reference.

Following this, the alarms are checked by simulating the inputs and verifying that the alarm activates and triggers the correct response: full stop, temporary stop, or alarm.

The actuators are checked by forcing them to activate and checking that the correct IO objects are activated and that the limiting parameters are functioning. The controllers are checked by simulating their activation conditions and observing the response. The controller's regulation mode should activate and the correct actuator should receive the commands.

5.13 Conclusion

Using the UNICOS framework a fully functional project was created and deployed. This included developing new templates for Siemens PLCs, creating SCADA panels and resolving hardware compatibility issues. This was accomplished with significant support from experienced colleagues and experts from the UNICOS development team. Corrections and bug fixes were made during commissioning to deliver a fully tested project.

A full set of alarms and hardware protection features was included in the system to keep it running preferring to sacrifice performance to avoid a shutdown where possible. The full description of these features is in the Functional Analysis in Appendix A.

Chapter 6

Modelling

Modelling is an important step in the design of control systems and new fluid processes. This system is a special case because the VTCS was in service for 10 years and its performance is well-known from that period. Additionally, the new chiller design was developed by the department and has been implemented in seven LUCASZ systems that have been used in many different roles.

There are several areas where a simulation may provide some insight: the new I2PACL process modification, the new refrigerant in the chiller, control loop tuning, and predicting performance when connected to different experiments. When the system is in I2PACL mode the steady state control action will be shifted to the heating side and may need a modified split-range configuration (Fig. 7.6) to compensate.

Several modelling software packages can simulate fluid systems including Modelica, EcosimPro and Simulink. MATLAB and Simulink were the most accessible and had well-developed libraries for modelling two-phase fluid and thermal properties.

The model was developed using Simscape, MATLAB's physical system modelling platform. It extends Simulink's environment to allow the modeller to use blocks that take the physical system properties as inputs and generate the differential equations.

6.1 Plant

The model is parameterised to allow it to be easily configured to represent the physical properties of the real system, especially those that may change during use or integration. Parameters can be changed in the configuration file or blocks can be commented out in Simulink to modify the system behaviour. The transfer line length and size can be changed to match the pipes used and the heat exchange block can be commented out to allow heat transfer or not which represents the use of concentric or non-concentric pipes.

The system can also be run in 2PACL and I2PACL modes by commenting the accumulator internal heat exchanger block (HX4a54b) out. Depending on the temperatures under test it may be advantageous to switch operation modes.

The model has been used to develop and test the controllers during the control system development. Unfortunately, due to unforeseeable and unavoidable delays in procurement and manufacturing caused by the pandemic, the system was not ready to be tested.

The technical drawing set for the original VTCS is available on NIKHEF's web server for the project [28]. The final report after the system was tested also contains datasheets and test information [17]. These documents were used to calculate the physical properties of the system that the Simscape blocks take as direct inputs or are used in calculations in the data file.

The plant volumes were verified from the final design report on the VTCS Verlaat [17]. The two systems are compared in Table 6.1. The volumes are all constant apart from the transfer lines. Their length is set as a parameter and can be set to simulate the system in a different configuration. The length was set to 50 m in this comparison for validation with the original system.

Table 6.1: Simulation volumes compared to the original system

Subsection	VTCS volume (ml)	Model volume (ml)
Evaporator	220.0	214.0
Liquid supply (50m)	944.4	981.74
Vapour return (50m)	6213.7	6283.2
Condenser	311.4	311.6
Liquid suction	59.1	63.3
Accumulator pipe	23.4	15.8
Accumulator	14 203.0	14 203.0

Additional physical properties were taken from the technical design documents produced by NIKHEF [28] and the technical design report Verlaat [17]. These were used to create representative heat transfer models of the system components.

The model of the system is shown in Figure 6.1. To simplify the model only half of the CO_2 system was included because the other half is identical. The P&ID of the system is shown in Figure 6.2 for comparison.

Table 6.2: Accumulator properties

Property	Value	Unit
Accumulator		
Material	Stainless Steel	319L
Mass	30	kg
Surface area	0.5	m^2
Thickness	7.11	mm
Thermal conductivity	16	$W\,m^{-1}\,K^{-1}$
Specific heat capacity	450	$J\,kg^{-1}\,K^{-1}$
Thermal resistance	888.75×10^{-6}	$K\,W^{-1}$
Armaflex insulation		
Thickness	32	mm
Surface area	0.5	m^2
Thermal conductivity	0.033	$W\,m^{-1}\,K^{-1}$
Specific heat capacity	Not specified	
Thermal resistance	1.92	$K\,W^{-1}$
Transfer lines		
Supply inner diameter	4	mm
Supply outer diameter	6	mm
Return inner diameter	14	mm
Return outer diameter	16	mm
Insulation thickness	25	mm

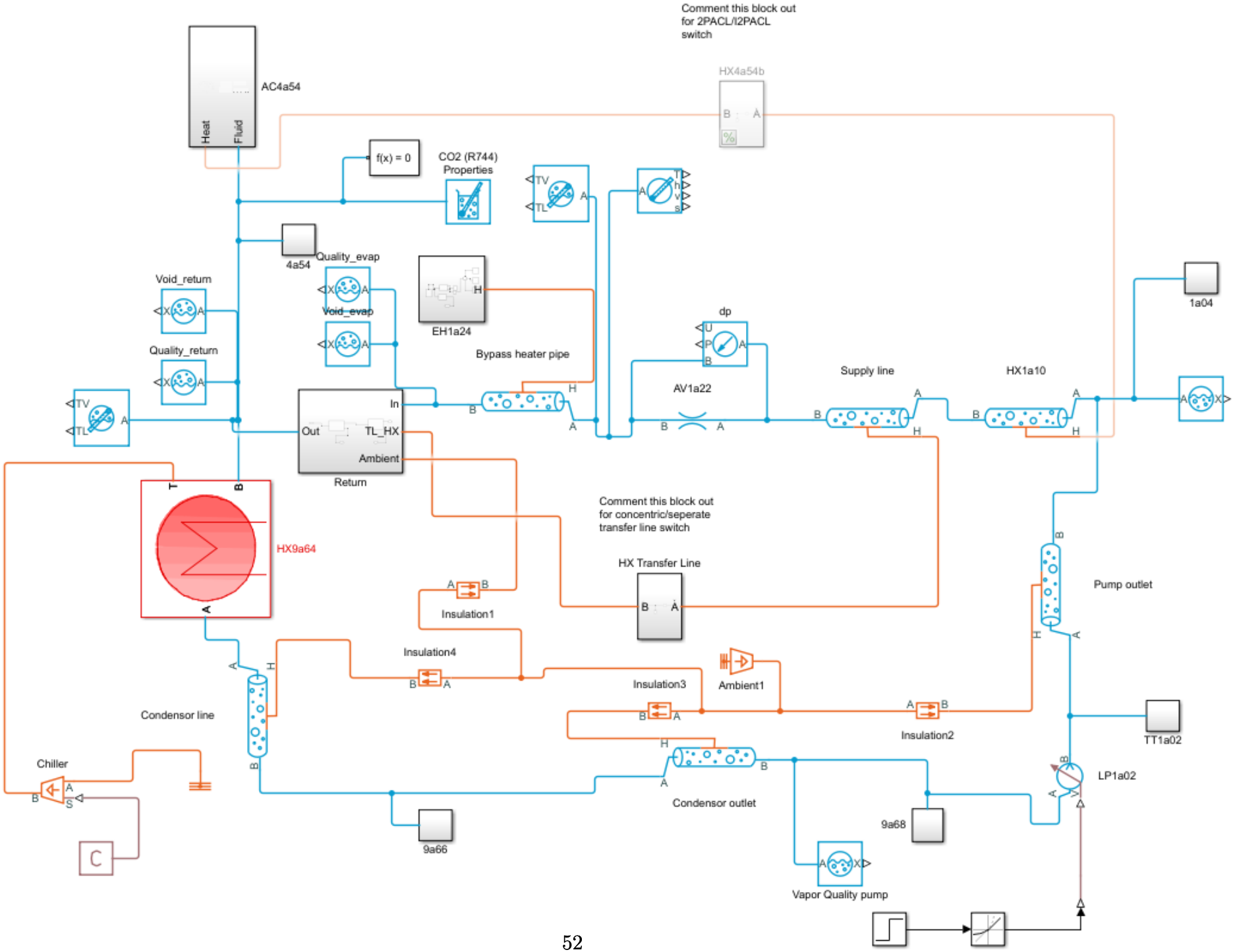

Figure 6.1: Simscape model of the plant

The phase change properties of the system are defined by the Two-Phase Fluid Properties block. This defines the characteristics of the fluid at different pressures and specific enthalpies. The fluid properties look-up table was exported from REFPROP [29] for the operating temperature and pressure range. They are then normalised and loaded into the MATLAB workspace to be accessed by the model.

The simulation script contains or calculates the parameters needed to run the model and loads them into the workspace. It also allows any parameter changes to be propagated to each element without editing the model. The file is included in Appendix B.

The initial conditions of the system are set by pressure and void fraction. This ensures the fluid is in a two-phase state and evenly distributed through the system, as it would be after a prolonged shutdown period.

Environmental conditions were selected to match the environmental heat leak documented in Section 11.5.3 of the Technical Description of the VELO Thermal Control System [17] to produce a similar heat leak rate.

6.2 Accumulator

One of the crucial subsystems is the accumulator, as it controls the response of the entire process. The accumulator has a specific design of being a large, two-phase volume which allows liquid but not gas to exit towards the rest of the system. This type of segregated vessel is more complicated to model as the liquid and vapour volumes need separate mass and energy balances when compared to a homogeneous two-phase fluid model. This doubles the number of equations that need to be solved and adds the equations for thermal energy and mass exchange between the two phases. This requires additional computation to solve the states which increases simulation run times.

Simscape's two-phase fluid library has a vessel which behaves in this way; however, it is part of the restricted library which does not allow it to be edited or the source to be viewed. For this block, the only heat flow port is connected to the vessel wall rather than to the fluid volume. The surface area of the vessel will be too small for effective and representative heat transfer to the fluid inside.

Both gas and liquid are taken from the accumulator and circulated through a constant volume fluid chamber, shown in Figure 6.3. This has a thermal port which acts directly on the fluid contained within it through thermal blocks, which set the surface area, thermal conductivity, specific heat and thickness of the heat exchanger material. This differs from the Accumulator heat port which acts on the vessel walls and is therefore connected to the ambient temperature through the insulation with parameters described in Table 6.2. This thermal port is where the controller output acts to maintain the set point.

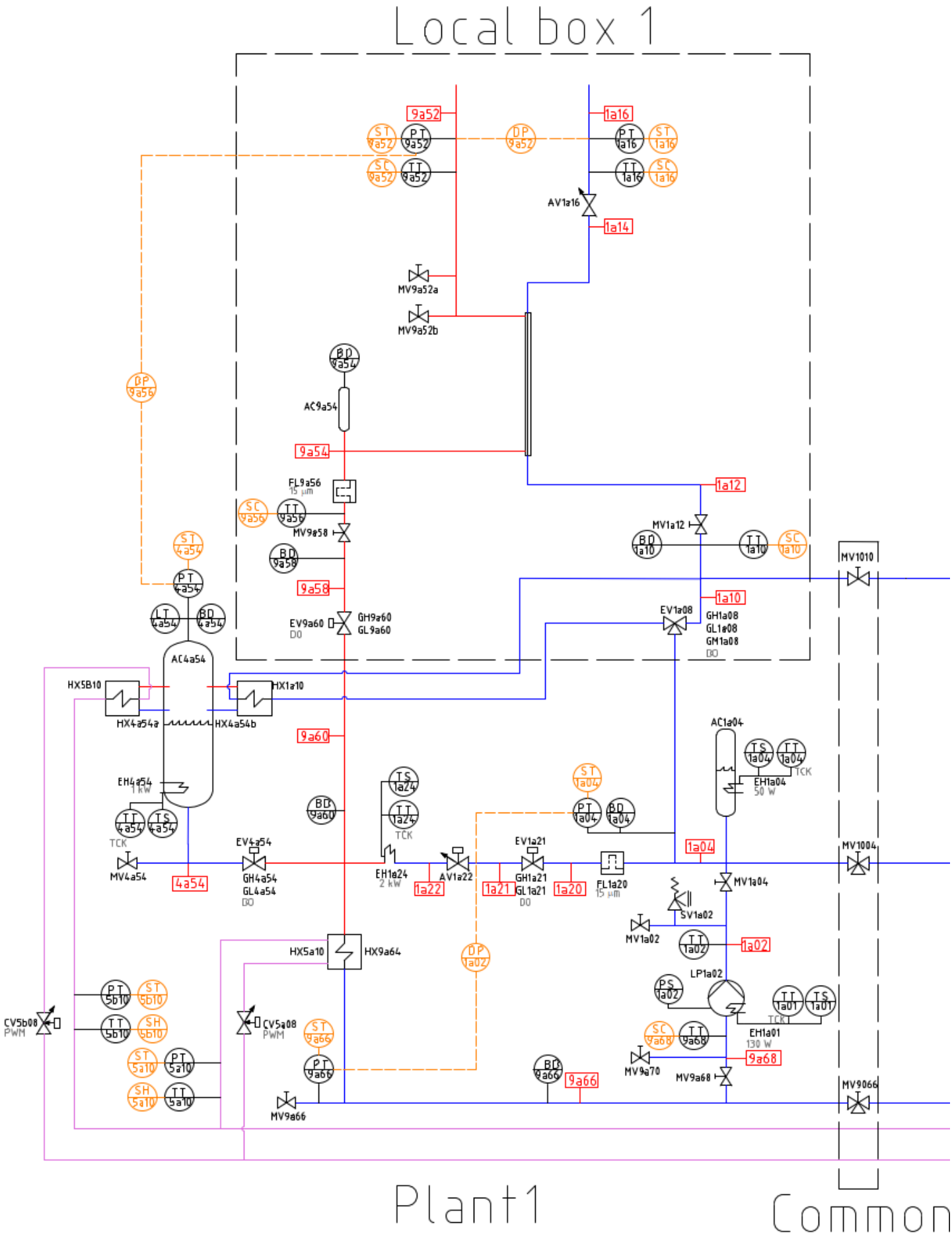

Figure 6.2: Plant P&ID

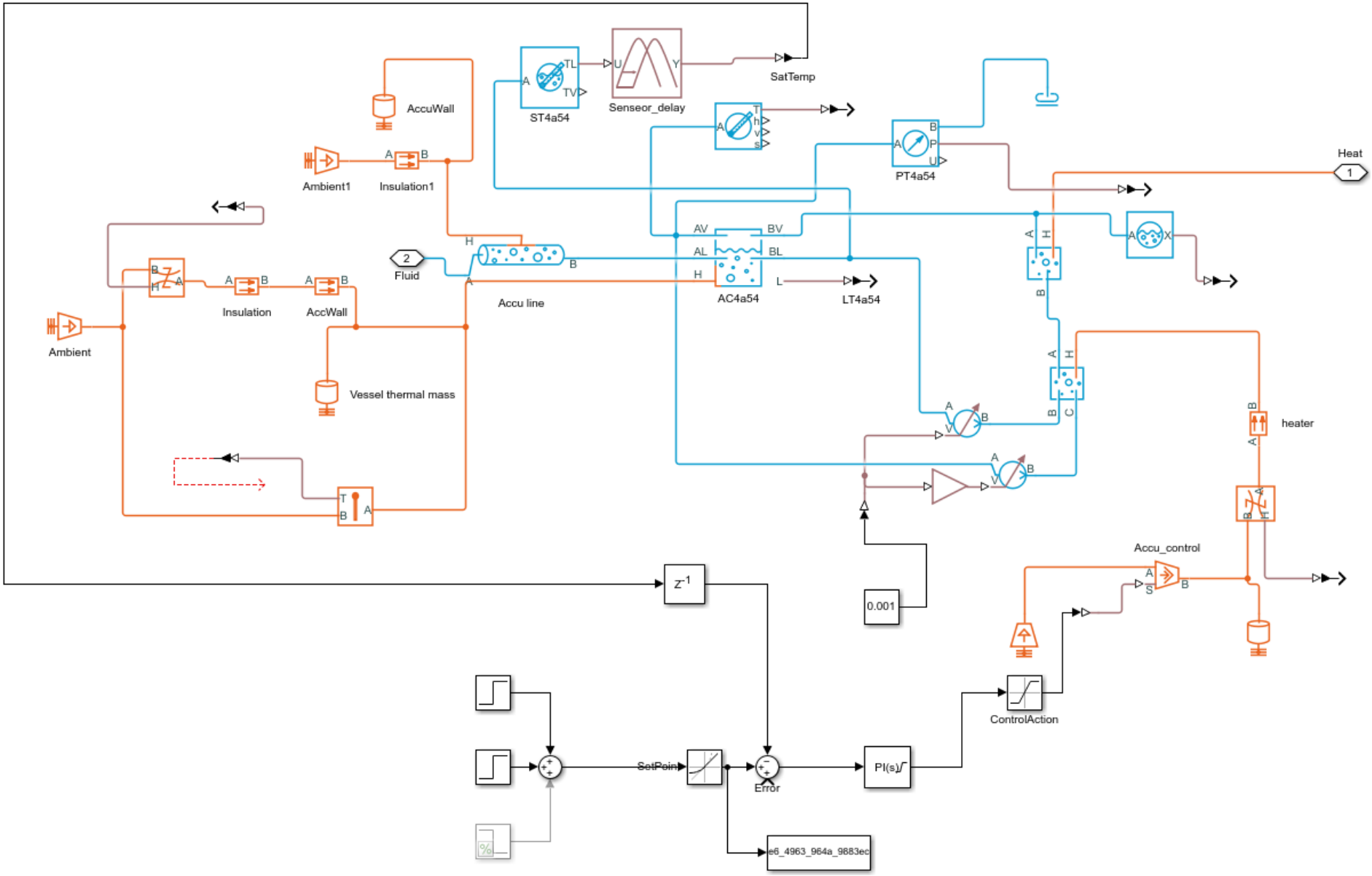

Figure 6.3: Accumulator Simscape model including controller

6.3 Validation

To verify that the Simscape model is representative of the real system, historic data from the testing of the original VTCS was used as validation. The start-up sequence shown in Figure 6.4, starting at 13:30 and ending with steady state operation at 14:45, was used to confirm the static effect of the accumulator heater. There are 10 minutes where an average power of 500 W is applied to raise the pressure of the system before starting. In this test, the inputs were fixed to get them to match the test done in the past.

The pressure is raised to bring the saturation temperature of the system above the ambient temperature. This causes the CO_2 in the lines to condense, shifting the mass from the accumulator to the lines of the plant, and reducing the liquid level in the accumulator. When there is sufficient sub-cooling at the pump inlet it can be started and the start-up process can continue.

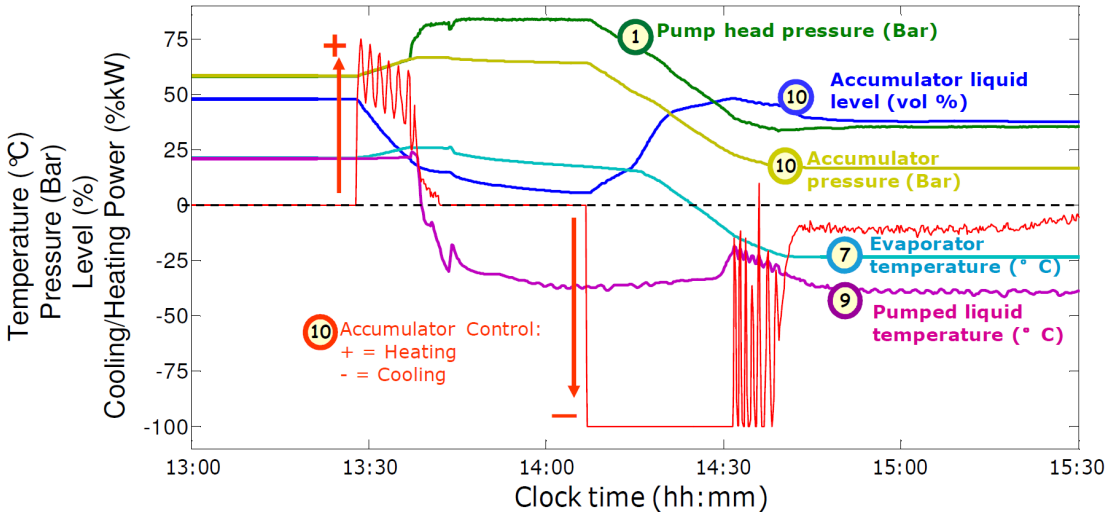

Figure 6.4: Startup of the VTCS from warm [17]

The model had to be adjusted to match the system characteristics of the original VTCS with 50 m long transfer lines. Figure 6.5 shows the result of the simulation and the data collected during commissioning [17]. The model was configured with the same set of initial conditions and a pulse input of 500 W was applied with a 10-minute duration. This causes the CO_2 vapour to condense, shifting the mass in the system out of the accumulator and into the lines.

To verify the dynamic performance of the model, the detector power on test was used. In this test, the system was on and stable at $-25\,^{\circ}\mathrm{C}$. The detector and module heat loads are applied as step heat inputs. A set point change to $-5\,^{\circ}\mathrm{C}$ is done while the detector is on and then the detector is switched off.

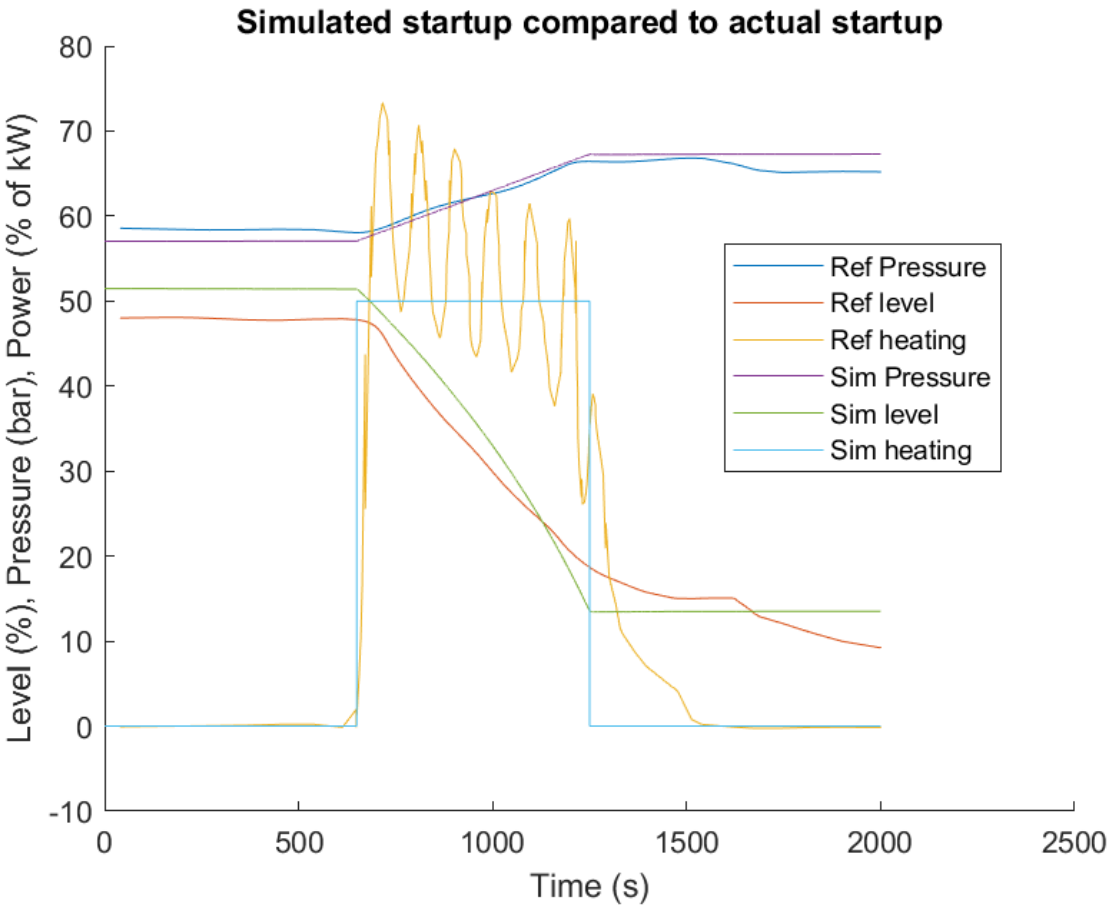

Figure 6.5: Simulink model output compared with the startup segment shown in Figure 6.4

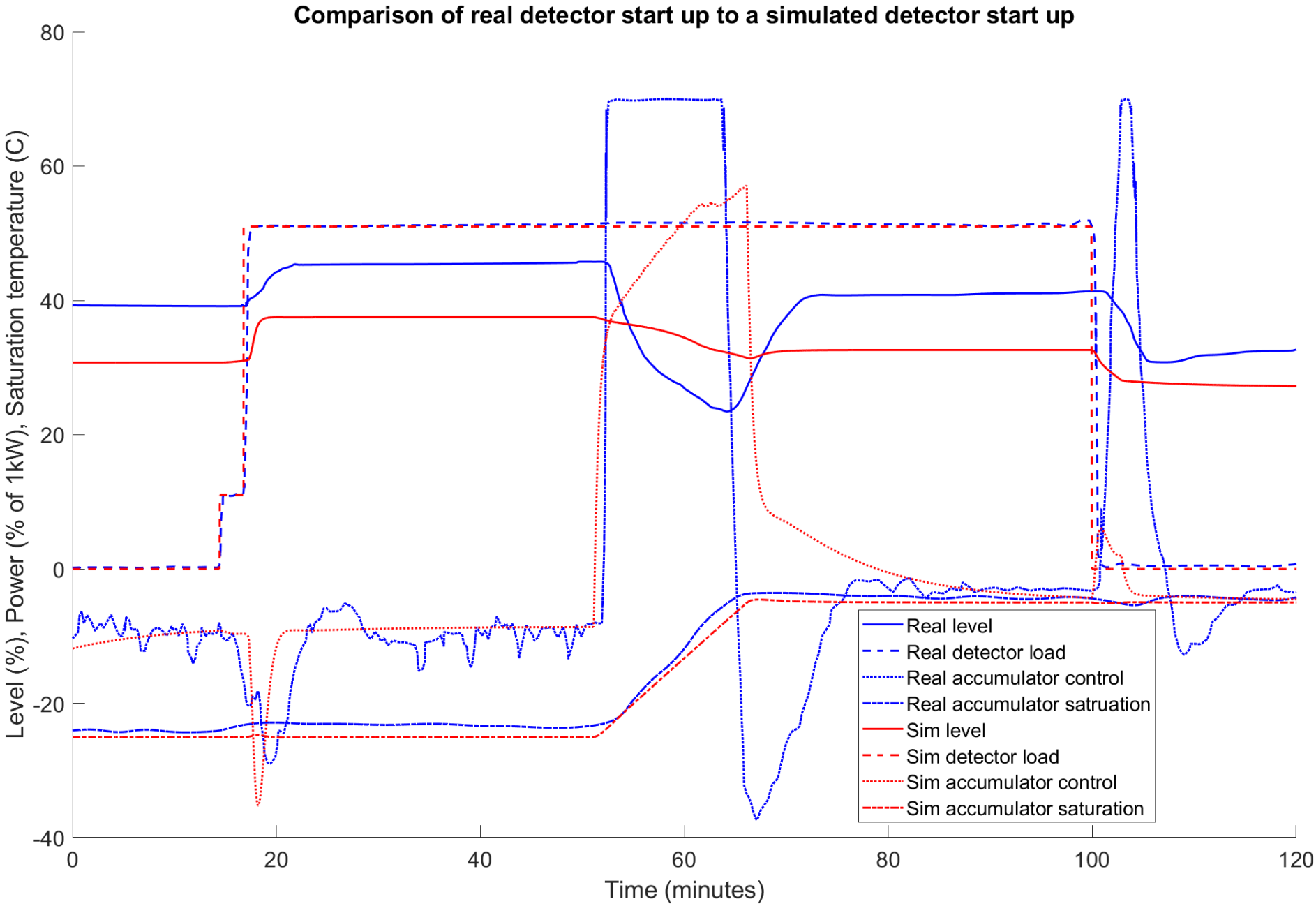

Figure 6.6: Performance comparison between simulation and real testing

Figure 6.6 shows the difference between the model's response to the detector switching on and the actual system's response during the VTCS commissioning [17]. The model captures the general response of the system to changes in heat input and saturation temperature.

The level in the accumulator rises when the detector is powered on after about 15 minutes. In the simulation, this is about 4% and in the test, it was about 6%. This is a similar fluid volume that is exchanged and the shape of the response also matches the response in the actual test. The controller response is also very similar, with a slightly larger magnitude in the simulated case.

The set point change around 60 minutes shows similar behaviour with both systems moving mass from the accumulator to the transfer lines, resulting in the level dropping and then recovering as the system reaches equilibrium at the new set point. The simulated level drops 15.5% and the tested system drops 22.5%.

This difference could be due to a few reasons. First, the model cannot capture all the dynamic responses of the real system which may cause some differences in the shape of the response. Secondly, the level sensor in the accumulator measures the cylindrical section of the vessel. Therefore, a 1% change in simulated level is a 142 mL change in volume where the same change in the accumulator is 130 mL. The difference in volume change is 724 mL.

The sensor in the accumulator is a capacitive sensor which uses the difference in the dielectric value of gaseous and liquid CO_2 to determine the level. The dielectric is not constant and changes with temperature, with the gas and liquid dielectric values getting closer as it gets warmer. This, combined with the position of the sensor directly above the heater, may impact the accuracy of the measurement.

When the detector is powered off there is a decrease in level when the mass returns to the lines as the transfer lines become fully liquefied. The simulated level continues to decrease and does not recover as the measured level does. This is likely also due to the model not capturing the effects of environmental heat. This was done as closely as possible using data from Verlaat [17] but it will never perfectly match the actual system.

6.4 Conclusion

The model provides a reasonable foundation on which to base the controller design given the unavailability of the real system. This initial design can be used as the baseline until the hardware build is complete. It also enables us to provide performance estimates which inform the end users of the probable performance limits and validate that the design will achieve the minimum requirements set out for the system.

Chapter 7

Controller design

After validating the model it was used to create a transfer function for the plant which was used to design the accumulator saturation temperature controller. This controller had to be fast enough to maintain safe set point change rates, respond to disturbances caused by changing load and maintain zero error set point tracking.

7.1 System identification

A thermal model of the accumulator was built to estimate heat flow rates using the thermal properties of the materials it will be constructed with, shown in Table 6.2. Using this model we can estimate the heat flow to the environment. Applying this model to the worst-case temperature difference at cold operation at $-40\,^{\circ}\mathrm{C}$ produces a maximum heat transfer from the environment of 30 W.

With the accumulator heating and cooling capacity of 1 kW, the system will not reach thermal equilibrium without departing from the operating range. If a step input of heat is applied to the accumulator the saturation temperature will increase or decrease continuously until a physical limit is reached. This can be modelled as an integrated first-order response, shown in Equation 7.1.

$$G(s) = \frac{A}{s(\tau s + 1)} \tag{7.1}$$

A step input of 500 W was used to identify the system which was applied to the model after 400 seconds to ensure that it started from a steady state. Plotting the derivative of the saturation temperature as shown in Figure 7.1 reflects the first-order response without the integrator, as described in Equation 7.1.

The DC gain A is defined as the ratio of the change in output to the change in input. The rise time τ is the time taken to reach 63% of the final value.

$$A = \frac{\Delta y}{\Delta u} \tag{7.2}$$

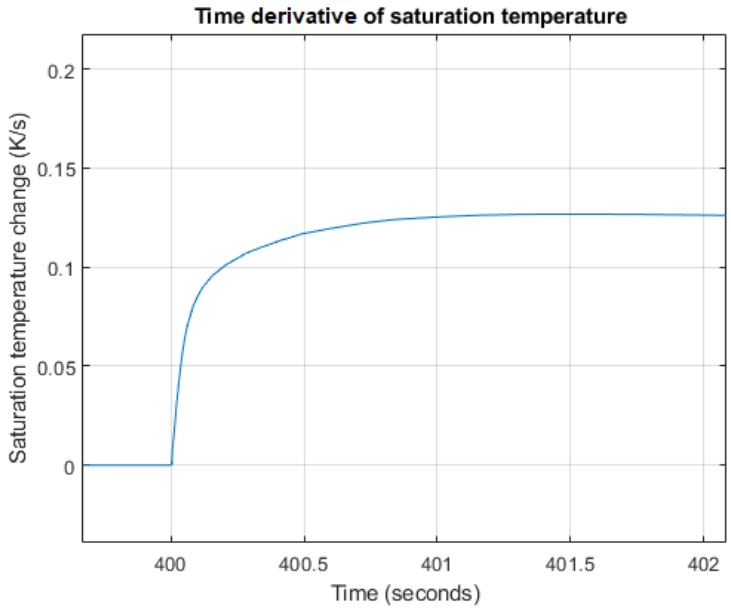

Figure 7.1: Derivative of the response to a 500W step input

Applying these principles $A = 25.4 \times 10^{-5}$ and $\tau = 0.084$, giving a plant transfer function:

$$G(s) = \frac{25.4 \times 10^{-6}}{s(0.084s + 1)} \tag{7.3}$$

7.2 Saturation temperature controller

The saturation temperature controller has several limits placed upon it by the detectors. These limits are that the set point should not change faster than $1\,^{\circ}\mathrm{C\,min^{-1}}$ and the steady state variation should be less than 0.1 K.

For maximum versatility, there is no planned communication between the plant and the device under test. The controller must be able to maintain the set point despite sudden changes in load.

7.2.1 VTCS controller

In the original system, this controller was implemented as only proportional with a gain of 100 [17] which produces closed-loop poles at $s = -0.293$ and $s = -0.00125$. This results in the dominant pole having a rise time of 800 seconds. This worked well for the time that VTCS was operational; however, it will not perform well with the I2PACL modification.

7.2.2 System feedback

A typical feedback model, shown in Figure 7.2, includes signals that impact the system but may not be controlled or desired. Environmental noise which may

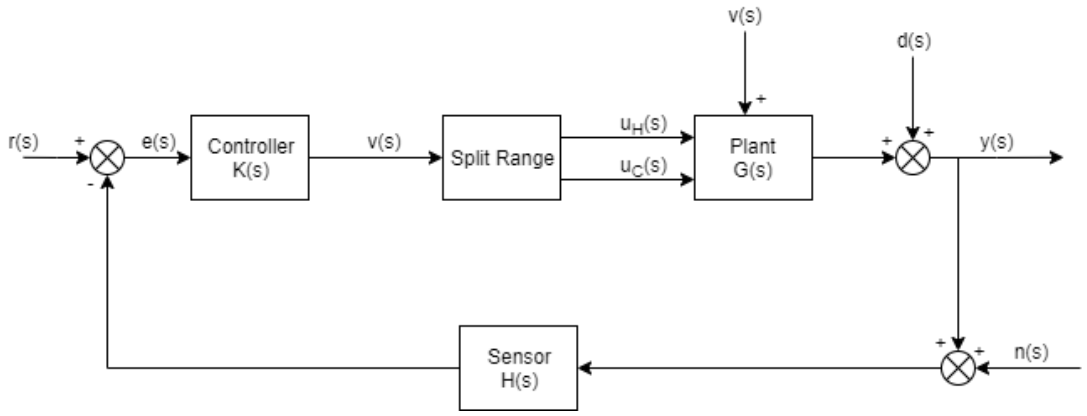

Figure 7.2: Feedback block diagram

impact the sensor reading is $n(s)$. Changes in saturation temperature caused by system pressure changes are output disturbances $d(s)$. Input disturbances caused by changes in the heat balance of the system are represented by $v(s)$. The saturation temperature set point is $r(s)$ and the evaporator temperature is $y(s)$. In the VTCS the controller would operate around zero at steady state as the only heat load on the system would be environmental, which is an input disturbance. This will change based on the set point but in data from Verlaat [17], this is less than 10 W. This would cause some steady state error which must have been negligible.

In the I2PACL configuration the combined thermal load from the cold CO_2 and environment could reach hundreds of watts as discussed in Section 3.2.1. The larger the input disturbance, the larger the steady-state error will be for a proportional type controller. To ensure that there is zero steady-state error to an input disturbance, an integrator must be included in the controller.

PLC cycle time

The PLC cyclically runs the program. First, the inputs are updated, then the code is run and finally, the outputs are set before restarting. The cycle time is the full duration of this process and it is not constant. The PLC reports average cycle times of 56 ms with a range between 45 ms and 60 ms. The cycle time variation can be caused by variations in program execution time and interrupts for other tasks such as communication.

Jitter is an important consideration when designing digital control systems as it can significantly impact the stability of the output [30]. The Siemens Step 7 software does show the parameters stated above however it does not provide a method to statistically analyse the distribution of cycle time, and thus allow the jitter to be modelled. Jitter can be compensated for by trying to minimise it or compensating for it as discussed by Lluesma, Cervin, Balbastre, *et al.* [31].

As the minimum and maximum PLC cycle times are significantly faster than the desired closed-loop response time jitter is not foreseen to be a significant

problem for the control system. It can be eliminated by setting the minimum PLC cycle time parameter to a level above the typical cycle time which would remove the variation in the cycle and instead introduce a fixed delay. The maximum cycle time parameter can also be used to trigger an alarm if the PLC is struggling to maintain the desired cycle time

Sensor dynamics

The sensor transfer function $H(s)$ describes the behaviour of the sensor in response to a change in the measured process. The Druck PTX 7500 series used in the accumulator has a 1 ms response time to a step change in pressure and uses a piezoresistive silicon sensor.

The sensors are attached to the process to keep them separate from the cold liquid, which would cause them to freeze. This is done by connecting them to the top of the vessel in the case of the accumulator or by a small vertical standpipe in the rest of the system. The speed of sound in gaseous CO_2 is approximately $260\,\mathrm{m\,s^{-1}}$ [29] which will add only 3 ms if the accumulator is empty. This is an order of magnitude faster than the PLC cycle time and is much faster than the process will change; therefore, it will be considered negligible in the controller design process.

The placement of the sensors at the top of the accumulators in the gaseous CO_2 also acts as a damper for pressure pulses produced by the pumps and other plant processes, reducing noise on the controller input signal.

Actuator dynamics

The heating and cooling actuators have a transfer function which modifies the control action before it acts on the plant. This is caused by the thermal mass and thermal conductance of the materials in the heat exchangers and the time for refrigerant to reach the heat exchanger from the expansion valve.

The time response of the heating segment had to be estimated using the heaters installed in another system. These heaters have the same cartridge design; however, they have different sizes and powers. The heaters used for testing were 15 kW with a length of 1000 mm and a diameter of 32 mm.

The heater's internal temperature was used as an indicator that the temperature had stabilised and the heater was delivering all its power to the fluid. This took 42 seconds with a rise time of 14 seconds.

The heaters installed in the DTCS have a power rating of 1 kW, a length of 300 mm, and a diameter of 14 mm. The power and volume of the two heaters change at a similar scale which is why the response time is considered to be representative of the system.

This transfer function is modelled as a first-order transfer function with a DC gain of 1 and a time constant of 14 s. This ensures that the full requested

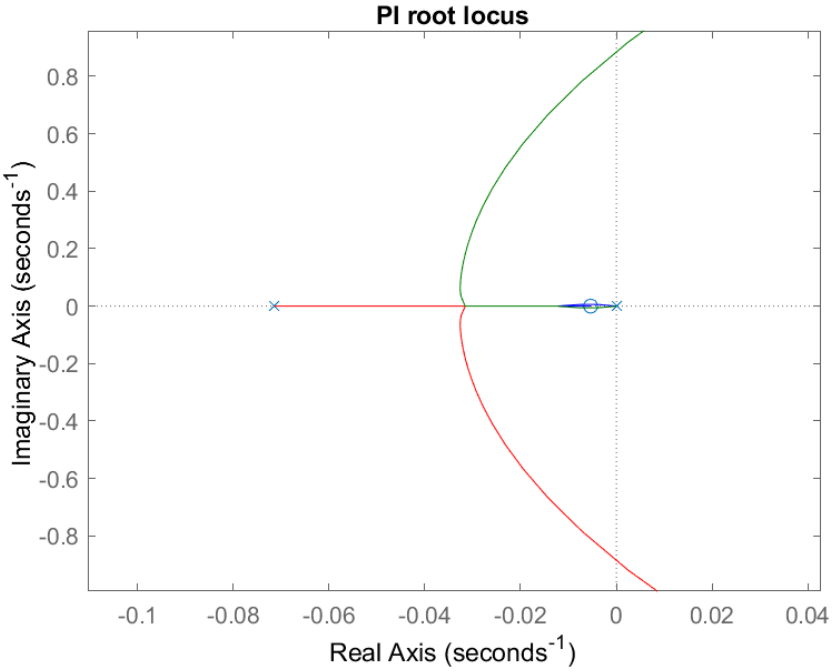

Figure 7.3: Root locus with a PI controller including actuator dynamics

cooling power from the controller will be applied; however, it modifies the lag in the application of that power.

7.2.3 Controller design

The PID controller implemented in UNICOS is the parallel equation shown in Equation 7.4 where T_{df} is the derivative filter time. This adds a pole at the origin and a zero at $\frac{1}{T_i}$ when the PI implementation is used.

$$K(s) = K_c(1 + \frac{1}{T_i s} + \frac{T_d s}{1 + \frac{T_d}{T_{df}} s}) \tag{7.4}$$

To meet the detector requirements and avoid damage the dominant pole of the closed-loop system should be slower than 60 seconds to keep within the one degree per minute limit on the rate of change. This is a limit set by the detector designers for the safe operation of their instruments. This limit is applied by the controller object to the feedback loop set point $r(s)$. Figure 7.3 shows the root locus of the plant under PI control. This reveals that a minimum gain is required to keep the poles on the negative real axis to avoid an underdamped response and the position of the zero dictates where the poles converge on the real axis, which will dictate the rise time of the controlled system.

The loop transfer function $L(s)$ can be calculated in terms of T_i where $L(s) = K(s)G(s)$

$$L(s) = \frac{25.4 \times 10^{-6}(T_i s + 1)}{T_i s^2(\tau s + 1)(14s + 1)} \tag{7.5}$$

The break-in point of the root locus is calculated by finding the turning points of the characteristic equation $1 + K_c L(s) = 0$. Therefore the point where the poles rejoin the real axis can be found in terms of T_i by finding the turning point of the characteristic equation. Choosing T_i to set a specific break-in point will ensure that the poles are on the real axis.

$$\frac{d}{ds}\left(-\frac{1}{L(s)}\right) = 0 \tag{7.6}$$

To make sure the dominant closed-loop pole has a time constant slower than 60 seconds the break-in point will be placed at $s = -0.01$ which provides some margin for variation in the plant model. Substituting this into Equation 7.6 and solving for T_i gives an integration time constant of 186 s.

The loop gain can then be calculated from the characteristic equation by substituting the desired closed-loop pole locations. Choosing to place the closed-loop pole at $s = -0.009$ will leave some margin for system and controller variation from external factors.

$$K = \left|\frac{1}{L(s)}\right| \tag{7.7}$$

Applying Equation 7.7 gives a gain $K_c = 711\,\mathrm{W\,K^{-1}}$. This value must be scaled when implemented in UNICOS as the controller output is the percentage of the maximum output value. In this case, with a 1 kW maximum output the value for the PLC is divided by 10.

From the root locus (Figure 7.3), it is clear that the system will become unstable at a high gain of $43\,500\,\mathrm{W\,°C^{-1}}$. This is much higher than will be reasonably implemented; however, the response of the actuators has a significant impact on the stability of the controller.

From experience with previous systems, it is necessary to implement different controllers for the heating and cooling modes of the accumulator. This is done to accommodate the more intricate dynamics of the chiller.

It is anticipated that the system will run in I2PACL mode more often than in 2PACL, making the heating side dynamics and control a higher priority for modelling and simulation.

Stability margins

The Bode and Nyquist plots can be used to analyse the gain and phase stability margins of the controller, shown in Figures 7.4 and 7.5. The system has 59°of

phase margin, 55.7 dB of gain margin and a delay margin of 56 seconds.

This indicates that the designed controller will remain stable despite some perturbation to the plant performance but significant delays in measured value or control action application will lead to oscillation and then instability.

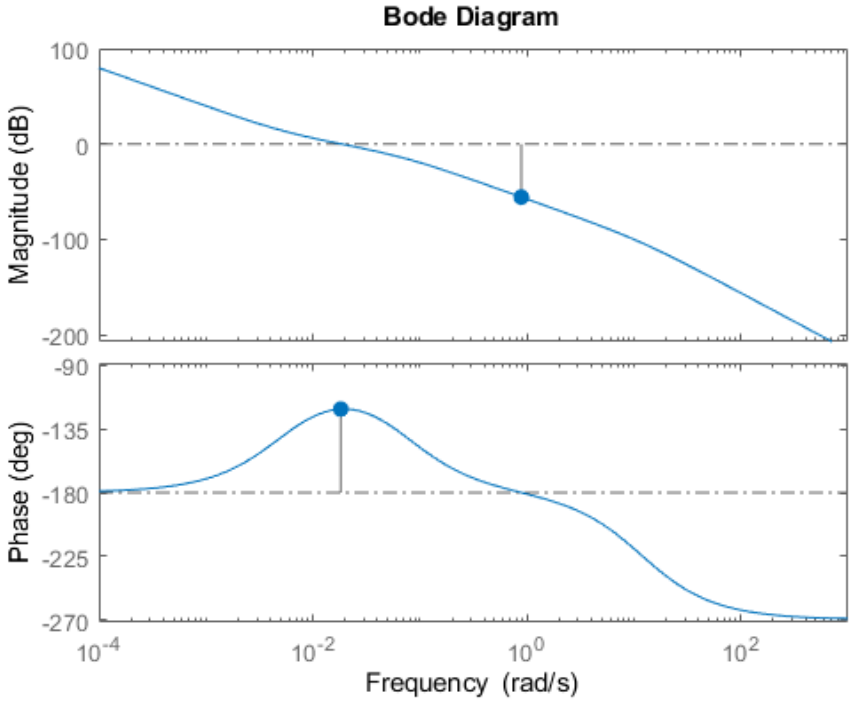

Figure 7.4: Bode plot of the controlled system

7.2.4 Split range design

The internal parameters $v(s)$ and $u_i(s)$ need to be defined to compensate for the differences in performance between the heating and cooling modes of the system. The internal parameter $v(s)$ has the interval $[0, 100]$ derived from the base implementation of the UNICOS controller object.

The heating (u_{Heat}) and cooling (u_{Cool}) actuator commands are also normalised internally to have an interval of $[0, 100]$; however, the actuators will have different maximum power outputs. For the heater, this is clearly defined by its nominal power of 1 kW.

The injection valve capacity is dependent on the performance of the chiller and therefore may be impacted by the load being applied to the system. The Emerson EX2 orifice 0 has a nominal power rating $Q_0 = 1.05\,\text{kW}$, as determined by the manufacturer's data sheet for the expected operating conditions. The capacity of the valve will be impacted by the opening of other valves in the system, with high loads leading to an increasing suction pressure of the compressor and reduced performance as a result.

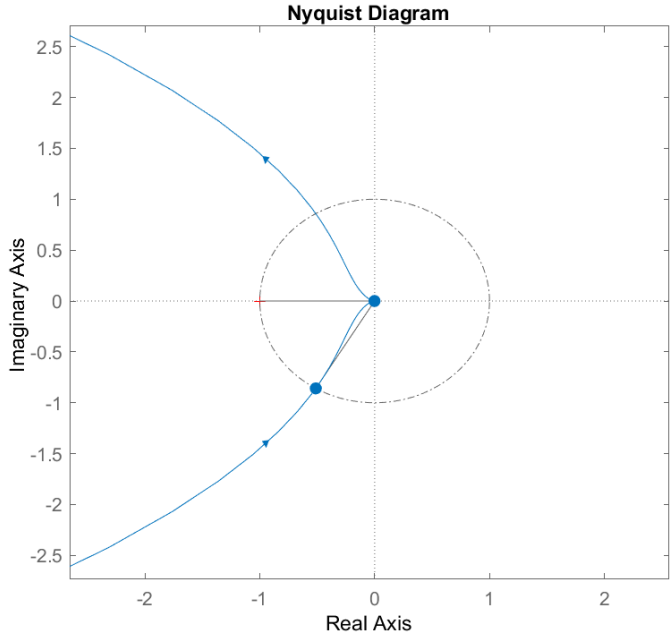

Figure 7.5: Nyquist plot of the controlled system

Step tests were done to determine the gain of each actuator. The accumulator was at equilibrium before starting and power was applied until a constant change in saturation temperature was observed. Using the rated power of the devices the gain can be found with the cooling gain $G_{Cool} = 7.84 \times 10^{-5}$ and the heating gain $G_{Heat} = 3.48 \times 10^{-5}$. Applying the controller design process the desired controller gain for each actuator is calculated, shown in Table 7.1.

u_i	$K_{C,i}$
u_{Heat}	73.46
u_{Cool}	-32.46

Table 7.1: Desired loop gain

As discussed earlier this is an integrating process, with the proportional gain being the most important parameter. The gain difference between each actuator gain ($K_{C,i}$) can be accounted for using the slope (α_i) of the split range function and the common controller gain (K_C) [32]. K_C and α_i can be found by solving Equations 7.8 and 7.9 which gives $\alpha_{Cool} = -1.49$, $\alpha_{Heat} = 3.01$ and $K_C = 24.41$, indicated in Figure 7.6.

$$K_{C,i} = \alpha_i K_c \quad \forall i \in \{1, .., N\} \tag{7.8}$$

$$v_{max} - v_{min} = \sum_{i=1}^{N} \frac{u_i^{max} - u_i^{min}}{|\alpha_i|} \tag{7.9}$$

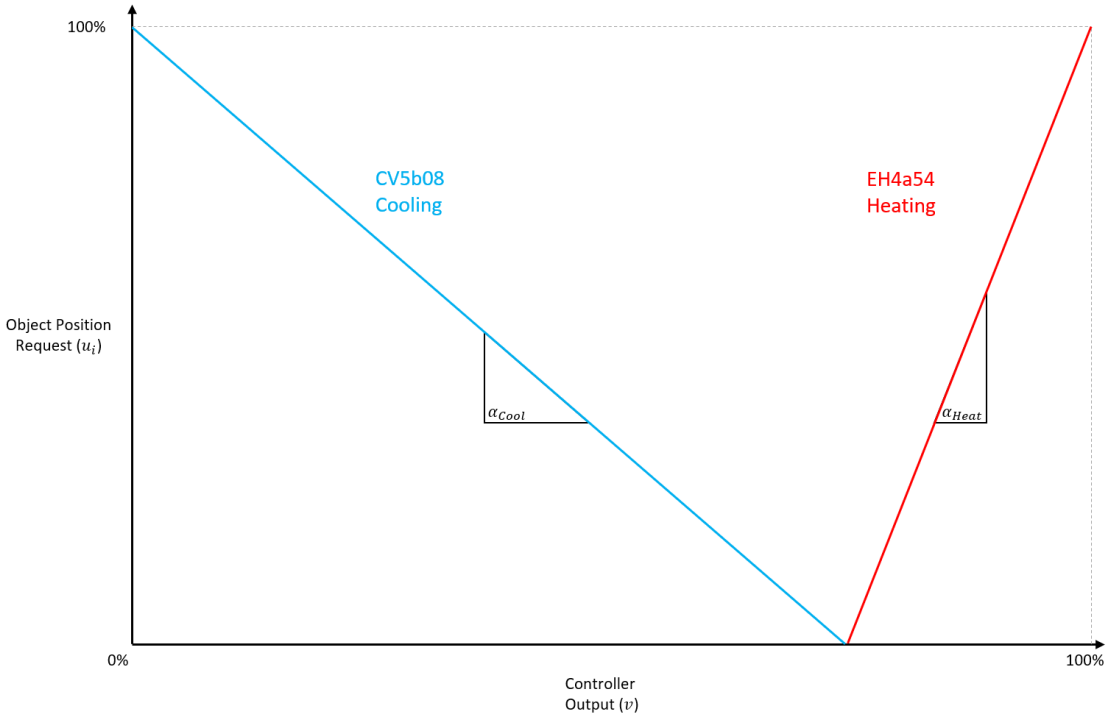

Figure 7.6: Saturation pressure controller split-range function

7.2.5 Conclusion

This controller will ensure zero steady-state error using the integrator which will keep the saturation temperature at set point. It also has good stability margins which will be able to cope with variance of the system as parameters such as ambient temperature and set point vary during operation. Additionally, the difference in performance between the heating and cooling actuators has been addressed.

Chapter 8

Results

Uniting all the elements discussed in previous chapters leads to the final system. Firstly the model was run in closed loop with varying parameters to develop a baseline performance level. Where possible actual performance data was gathered and used to verify that the performance meets the requirements.

In simulation, the controller was tested in all operating conditions and in all phases of the cooling cycle. It was configured to run in both standard 2PACL and I2PACL modes. The impact of transfer line length and heat transfer was also tested to determine the impact it has on the controller and system performance.

The limits on I2PACL operating conditions were also tested to verify the trends shown in Figure 3.4. This will define the operating limits for this mode and help operators decide which mode should be used.

The test goes through a full cooling cycle starting from warm. The system was allowed to stabilise before the next step was started. The test started at room temperature where the system is liquefied. The accumulator saturation set point was then decreased to $-25\,^{\circ}\mathrm{C}$ and then the detector was turned on. The set point was changed to $-5\,^{\circ}\mathrm{C}$ with the detector power on. It was switched off and the test ended having followed a similar profile to the test shown in Figure 8.1.

8.1 2PACL operating mode

Figure 8.2 shows the startup, set point change and detector power cycling test. It compares the performance of two different transfer line configurations, showing how each configuration impacts the performance of the system. The overshoot of the set point was $0.4\,^{\circ}\mathrm{C}$ when decreasing and $0.43\,^{\circ}\mathrm{C}$ when increasing. Due to the gradual set point changes the overshoot will be more significantly impacted by the slope rather than the magnitude of the set point change.

The disturbance caused by the detector power on and off caused a set point deviation of $0.43\,^{\circ}\mathrm{C}$ and $-0.12\,^{\circ}\mathrm{C}$ respectively. The controller never saturates and is always able to maintain the set point in steady-state conditions.

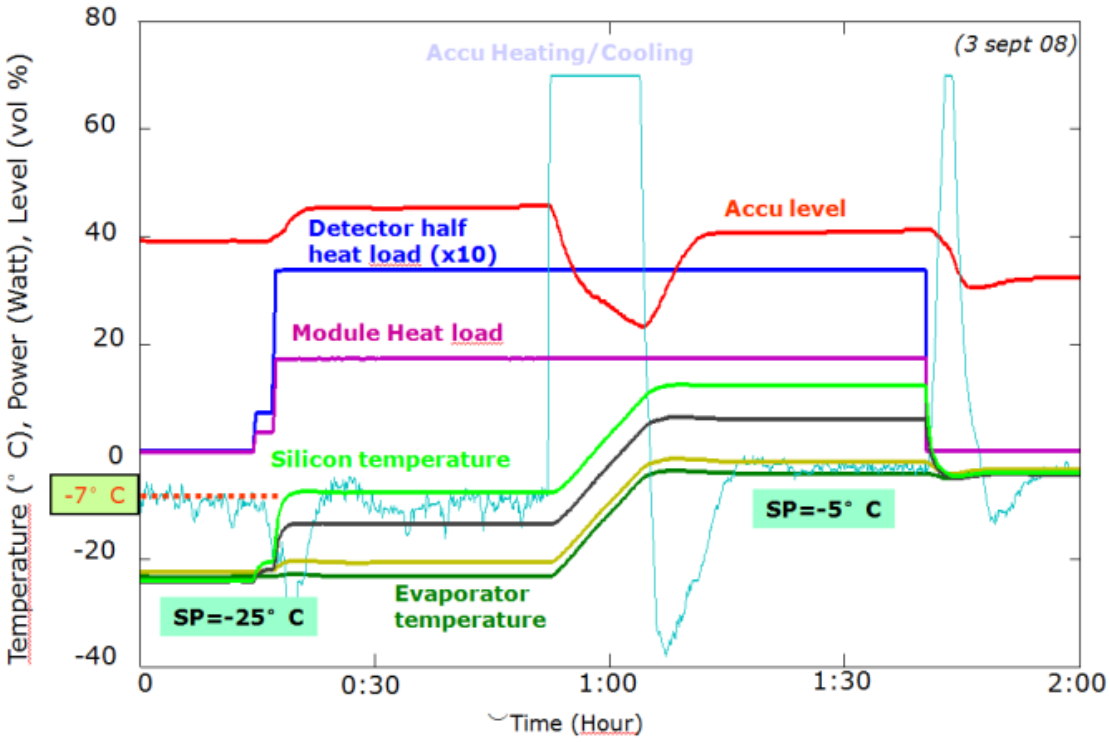

Figure 8.1: Detector power on and set point change [17]

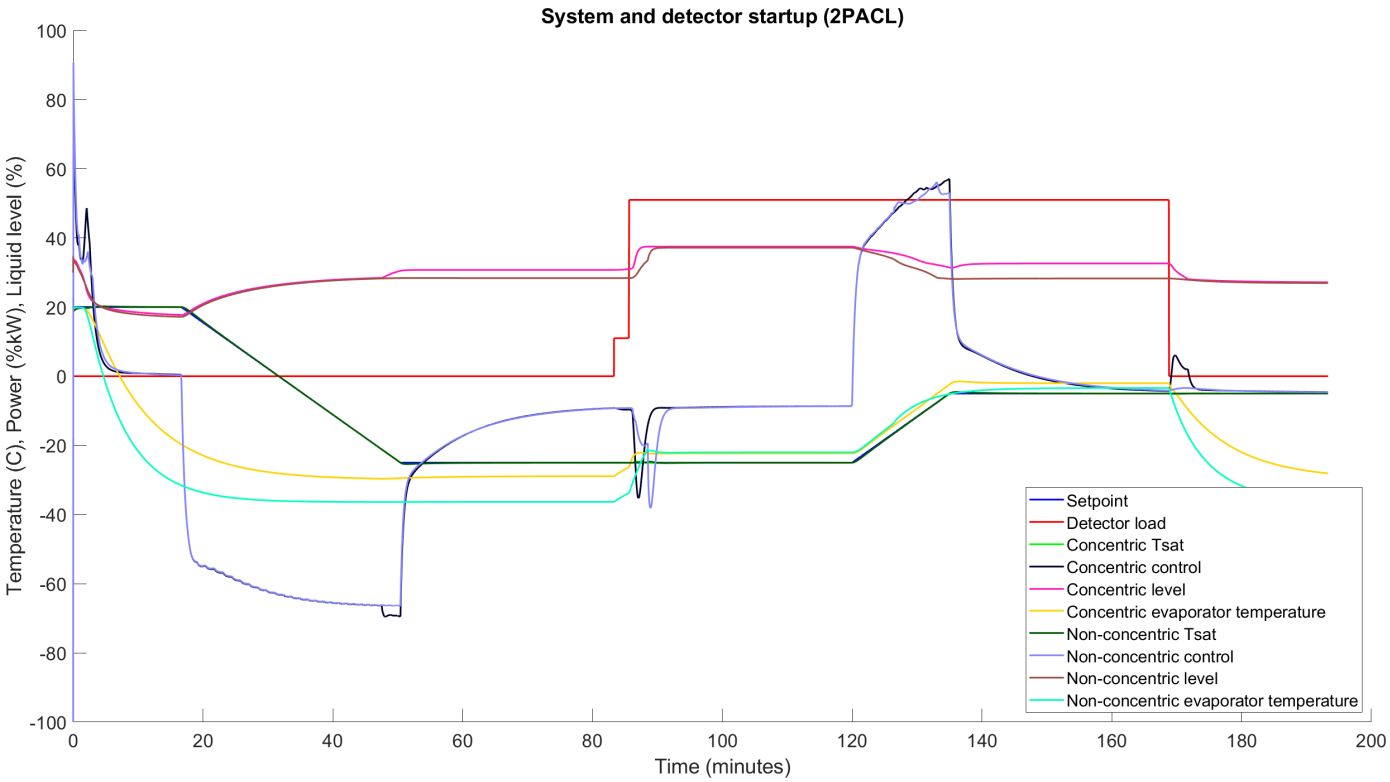

Figure 8.2: Simulated startup in 2PACL mode

8.2 I2PACL operation mode

In this mode both the real system and simulation were tested. The designer of the local box decided to replace the concentric lines with a heat exchanger for better packaging and heat transfer. This exchanger was not ready at the time of testing. I2PACL operating mode was the only way to saturate the CO_2 before it reached the dummy load that had been connected. The dummy load was controlled by an external heater controller which was not controlled by the PLC and therefore was not logged. Its effect can be seen in the response of the other attributes.

8.2.1 Simulation

Figure 8.3 shows the same test as the previous section with the system in I2PACL operating mode. The controller overshoots by $-0.38\,^{\circ}\mathrm{C}$ when decreasing the set point and $0.23\,^{\circ}\mathrm{C}$ when increasing it. The detector power cycle caused a deviation of $0.24\,^{\circ}\mathrm{C}$ and $-0.15\,^{\circ}\mathrm{C}$ when turning on and off respectively.

There are some important performance differences to note between the 2PACL and I2PACL modes that can be seen in Figure 8.3. In the first 20 minutes, the controller saturates its output with maximum heating. This occurs because the heater is not powerful enough to overcome the cooling of the sub-cooled CO_2 in the supply line. This causes the set point deviation seen. This may be more pronounced in the physical accumulator as the densities of gaseous and liquid CO_2 get closer with increasing saturation temperature. This reduces the effectiveness of the thermosyphon design of the heater which in turn may reduce its maximum sustained power output.

Another key point is the set point change at 130 minutes when the saturation temperature change causes the heater to reach its limit but for a shorter time. This may reduce the controller's effectiveness at warm saturation temperatures as more heating is required to maintain steady-state conditions.

The evaporator temperatures are also significantly different between the operating modes. In I2PACL mode the evaporator temperatures closely follow the saturation temperature at all times; however, in 2PACL mode the detector temperatures drop below $-30\,^{\circ}\mathrm{C}$ when not running because the CO_2 is sub-cooled when it arrives at the evaporator. The CO_2 arriving sub-cooled can create uneven cooling of the detector as the liquid is first heated to saturation before boiling. If the system needs to be run at temperatures greater than $5\,^{\circ}\mathrm{C}$ it will need a pre-heater or heat exchanger in the local box to warm up the supply before it enters the detector.

8.2.2 Real

A test of the real system was done in I2PACL mode, shown in Figure 8.4. This operating mode was used because the heat exchanger which would replace the concentric lines was not yet delivered. The internal accumulator heat exchanger

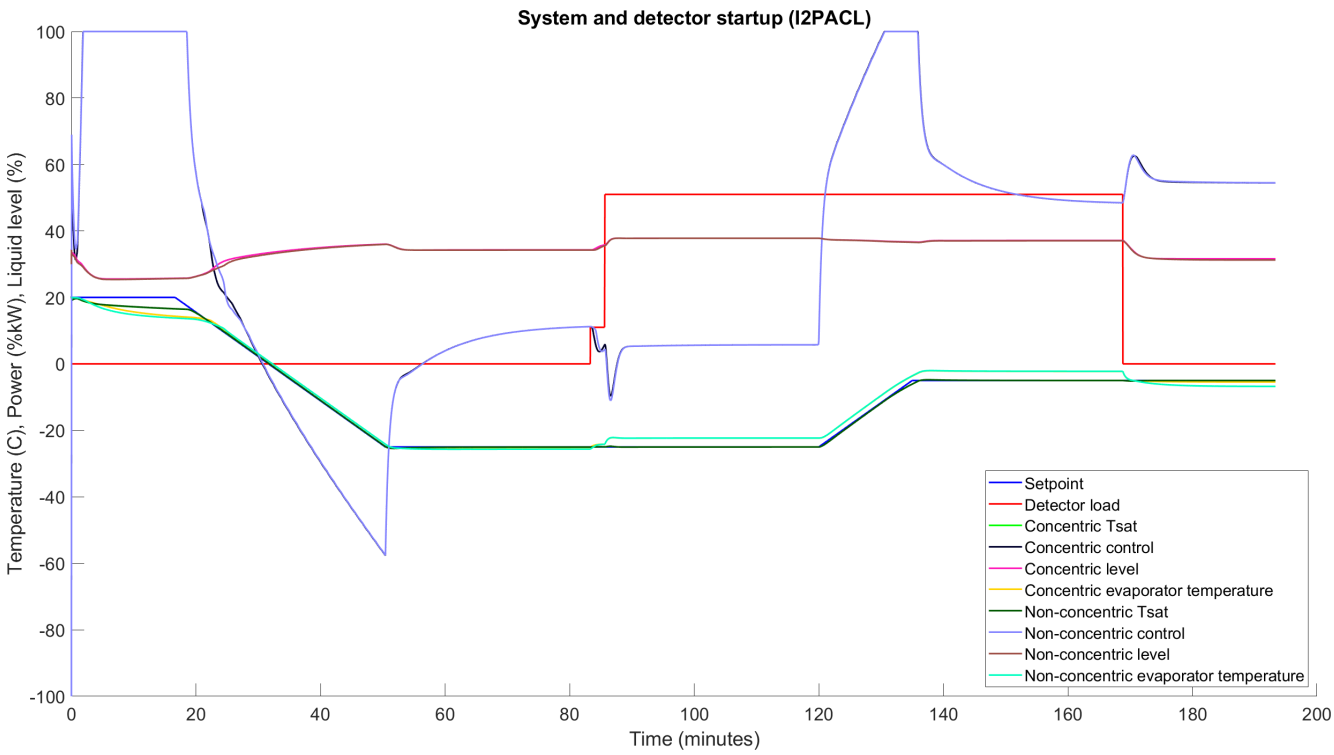

Figure 8.3: Simulated startup in I2PACL mode

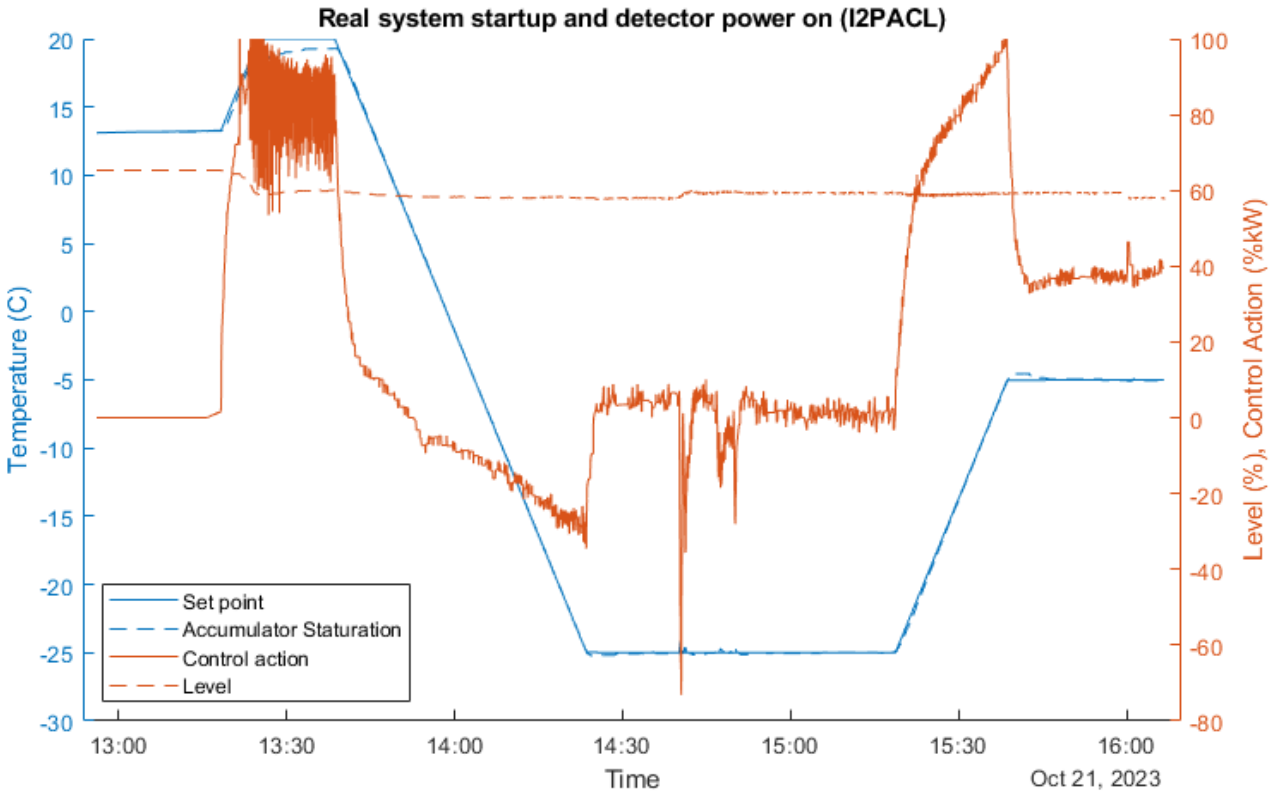

Figure 8.4: Real start-up in I2PACL mode

was the only other way of warming up the supply line before it went to the local box.

In the first 30 minutes, the start-up process occurs automatically. The set point is raised to generate sub-cooling at the pump inlet. The significant oscillation is caused by the internal heater temperature power limit being reached. At 13:40 the sub-cooling threshold is reached and the pump is switched on. The set point now moves at the user-defined rate to the current active set point −25 °C. The set point is reached at 14:25 with a small overshoot and it is allowed to stabilise.

At 14:40 the dummy load is activated, clearly shown by the small increase in level and corrective control action. The two distinct peaks of control action are caused by the chiller protection parameters reducing the opening of the valve to prevent liquid refrigerant from returning to the compressor. This is more pronounced at lower operating temperatures.

At 15:20 a set point change to −5 °C is started still under load. When it reaches the set point there is a small overshoot of 0.5 °C. The Engineering Office was involved with the test and agreed that it was within their expectations.

The dummy load power is removed at 16:00 visible as a drop in level and a small peak in control action. After observing a period of stability the test was ended.

8.2.3 I2PACL set point limits

This problem was discussed in Section 3.2.1 where a theoretical maximum set point was illustrated at different flow rates in Figure 3.4. This limit is most significant when no heat load is present because this is the point where sub-cooling at the pump outlet is highest. The model was run with no detector heat load, only ambient heating, and the set point was changed in steps of 10 from −25 °C to 25 °C.

Figure 8.5 shows the results of the simulation. The control action first saturates at −5 °C but settles at about 500 W of heating power. At 5 °C the heating input starts settling at 800 W but the saturation during the transition causes a significant set point deviation. The actual limit must be verified experimentally during commissioning.

This simulation was validated on the real system using the same set point steps, shown in Figure 8.6. The real system managed to reach 15 °C which was not predicted by the model. This indicates that heat transfer was better in the simulation also indicated by the different steady state controller inputs. Given that the mass flow meter had not yet been delivered the flow can only be estimated based on pump data. This may contribute to the differences observed. The heater's high-temperature limits can be seen activating in the last 20 minutes, resulting in the derating of the heater's output.

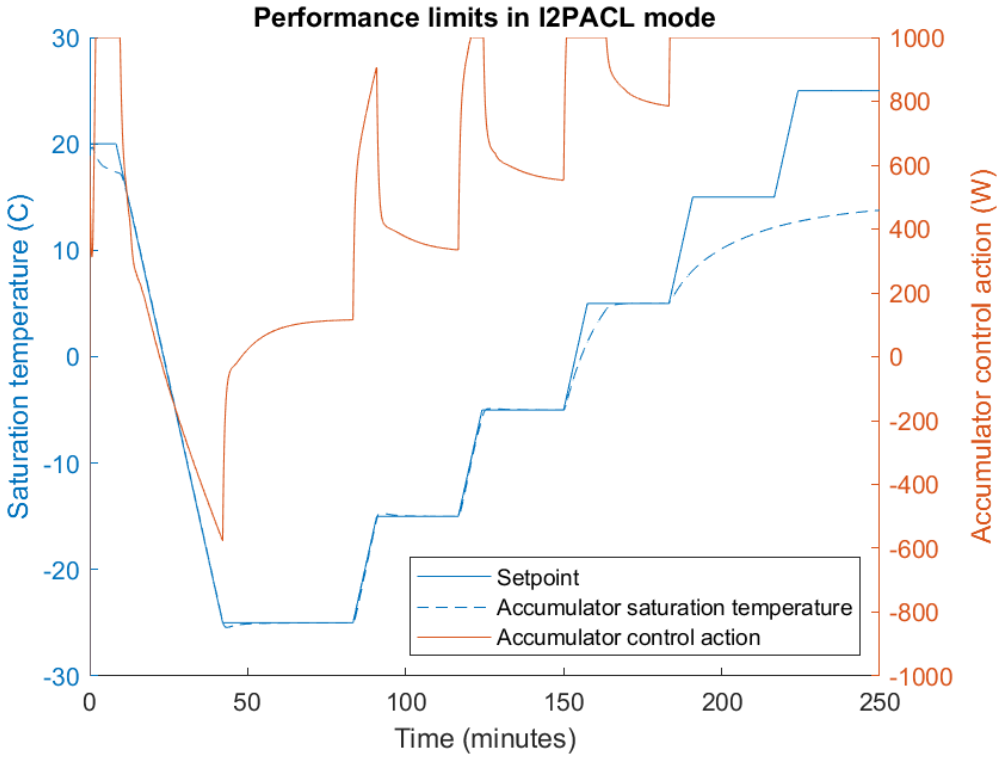

Figure 8.5: Simuated I2PACL limit shown by increasing set point ($45\,\mathrm{l\,h^{-1}}$)

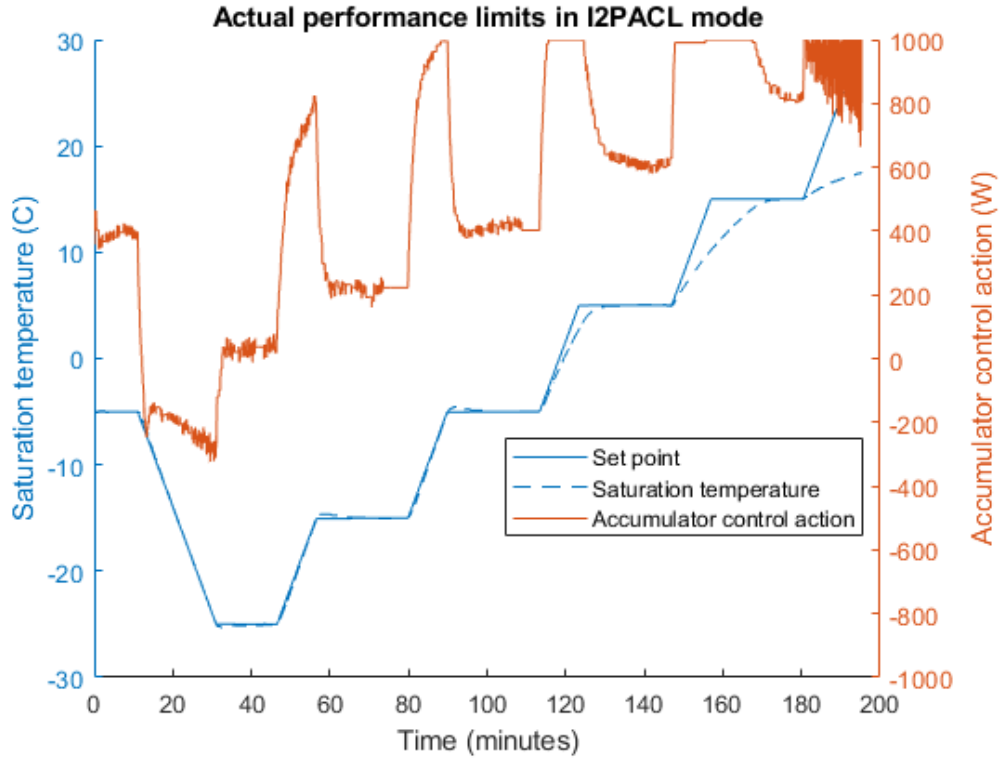

Figure 8.6: I2PACL performance limit test on the real system (10 mm stroke)

Additionally, this confirms the model's reliability and the conclusion of Chapter 6. While there are areas of inaccuracy it provides a good baseline for estimating the performance of the larger system.

8.2.4 Sub-cooling performance with different configurations

To ensure good performance of evaporative cooling systems the fluid should arrive at the evaporator at saturation temperature. This requires heat exchange after the pump because the CO_2 is sub-cooled at the outlet.

This can be done in a combination of two ways; the system can be run in I2PACL mode, which warms the outgoing CO_2 in an accumulator heat exchanger (HX4a54b) before it flows to the transfer line secondly; further heat exchange can occur in a concentric transfer line or heat exchanger on the client side.

Figure 8.7 shows the difference in pre-evaporator sub-cooling in each test scenario. This clearly shows that operating in I2PACL mode, when possible, is the most effective way of eliminating sub-cooling. If possible a concentric transfer line should be used to significantly reduce sub-cooling in 2PACL mode and still has benefits in I2PACL mode.

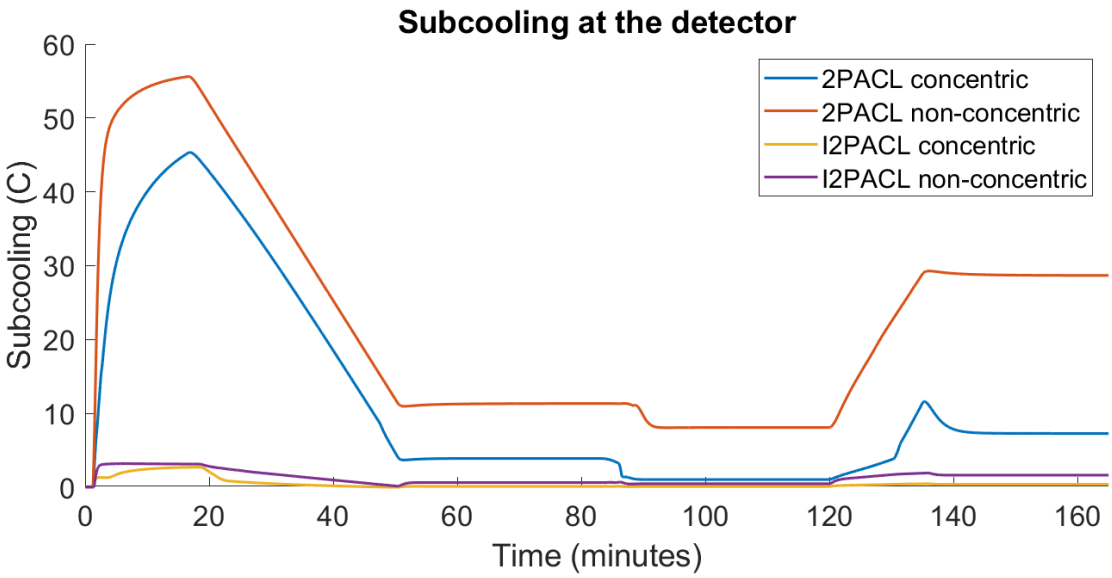

Figure 8.7: Sub-cooling at the evaporator in different operating modes

8.3 Transfer line length

The transfer line length influences both the volume that must be absorbed by the accumulator during changes in load and the heat exchange between the liquid and return lines. Requiring more mass to be absorbed by the accumulator requires more power from it. Longer transfer lines allow more heat transfer between the

supply and return which improves performance by reducing the sub-cooling of the fluid arriving at the detector.

Figure 8.8 shows the impact on the sub-cooling at the detector with different transfer line lengths. After the set point changes to −5 °C around 140 minutes the sub-cooling is significant. An increase in transfer line length to 20 m improves it significantly with diminishing returns thereon.

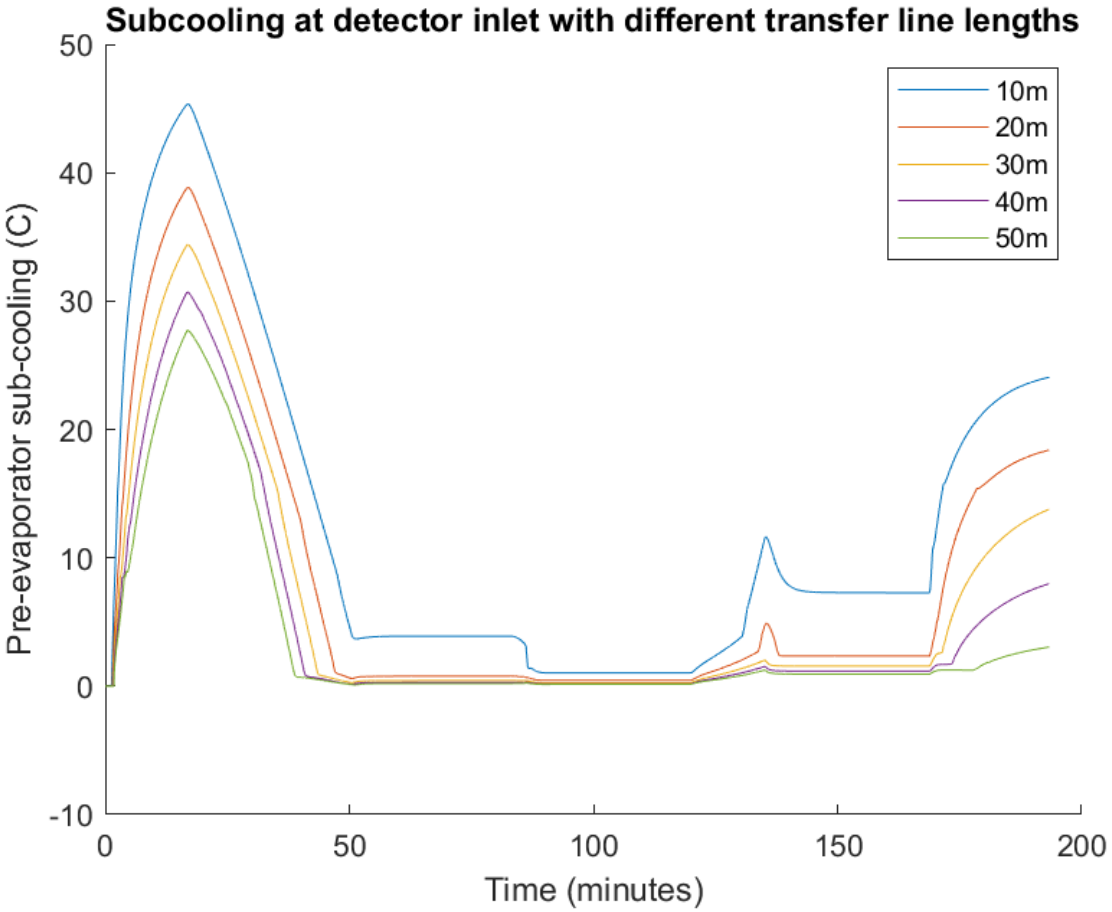

Figure 8.8: Sub-cooling at the detector inlet (SC1a16) with different transfer line lengths in 2PACL mode

Figure 8.9 shows the impact of the transfer line length on the controller's performance. The overshoot and disturbance response of the measured value stay at similar values; however, the control action changes significantly. This is clearest at 40 minutes where the 40 and 50-metre transfer lines saturate the control output starting to deviate from the set point. If a long transfer line is connected to this system again, this should be checked experimentally to verify these results.

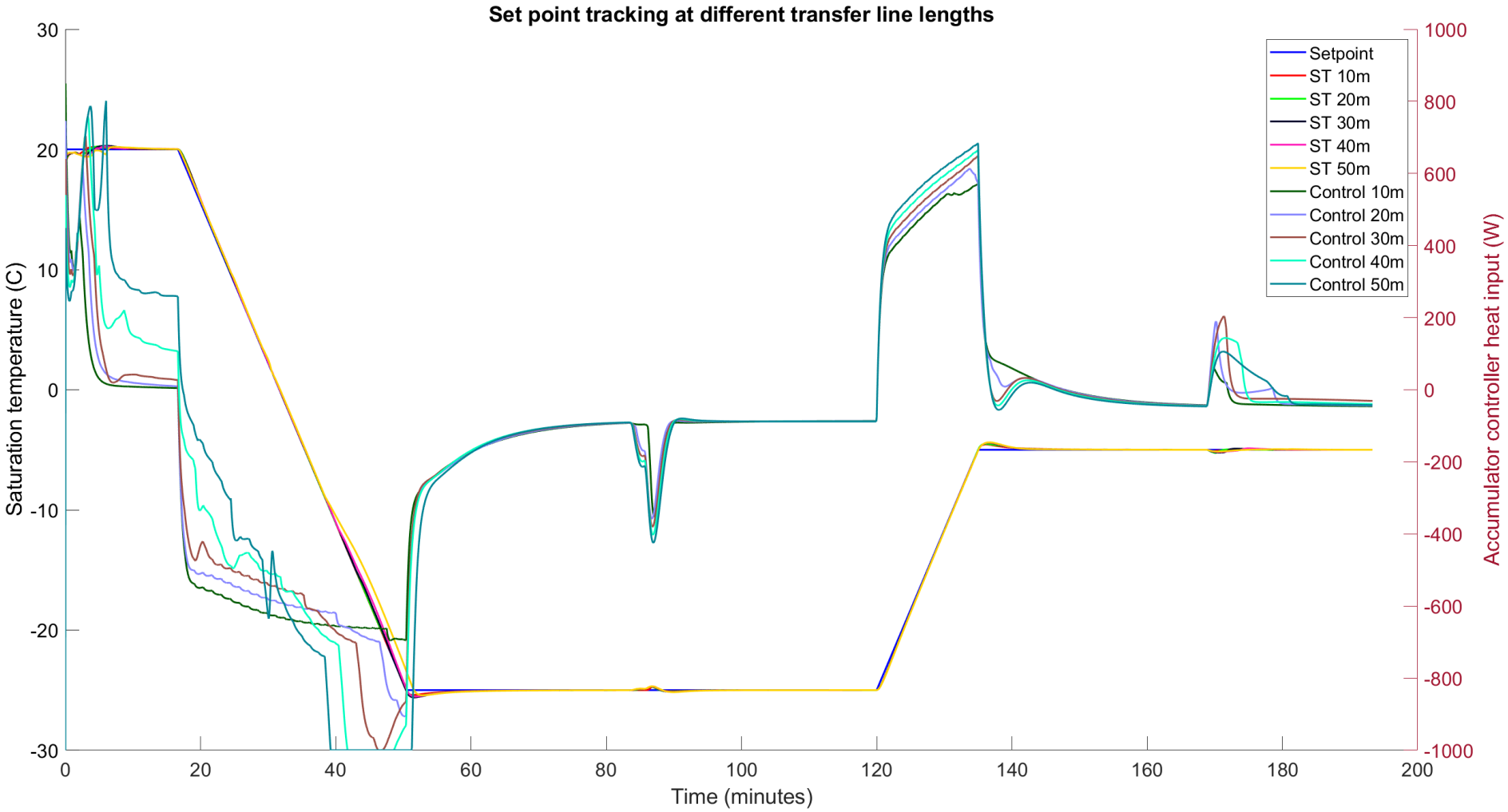

Figure 8.9: Impact of transfer line length on controller performance

8.4 Conclusion

The fluid system was modified to improve performance with short transfer lines and at warmer temperatures with the I2PACL running mode; the electrical system was redesigned to meet the group's standards, improving its usability. The control software was written with the latest version of UNICOS and integrated into the group's SCADA systems; to understand the performance of the new system and test the controller and system configurations, a model was developed.

Unfortunately, these elements could not be united and commissioned into a working system within the time frame of this project. Travel restrictions, material shortages and procurement delays caused by the pandemic resulted in some components not being available for evaluation in this project.

The new electrical design is much simpler and matches the norms of the EP-DT section. It ensures that the design can be maintained by others in the group while also reusing as many parts from the original system as practical. It provides a more open presentation allowing easier access for technicians and better visualisation of the status of the electrical components.

The new fluid systems are an elegant reuse of the original VTCS components making the system more usable. The 2PACL and I2PACL option modes allow the operator to choose what best suits their needs at the time and increase the temperature of the CO_2 to bring it closer to saturation before entering the test section.

Running in the internal bypass heater allowed a 1.5 kW load to be applied to both CO_2 systems simultaneously. At this point the chiller nears its maximum capacity: the saturation temperature drifts warmer but remains at acceptable levels.

It is capable of reaching −30 °C; below this, the system protection parameters begin to activate and may result in deviation from the set point. −35 °C is the minimum operating temperature and may only be achievable under limited conditions.

The controller was able to maintain the standard temperature change rate, even when a heat load was added during the change in set point. It caused a small deviation which the controller corrected for. The integrator ensured zero steady-state error, an exact measurement of the error is difficult to specify due to data archiving dead bands.

The chiller can run in stand-alone operation without any load on the CO_2 systems. It has winterisation protection to maintain performance in cold temperatures and can provide the 3 kW design power.

The control system was built using the most recent versions of UNICOS and was integrated into the Fluid Systems section SCADA server allowing remote monitoring and control through the server's web interface and logging of system

parameters via LHCLogging. The program was developed in a standardised and modular manner allowing further development and updates as needed.

A model of the system was built to show the system's expected performance. The controller design was developed from this model. This was the best alternative available because the chiller rack and its components were not available to collect real-world data. Developing a digital twin model of the system was beyond this project's scope; however, the model was validated against data collected when the VTCS was commissioned. This ensures that, when the hardware is ready, it will be sufficiently accurate to provide a stable base for the final design.

The final system design provides a simple and powerful basis for the detector development team to do their work. Each CO_2 half is five times more powerful than the previous test facility it replaces

While the results shown in this chapter are not taken from the system in its final configuration, they are representative of the final performance and the components yet to be received will only improve it. The system has met or exceeded the outcomes defined in Section 1.2 and, during the handover process, the Engineering Office team were satisfied with the performance shown.

Bibliography

[1] E. Mobs, "The CERN accelerator complex - 2019," *The CERN accelerator complex - August 2018*, Jul. 29, 2019, Number: CERN-GRAPHICS-2019-002. [Online]. Available: https://cds.cern.ch/record/2684277 (visited on 08/22/2021).

[2] V. Ramanathan, "Greenhouse effect due to chlorofluorocarbons: Climatic implications," *Science*, vol. 190, no. 4209, pp. 50–52, Oct. 3, 1975, ISSN: 0036-8075, 1095-9203. DOI: 10.1126/science.190.4209.50. [Online]. Available: https://www.sciencemag.org/lookup/doi/10.1126/science.190.4209.50 (visited on 04/07/2021).

[3] S. Solomon, I. P. on Climate Change, and I. P. on Climate Change, Eds., *Climate change 2007: the physical science basis: contribution of Working Group I to the Fourth Assessment Report of the Intergovernmental Panel on Climate Change*, OCLC: ocn132298563, Cambridge ; New York: Cambridge University Press, 2007, 996 pp., ISBN: 978-0-521-88009-1.

[4] D. Ehhalt, M. Prather, F. Dentener, R. Derwent, E. Dlugokencky, E. Holland, I. Isaksen, J. Katima, V. Kirchhoff, P. Matson, P. Midgley, M. Wang, T. Berntsen, I. Bey, G. Brasseur, L. Buja, W. J. Collins, J. Daniel, W. B. DeMore, N. Derek, R. Dickerson, D. Etheridge, J. Feichter, P. Fraser, R. Friedl, J. Fuglestvedt, M. Gauss, L. Grenfell, A. Grübler, N. Harris, D. Hauglustaine, L. Horowitz, C. Jackman, D. Jacob, L. Jaeglé, A. Jain, M. Kanakidou, S. Karlsdottir, M. Ko, M. Kurylo, M. Lawrence, J. A. Logan, M. Manning, D. Mauzerall, J. McConnell, L. Mickley, S. Montzka, J. F. Müller, J. Olivier, K. Pickering, G. Pitari, G. J. Roelofs, H. Rogers, B. Rognerud, S. Smith, S. Solomon, J. Staehelin, P. Steele, D. Stevenson, J. Sundet, A. Thompson, M. van Weele, F. Joos, and M. McFarland, "Atmospheric chemistry and greenhouse gases," p. 50, [Online]. Available: https://www.ipcc.ch/site/assets/uploads/2018/03/TAR-04.pdf.

[5] O. US EPA. (Dec. 23, 2015). "Overview of greenhouse gases," [Online]. Available: https://www.epa.gov/ghgemissions/overview-greenhouse-gases (visited on 11/16/2021).

[6] G. J. M. Velders, C. Clerbaux, R. Derwent, M. Grutter, D. Hauglustaine, S. Incecik, M. Ko, J.-M. Libre, O. J. Nielsen, F. Stordal, T. Zhu, D. Blake, D. Cunnold, J. Daniel, P. Forster, P. Fraser, P. Krummel, A. Manning, S. Montzka, G. Myhre, S. O'Doherty, D. Oram, M. Prather, R. Prinn, S. Reimann, P. Simmonds, T. Wallington, R. Weiss, I. S. A. Isaksen, and B. P.

Jallow, "Chemical and radiative effects of halocarbons and their replacement compounds," p. 48,

[7] O. US EPA. (Jan. 12, 2016). "Global greenhouse gas emissions data," [Online]. Available: https://www.epa.gov/ghgemissions/global-greenhouse-gas-emissions-data (visited on 11/16/2021).

[8] M. W. Roberts, "Finishing the job: The montreal protocol moves to phase down hydrofluorocarbons," *Review of European, Comparative & International Environmental Law*, vol. 26, no. 3, pp. 220–230, Nov. 1, 2017, Publisher: John Wiley & Sons, Ltd, ISSN: 2050-0386. DOI: 10.1111/reel.12225. [Online]. Available: https://onlinelibrary.wiley.com/doi/full/10.1111/reel.12225 (visited on 04/06/2021).

[9] Y. Heredia-Aricapa, J. M. Belman-Flores, A. Mota-Babiloni, J. Serrano-Arellano, and J. J. García-Pabón, "Overview of low GWP mixtures for the replacement of HFC refrigerants: R134a, r404a and r410a," *International Journal of Refrigeration*, vol. 111, pp. 113–123, Mar. 1, 2020, ISSN: 0140-7007. DOI: 10.1016/j.ijrefrig.2019.11.012. [Online]. Available: https://www.sciencedirect.com/science/article/pii/S0140700719304773 (visited on 06/10/2021).

[10] *Regulation (EU) no 517/2014 of the european parliament and of the council of 16 april 2014 on fluorinated greenhouse gases and repealing regulation (EC) no 842/2006 text with EEA relevance*, Legislative Body: CONSIL, EP, May 20, 2014. [Online]. Available: http://data.europa.eu/eli/reg/2014/517/oj/eng (visited on 06/14/2021).

[11] (Jun. 21, 2021). "Regulation of climate-damaging gases: Update f-gas-regulation," Regulation of climate-damaging gases: Update F-Gas-Regulation, [Online]. Available: https://frigoconsulting.ch/en/regulation-of-climate-damaging-gases-update-f-gas-regulation/ (visited on 10/20/2021).

[12] D. Bortoletto, "Detectors for particle physics," p. 65, Jul. 17, 2012. [Online]. Available: https://indico.cern.ch/event/190055/.

[13] *IMG_3400*. [Online]. Available: https://www.nikhef.nl/pub/departments/mt/projects/lhcb-vertex/VELO_PICTURES/pages/IMG_3400.htm (visited on 10/20/2021).

[14] M. Gupta, *Calculation of radiation length in materials*, Jul. 22, 2010. [Online]. Available: https://cds.cern.ch/record/1279627/files/PH-EP-Tech-Note-2010-013.pdf (visited on 05/24/2021).

[15] P. Jałocha, *LHCb VELO detector cooling requirements*, Apr. 2, 2016. [Online]. Available: https://indico.cern.ch/event/487201/contributions/1997116/subcontributions/180176/attachments/1227161/1797159/LHCb_VELO_Detector_Cooling_Requirements.pdf (visited on 05/24/2021).

[16] H. Postema and B. Verlaat, "Cooling in HEP vertex and tracking detectors," in *Proceedings of The 20th Anniversary International Workshop on Vertex Detectors — PoS(Vertex 2011)*, vol. 137, SISSA Medialab, Jun. 27, 2012, p. 003. DOI: 10.22323/1.137.0003. [Online]. Available: https://pos.sissa.it/137/003 (visited on 03/14/2021).

[17] B. Verlaat, *Technical description of the velo thermal control system*, Aug. 31, 2010. [Online]. Available: https://edms.cern.ch/ui/file/1056946/3.0/VTCSdesignReport31aug10_EDMS1056946ver3p0.pdf (visited on 04/02/2020).

[18] O. Postma, H. B. Rookhuizen, M. Doets, and M. Ferro-Luzzi, "Preliminary studies for the LHCb vertex detector cooling system," p. 7, Dec. 22, 1999.

[19] B. Verlaat, "CO2 cooling," 2011, [Online]. Available: https://indico.cern.ch/event/132770/ (visited on 08/22/2021).

[20] B. Verlaat and A. P. Colijn, "CO2 cooling developments for HEP detectors," in *Proceedings of VERTEX 2009 (18th workshop) — PoS(VERTEX 2009)*, vol. 95, SISSA Medialab, Aug. 10, 2010, p. 031. DOI: 10.22323/1.095.0031. [Online]. Available: https://pos.sissa.it/095/031 (visited on 03/15/2021).

[21] B. Verlaat, "Controlling a 2-phase CO2 loop using a 2-phase accumulator," p. 8, 2007.

[22] H. Jan van Gerner and N. Braaksma, "Transient modelling of pumped two-phase cooling systems: Comparison between experiment and simulation," Jul. 10, 2016. [Online]. Available: https://ttu-ir.tdl.org/handle/2346/67471 (visited on 09/18/2023).

[23] J. Sanchez, J. M. Heuser, C. J. Schmidt, P. Petagna, B. Verlaat, L. Zwalinski, and H. R. Schmidt, "TRACI-XL, the test cooling system for the CBM silicon tracking system," p. 1, 2012.

[24] B. Verlaat, "LUCASZ user training for FPIX," 2017, [Online]. Available: https://indico.cern.ch/event/688678/ (visited on 10/08/2021).

[25] ABB, *Comparison of tripping characteristics for miniature circuit-breakers*. [Online]. Available: https://library.e.abb.com/public/114371fcc8e0456096db42d614be2CDC400002D0201_view.pdf (visited on 11/09/2021).

[26] M. Baezner and P. Robin, *Hotspot analysis: Stuxnet*, 2017. [Online]. Available: https://css.ethz.ch/en/publications/risk-and-resilience-reports/details.html?id=%2Fs%2Ft%2Fu%2Fx%2Fstuxnet (visited on 03/30/2022).

[27] H. Milcent, E. Blanco, F. Bernard, and P. Gayet, "UNICOS: An open framework," p. 3, 2009.

[28] NIKHEF. (). "Mechanical design LHC-b vertex," [Online]. Available: https://www.nikhef.nl/pub/departments/mt/projects/lhcb-vertex/index_current.html (visited on 03/13/2022).

[29] M. Huber, A. Harvey, E. Lemmon, G. Hardin, I. Bell, and M. McLinden, *NIST reference fluid thermodynamic and transport properties database (REFPROP) version 10 - SRD 23*, Type: dataset, 2018. DOI: 10.18434/T4/1502528. [Online]. Available: https://www.nist.gov/srd/refprop (visited on 12/10/2021).

[30] E. Boje, "Approximate models for continuous-time linear systems with sampling jitter," *Automatica*, vol. 41, no. 12, pp. 2091–2098, Dec. 1, 2005, ISSN: 0005-1098. DOI: 10.1016/j.automatica.2005.06.011. [Online].

Available: https://www.sciencedirect.com/science/article/pii/S000510980500261X (visited on 12/16/2022).

[31] M. Lluesma, A. Cervin, P. Balbastre, I. Ripoll, and A. Crespo, "Jitter evaluation of real-time control systems," Jan. 1, 2006, pp. 257–260. DOI: 10.1109/RTCSA.2006.41.

[32] A. Reyes-Lúa, C. Zotică, K. Forsman, and S. Skogestad, "Systematic design of split range controllers," *IFAC-PapersOnLine*, vol. 52, pp. 898–903, Jan. 1, 2019. DOI: 10.1016/j.ifacol.2019.06.176.

Appendix A

DTCS documentation

All official CERN documentation can be accessed through CERN's Engineering Data Management System (EDMS). This repository contains the current state of the files and changes may have been implemented after writing. If there are access problems please contact me by email.

The EDMS repository contains:

1. Process and Instrumentation Diagram
2. Electrical schematics
3. Functional analysis
4. Specification file
5. Commissioning file

Appendix B

Modelling and data files

Files not stored by CERN can be found in a GitHub repository. It contains the MATLAB scripts, Simulink files, model data files and additional engineering material not stored on EDMS.

Due to size limitations in git, the full data output files from the simulations cannot be included in the repository. They can be found at the following DropBox link: Model output

Appendix C

Component naming convention

A new naming convention for the components of the system is being used that matches the norms used in the FS section. Component labels are 6 characters long and have the following structure:

ABCd_EF_XXNYZZ

C.1 Function identifier (A)

This letter identifies the function that the system performs: C is cooling, G is gas

C.2 Location identifier (BC)

Character B indicates if the system is on the surface (S) or underground (U). Number C is the LHC point at which it is installed. There are 8 designated points on the LHC ring with CERN's Meyrin site being designated point 0.

C.3 System identifier (d)

This is a lowercase letter that differentiates systems installed at the same location. It starts at a and decreases as new systems are added.

C.4 Plant identifier (EF)

This identifies the subsystems that make up a system. The CO_2 systems are P1 and P2, the common chiller is C0 and the local boxes are L1 and L2.

C.5 Component identifier (XX)

The component identifier is the first two characters of the label and is shown in Table C.1.

Table C.1: Component identifiers

Label	Description
TT	Temperature transmitter
PT	Pressure transmitter
LT	Level transmitter
PS	Pressure switch
TS	Thermal switch
CV	Control valve
EV	Electrical valve (shut-off)
MV	Manual valve
AV	Adjustable restriction valve
EH	Electrical heater
HX	Heat exchanger
AC	Accumulator
SG	Sight glass
LP	Liquid pump
GP	Gas pump (compressor)
BD	Burst disk
SV	Safety valve
FL	Filter
ST	Saturation pressure
SC	Sub-cooling
SH	Super-heating
DP	Differential Pressure
GH, GL, GM	Limit switch feedback

C.6 Subsystem (N)

The subsystem identifier is a single number that tells where the component is installed as indicated in Table C.2.

C.7 Parallel identifier (Y)

This is a single character which indicates if there are similar components at the same state point. If it is 0 it is the only device at that state point. If there are two components with the same identifier at the same state point they are differentiated with letters starting at a. In this system, it will be used to differentiate between the A and C CO_2 systems.

Table C.2: Subsystem identifier

Identifier	Subsystem
1	Liquid CO_2
4	Accumulator
5	Chiller
9	Two phase CO_2

C.8 State point (ZZ)

The state point is a two-digit number that indicates where in the process loop the component is placed. It is incremented every time there may be a change in the state of the process, for example across a heater or valve.

Appendix D

Standard wire colours

Table D.1 shows the standard wire colours used at CERN.

Table D.1: Standard wire colours

Description	Colour	Code
Three-phase 400V AC L1-L2-L3	Brown-Black-Grey	BRN-BLK-GRY
Single-phase 230V AC	Brown	BRN
24V AC	Violet	VIO
Neutral	Blue	BLU
Protective earth	Green-Yellow	GRN-YEL
24V DC	Red	RED
0V DC	White	WHT
Digital input	Orange	ORG
Digital output	Grey	GRY
Analogue input	Green	GRN
Analogue output	Yellow	YEL

Appendix E

Unused models

A model of the chiller was developed in Simscape (Fig. E.1). However, to reduce complexity, it was not included in the final plant model. The plant model takes 20 minutes to run depending on the dynamics being modelled and the performance of the computer that it is being run on. To avoid increasing the run time and computation demands, the chiller was represented as a cold source on the other side of the condenser heat exchanger.

The chiller design has been widely used in the DT group with at least eight examples in operation. As a result, more work was done on the modelling and performance analysis of the CO_2 systems. It features hot gas bypass and cold liquid injection valves to allow it to run with no load being applied. This configuration is unusual in commercial applications with more consistent heat loads.

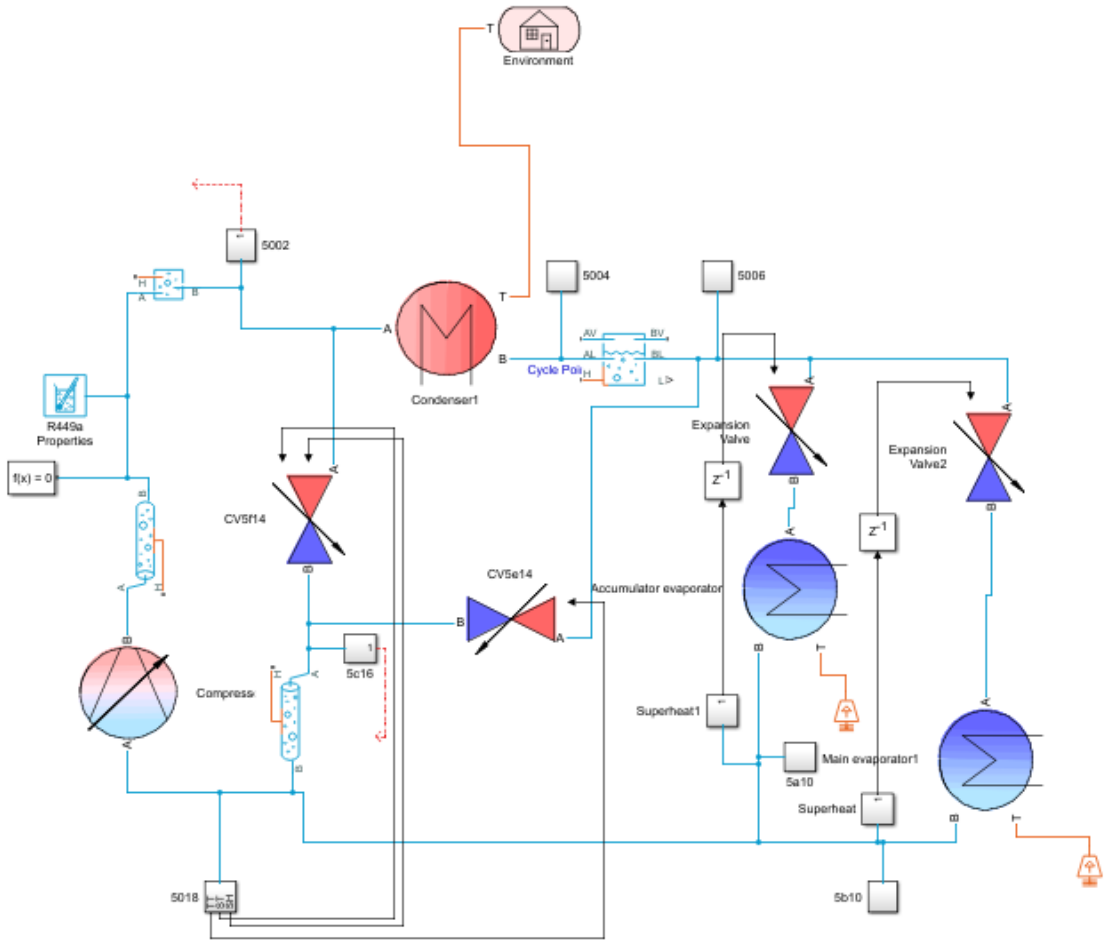

Figure E.1: Chiller Simscape model

Appendix F

UNICOS

UNICOS documentation can be found on their website.

The UNICOS templates can be provided on request. A sample of the CO_2 general logic template is available in the GitHub repository.

Appendix G

Publications

A paper on the design was presented at the 18th International Conference on Accelerator and Large Experimental Physics Control Systems (ICALEPCS) 2021. The paper can be accessed on CERN's website https://accelconf.web.cern.ch/icalepcs2021/papers/tupv030.pdf